

# EUR 4638 e

COMMISSION OF THE EUROPEAN COMMUNITIES

EXPERIMENTAL AND THEORETICAL DETERMINATION  
OF BURNUP AND HEAVY ISOTOPE CONTENT IN A FUEL ASSEMBLY  
IRRADIATED IN THE GARIGLIANO BOILING WATER REACTOR

by

A. ARIEMMA, I. BRAMATI, M. GALLIANI,  
M. PAOLETTI GUALANDI, B. ZAFFIRO  
(ENEL)

and

A. CRICCHIO, L. KOCH  
(EURATOM)

1971



Report prepared by ENEL  
Ente Nazionale per l'Energia Elettrica - Rome (Italy)

Euratom Contract No. 092-66-6 TEEI

## ABSTRACT

Under the joint ENEL-EURATOM program for the utilization of plutonium in thermal reactors, post-irradiation analyses were carried out on an enriched-uranium assembly irradiated at about 10,000 MWd/MTU in the Garigliano boiling water reactor.

The objective was the determination of burn-up, uranium and plutonium concentration in order to supplement the experimental data to be used for the verification of the calculation method on irradiated fuel. Burn-up was measured non-destructively by means of a high-resolution solid-state detector and destructively through Nd-148 determination, whereas heavy isotope concentrations by mass spectrometry combined with isotopic dilution techniques.

The measurements, carried out at the Institute for Transuranium Elements in Karlsruhe, compare favourably with the five-group BURSQUID calculation; the burn-up values agree within  $\pm 1.5\%$ , whereas the concentrations of U-235, Pu-239 and Pu-240 are within less than 4%.

The report discusses several correlations of general interest that were found among different isotopic ratios or between isotopic abundances and burn-up parameters. The correlations were used only to check the consistency of experimental results, although their validity to determine also burn-up and isotopic abundances is recognized.

## KEYWORDS

BURNUP	NEODYMIUM 148
URANIUM	MASS SPECTROMETERS
PLUTONIUM	ISOTOPE DILUTION
ISOTOPE RATIO	URANIUM 235
GAMMA SPECTROMETERS	PLUTONIUM 239
GAMMA FUEL SCANNING	PLUTONIUM 240
ALPHA SPECTROMETERS	DATA PROCESSING
SPECTRA	CONSISTENCY

I N D E X

	Page
1. INTRODUCTION	7
2. DESCRIPTION OF THE PROGRAM	8
2.1 Objectives of the program	8
2.2 Program administration	10
3. FUEL ELEMENT CHARACTERISTICS	12
3.1 Description of A-106 assembly	12
3.2 Irradiation history	12
3.3 Problems associated with irradiated rod handling	18
4. BURN-UP CALCULATION METHOD AND MODEL	20
5. POST-IRRADIATION ANALYSES	25
5.1 Non-destructive gamma spectrometry	25
5.1.1 Data processing	29
5.1.2 Precision of the measurements	33
5.2 Axial gamma scanning on rods A-1 and E-5	37
5.3 Destructive gamma spectrometry	41
5.3.1 Data processing	42
5.3.2 Precision of the measurements	45
5.3.3 Burn-up determination from Cs-137 activity	47
5.4 Analyses of heavy isotopes	48

	Page
5.4.1 Mass spectrometry	48
5.4.2 Alpha spectrometry	49
5.4.3 Data processing	49
5.5 Nd-148 analyses	51
5.5.1 Accuracy of $F_T$ derived from Nd-148 analyses	51
6. DISCUSSION OF RESULTS	52
6.1 Evaluation of burn-up analyses	52
6.2 Correlation between isotope ratios and burn-up parameters	54
6.2.1 Consistency of experimental data	56
6.2.2 Discussion of correlations	62
6.3 Comparison between theoretical and experimental data	63
6.3.1 Burn-up	63
6.3.2 Isotopic content	66
7. CONCLUSIONS	76
8. ACKNOWLEDGEMENTS	78
9. REFERENCES	79
APPENDIX 1 BURN-UP CODES USED IN THE CALCULATIONS	82
A.1-1 FLARE code	82
A.1-2 BURNY code	84
A.1-3 BURSQUID code	85

		Page
APPENDIX 2	GAMMA SPECTROMETRY TECHNIQUES	86
A. 2-1	Non-destructive gamma spectrometry	86
A. 2-2	Gamma spectrometry of the solutions	88
A. 2-3	Burn-up determination from Cs-137 activity	99
APPENDIX 3	MASS AND ALPHA SPECTROMETRY	104
A. 3-1	Dissolution of samples and analyses of fission gases	104
A. 3-2	Isotopic dilution analyses	106
A. 3-3	Uranium and plutonium isotopic concentration	107
A. 3-4	Determination of other transuranic isotopes	108
A. 3-5	Nd-148 concentration analyses	110
A. 3-6	Burn-up determination from Nd-148 content	112
APPENDIX 4	ANALYTICAL RESULTS	114

## 1. INTRODUCTION \*)

In 1966 ENEL and EURATOM entered a research contract to study the recycle of plutonium in light water power reactors. One of the main purposes of the contract was to develop a design criterion for elements containing plutonium, employing adequate calculation methods. For this purpose it was deemed appropriate to take the largest number of measurements possible so as to adjust the calculation methods and codes to be used.

To complete and supplement the available experimental results, post-irradiation measurements of burn-up and isotopic contents were taken on an irradiated enriched-uranium assembly presenting plutonium contents of the same order of magnitude as is expected to be used for the design of the plutonium assemblies.

This topical report describes the main results of the investigations carried out under the ENEL-EURATOM Contract 092-66-6 TEEI at the Common Research Center in Karlsruhe, Institute for Transuranium Elements, on a fuel assembly that was irradiated in the Garigliano reactor, and the accuracy achieved by ENEL calculation methods.

---

\*) Manuscript received on February 9, 1971

## 2. DESCRIPTION OF THE PROGRAM

### 2.1 Objectives of the program

Task IV of the Contract calls for the execution of isotopic composition measurements on irradiated uranium fuel assemblies with an aim at obtaining experimental data to be used for the verification of the precision of the calculation methods developed within the framework of the referred Contract.

The main difficulties in carrying out such a program arose from disassembly, transport and handling of the fuel assembly (about 3 m long) in the hot cells at the Karlsruhe Center. Since a fuel assembly of the Garigliano first load had been removed from the reactor during the May 1967 shutdown for other research purposes and was already available disassembled in the Garigliano fuel pool, it was decided that this assembly should not be reassembled, but that it should be made available for the program.

This assembly, A-106, had reached a burn-up level of about 10,000 MWd/MTU<sup>(\*)</sup>. Thus, the fuel rods had been sufficiently exposed to contain an appreciable amount of plutonium. The estimated isotope content was, in fact, as follows:

U-235	1.18%
Total Pu	0.44%
Pu-239	0.32%
Pu-240	0.08%
Pu-241	0.03%
Pu-242	0.005% approx.

In addition, assembly A-106 had been irradiated in a fairly central position of the core so that the power tilting effect could be expected to be rather limited.

---

(\*) MTU = metric ton of uranium

The results of the post-irradiation analysis on assembly A-106 were therefore considered sufficiently reliable to check the burn-up calculations, and especially to check the concentrations of produced plutonium.

In view of the long period of decay that had elapsed before the beginning of the hot cell measurements, the program was limited to the measurements of burn-up and fuel isotopic composition.

The program was then logically broken down into two parts: non-destructive measurements based on gamma spectrometry and gamma scanning, and destructive analyses of burn-up and isotopic composition based on gamma, alpha, and mass spectrometric measurements of dissolved samples.

The non-destructive gamma-activity measurements were to determine the burn-up distribution at a pre-set level on the largest possible number of rods. These measurements are actually easier and more amenable than the destructive measurements, even though they cannot provide the absolute value of burn-up, because the results are dependent on the geometry of the measurement. On the contrary, destructive measurements permit an assessment of the heavy atom content, and specifically the depletion of U-235 and formation of plutonium. These measurements also offer the possibility of determining burn-up through the measurement of the concentration of a stable fission isotope. One of the isotopes most suited for this purpose is Nd-148, but its determination is not so simple as a non-destructive direct measurement and it requires the use of a mass spectrometer.

Therefore, it was decided that the absolute value of burn-up should be determined on a limited number of rods and then correlated with the results of the non-destructive measurements of burn-up distribution. In addition, the availability of the dissolved fuel samples prepared for the destructive measurements, offered the possibility of checking the burn-up by means of an additional destructive measurement, that is, through the determination of the specific activity of Cs-137.



For the purpose of adjusting the calculation method, it was of interest to determine the burn-up reached by the assembly at a given level, in order to apply the x-y geometry technique. In brief, the non-destructive measurements were taken on 34 rods at two levels corresponding to the positions of the in-core instrumentation (levels C and D; see Para 3.1), whilst the destructive measurements were limited to 18 fuel sections taken all at the same level (level C). For a check of the axial distribution calculations, two rods were subjected to gamma scanning over their entire length.

One reason for the choice of the particular level C was that the void fraction in operation at that point is representative of the average void content in the core.

These measurements permitted an integral and analytical verification of the calculation models and methods used in the nuclear design of the plutonium fuel assemblies. More specifically, the purpose of the measurements was to ascertain that the calculation technique was capable of:

- determining the correct burn-up distribution among the various rods;
- adequately assessing the concentrations of the heavy nuclides as a function of burn-up, with special reference to plutonium, while allowing for the effects of spectrum variations.

The measurements carried out in the Karlsruhe laboratories provided an adequate verification of the two above-mentioned stages in the calculations, and constitute an interesting source of information, considering the limited amount of experimental data at present available on power reactors.

## 2.2 Program administration

The measurement program was implemented by ENEL and the Institute for Transuranium Elements in Karlsruhe, working in close cooperation. ENEL undertook to deliver the irradiated rods of assembly A-106 to the Institute in such conditions as to be easily handled. For this purpose the rods had been

st firstly halved and then transported to Karlsruhe in a special shipping container.  
The rods were subjected to non-destructive gamma-spectrometry by a joint  
team of ENEL and EURATOM personnel. The cutting of the fuel sections and  
the performance of the destructive measurements were handled completely  
by the Institute.

ne The nuclear burn-up and isotopic composition calculations were performed  
by ENEL on the digital computer IBM 360/65 of CETIS at the Common Research  
Center at Ispra.

te  
NEL

### 3. CHARACTERISTICS OF THE FUEL ASSEMBLY

This Chapter will deal with the main characteristics of assembly A-106, its irradiation history and a brief description of the problems solved to handle the irradiated rods from Garigliano station to the hot cells at the Institute.

#### 3.1 Description of assembly A-106

Assembly A-106 belongs to the first core load of the Garigliano reactor; it is constituted of 81 rods arranged in a 9x9 array. Each of the eighty-one rods consists of four segments, containing pellets of ceramic uranium oxide enriched on the average to 2.02% in U-235 and clad in Zircaloy-2. The main geometrical dimensions of the element are given in Fig. 3-1.

The four segments of each rod are separated by zirconium connectors on which the steel grid rests; thus the fuel assembly is divided into four axial zones. All the pellets adjacent to the connectors have a lower enrichment in U-235 (1.6%); in addition, the peripheral rods contain also erbium oxide ( $\text{Er}_2\text{O}_3$ ) which acts as a neutron poison to flatten the flux peaking in the grid area.

Fig. 3-2 shows the enrichment distribution in the individual rods in the assembly. The outer diameter of the rods is 13.56 mm, and the cladding thickness 0.76 mm.

The axial position of the fission chambers for the measurement of the in-core neutron flux is at about mid-height of each fuel segment; the identification of levels at which the measurements were performed is shown in Fig. 3-3.

#### 3.2 Irradiation history

On the basis of the information contained in the station files, the history of assembly A-106 has been put together up to the time of discharge from the reactor at the end of Cycle 1B. Throughout Cycle 1, the assembly was irradiated in position 62-07 (Fig. 3-4); the steel sheath used in Cycle 1A was replaced by a Zircaloy sheath in Cycle 1B. Fig. 3-5 summarizes the main history of the assembly during irradiation, especially

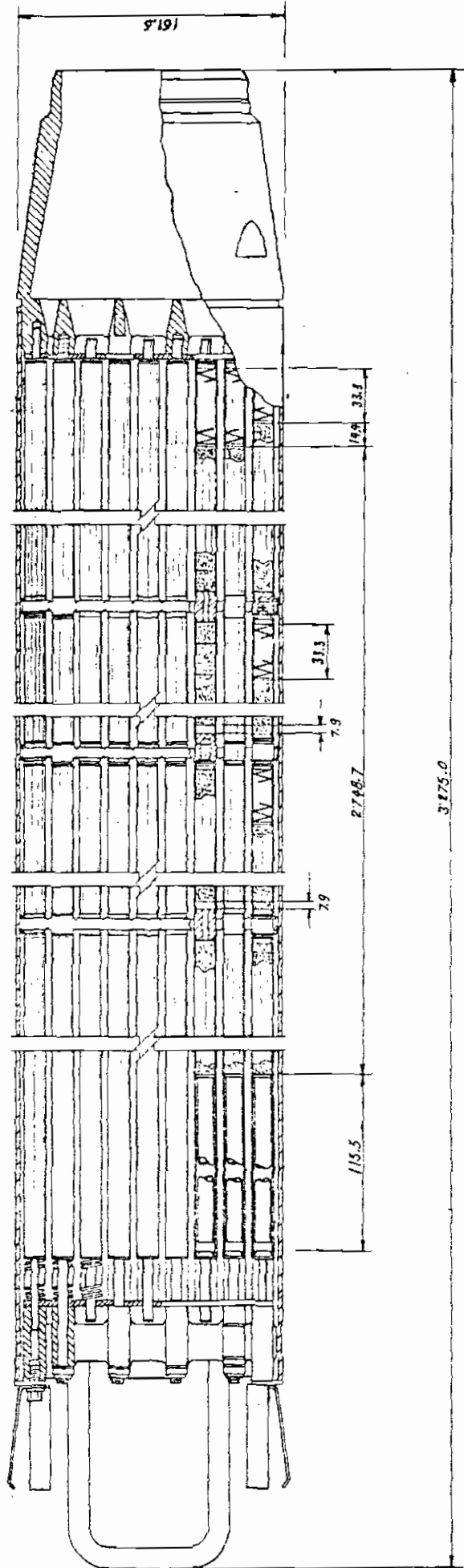
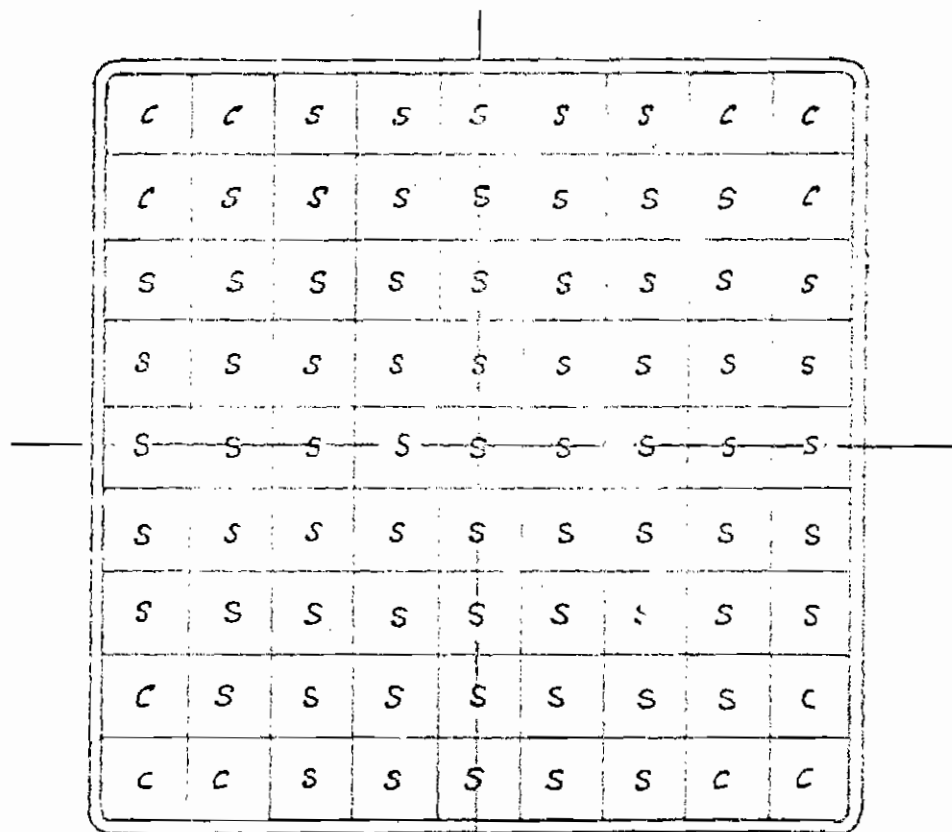


FIG. 3-1 GARIGLIANO FIRST CORE FUEL ELEMENT

3.

1

n



S = STANDARD ROD ; ENRICHEMENT 2,1%  
C = CORNER ROD ; ENRICHEMENT 1,6%

FIG. 3-2 ENRICHEMENT DISTRIBUTION IN THE GARIGLIANO FIRST CORE FUEL ASSEMBLY

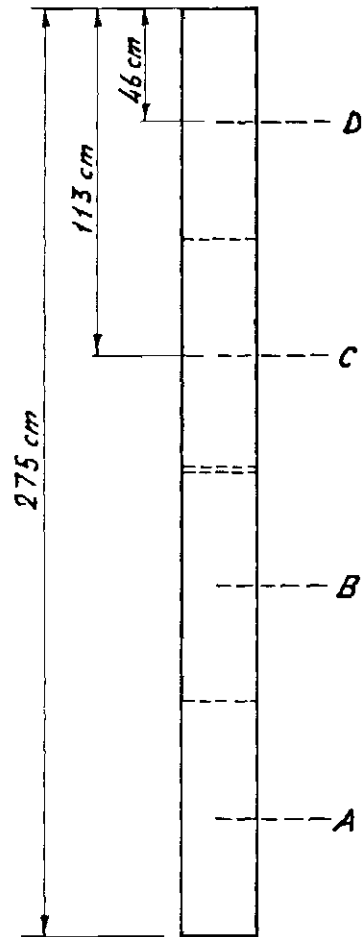
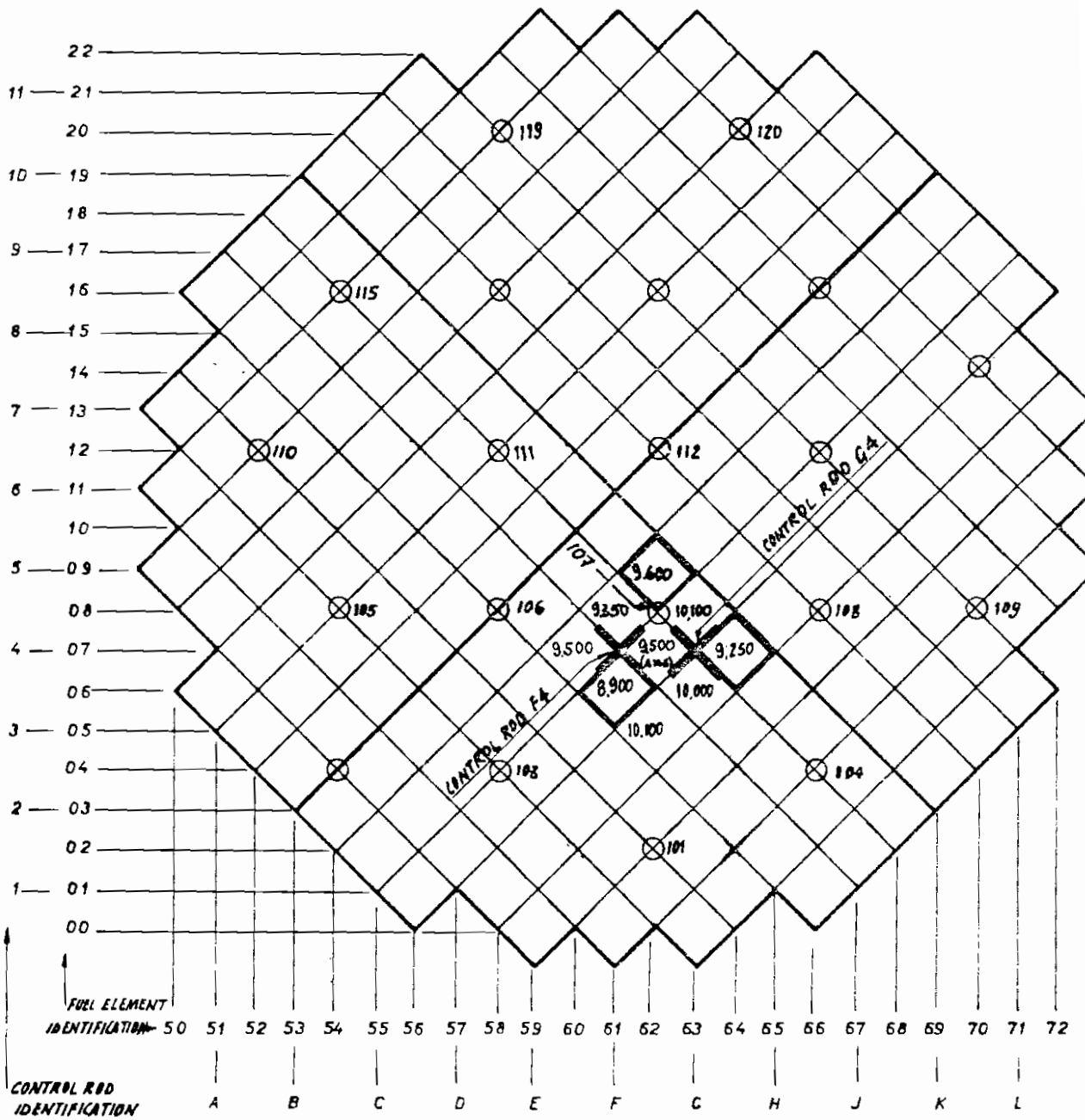


*FIG. 3-3 - IDENTIFICATION OF LEVELS "C" AND "D" ON THE FUEL ELEMENT*



BURN-UP AT THE END OF CYCLE 1B

⊕ SS IN-CORE TUBE

xxx SS CHANNEL

xxx AVERAGE FUEL ASSEMBLY BURN-UP

FIG. 3-4 POSITION OF ASSEMBLY A-106 IN THE CORE DURING OPERATION



72

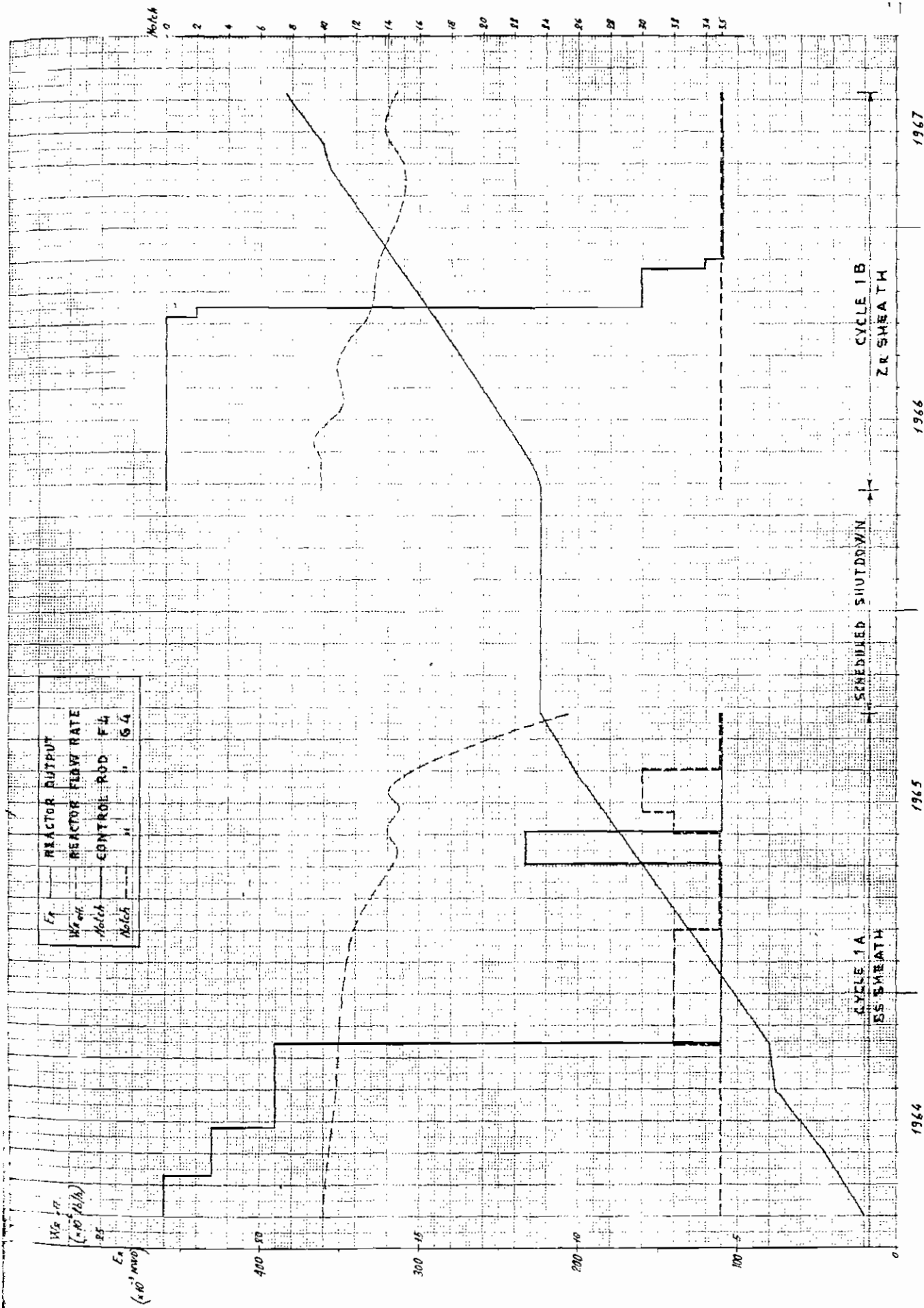


FIG. 3-5 - IRRADIATION HISTORY OF ELEMENT A-106 IN THE GARIGLIANO REACTOR



as concerns the reactor output, the position of the control rods directly affecting the element, the coolant flow rate and the type of sheath. This information was used in the tridimensional FLARE code to simulate the history of the core during Cycles 1A and 1B, and thus to determine the operating conditions in which the assembly was irradiated; particularly, the variation in average void fraction with exposure at the elevations of interest and the associated burnup levels. Figure 3-6 shows the curve of the void fraction variation at levels C and D, as calculated by the FLARE code. The burn-ups, calculated at the end of Cycle 1B, were:

Average irradiation	9,458 MWd/MTU
Average irradiation at level C	10,582 MWd/MTU
Average irradiation at level D	7,276 MWd/MTU

### 3.3 Problems associated with irradiated rod handling

The assembly selected for the analyses had already been disassembled in the Garigliano fuel pool for testing during the 1967 shutdown. Full-length pins were thus available in special stainless steel baskets. For reasons concerning handling in the hot cells it was necessary to halve the length of the pins before transporting them to the Karlsruhe Center. The halving operations were carried out at CNEN's Eurex Center in Saluggia, Italy, where adequate facilities were available. For the requirements of the final measurement program, thirty-six half-rods were selected and shipped to the Institute.

fect-  
a-  
idi-

ed  
th

al

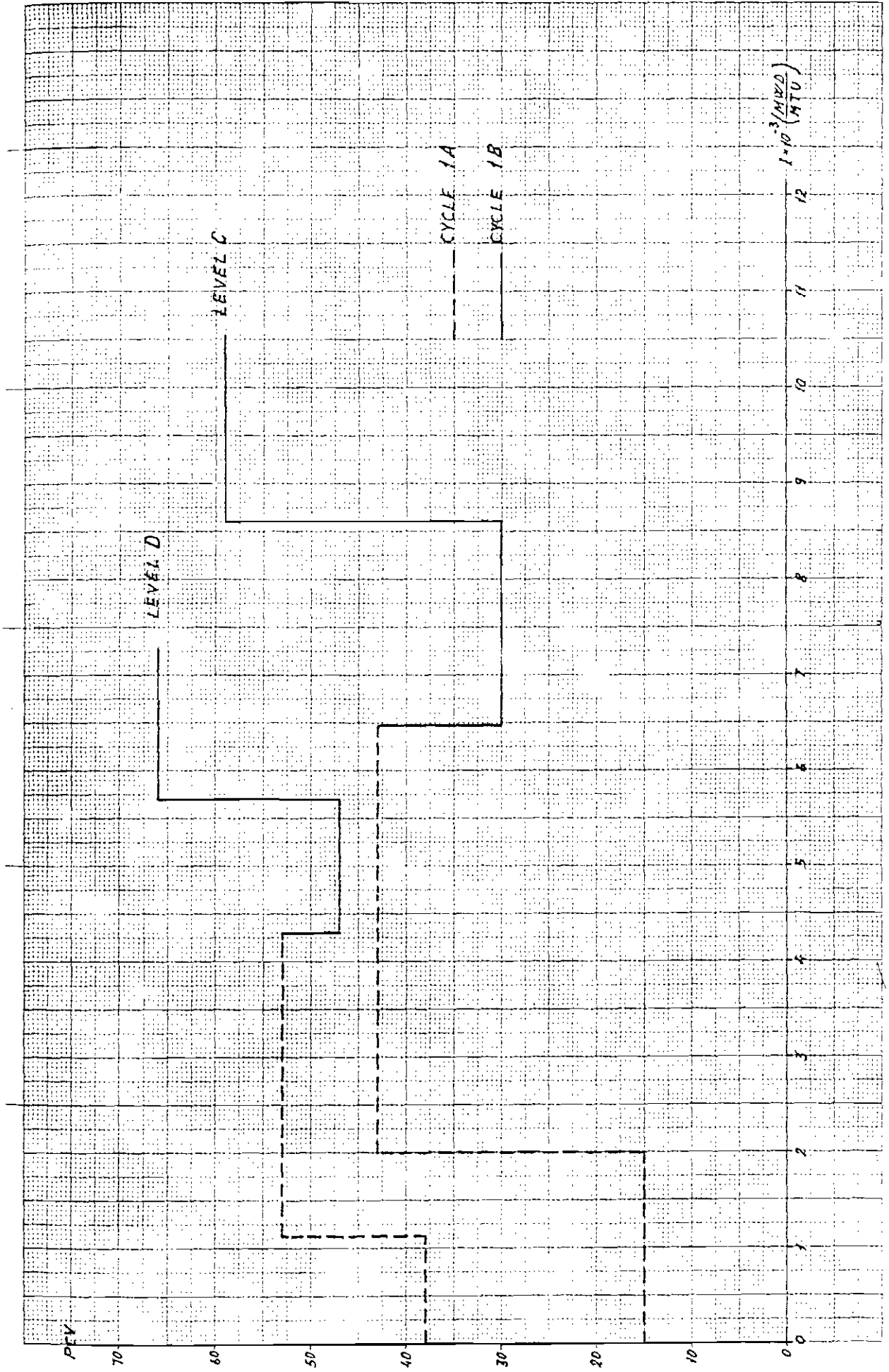


FIG. 3-6 - ELEMENT A-106 : AVERAGE VOID PROFILE DURING IRRADIATION

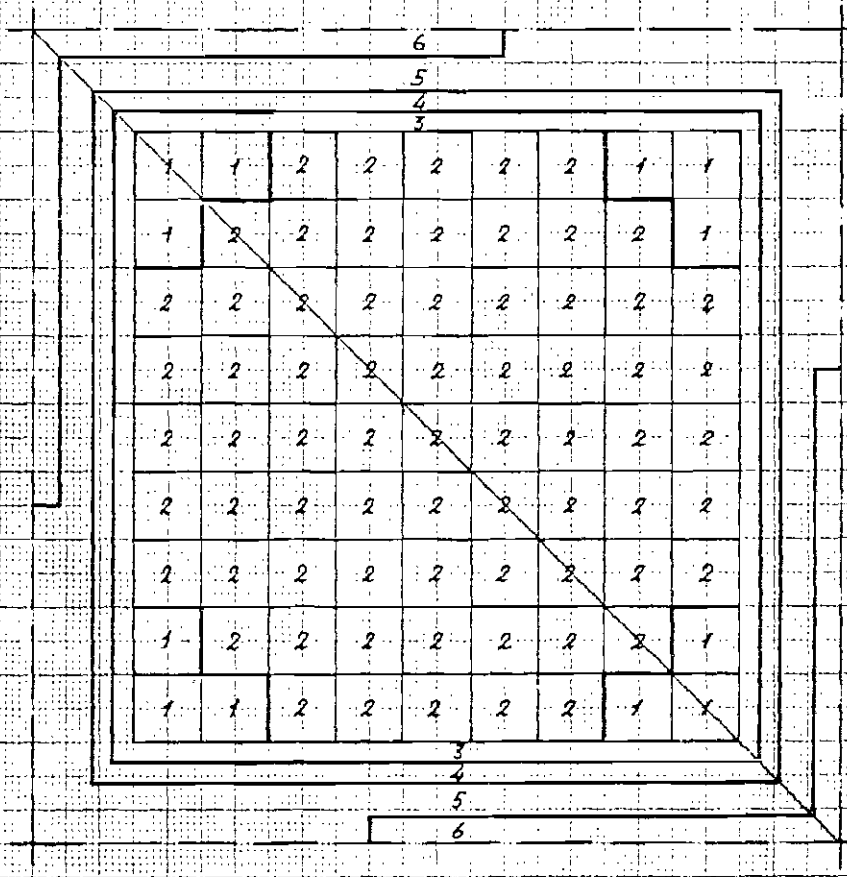
#### 4. BURN-UP CALCULATION METHOD AND MODEL

A brief description of the computer codes used by ENEL to carry out irradiation calculations is contained in Appendix 1. The main aspects of the calculations relating to the A-106 fuel assembly are summarized below.

The calculations of the exposure and fuel isotopic composition were performed initially with the two-group BURNY code on the calculation model as shown in Fig. 4-1. In the calculations it was assumed that the neutron current was nil around the assembly only during the exposure times when the assembly was not affected by the presence of control rods. On the contrary, when a control rod was inserted, use was made of extrapolation lengths calculated by means of the transport code DTK. It was also assumed that during irradiation a diagonal symmetry existed, this assumption simplified the calculations, but made it necessary to neglect the presence of the in-core instrumentation guide tube near one edge of the assembly.

The calculations related to level D were performed at a later date and the model was changed in respect of the intersection of the control rod blades. In the calculations, the related area was represented by lattice constants of steel-water mixture instead of the extrapolated length pertinent to the absorbing material used in the preceding calculations for the whole control rod. Actually, the control rod is constituted by four absorbing blades formed of steel-clad boron carbide pins sheathed in a steel frame and connected with a central steel support. If this detail is omitted in representing the rod, the absorbing effect on the corner rod facing the control rod is overrated. This effect was observed for the first time in the experimental results of the measurements of the control-rod-affected power distribution carried out at the Garigliano in the 1968 summer shutdown<sup>(1)</sup>, and it has been confirmed by the theoretical-experimental comparison performed for level C (see Chap. 6).

The calculations were repeated with the five-group BURSQUID code (a link of the five-group RIBOT and SQUID codes). This five-group code



AREAS

- 1. RODS ENRICHED TO 1.6% IN U235
- 2. RODS ENRICHED TO 2.1% IN U235
- 3. WATER INSIDE THE ELEMENT
- 4. SS. BR. ZK SHEATH
- 5. WATER GAP
- 6. CONTROL RODS

FIG. 4-1 - MODEL USED FOR THE CALCULATION OF IRRADIATION OF ELEMENT A-106

retains the main features of the calculation model of the two-group BURNY code, the difference being the subdivision of the thermal spectrum into two groups, whilst the condensation of the fast group is no longer carried out. This code was developed under the ENEL-EURATOM contract on the basis of the preliminary information obtained from the analysis of the relationship between Pu-239 and U-235 fission rates measured on the DIMPLE critical assemblies<sup>(2)</sup>. This analysis had indicated as the most promising for burnup and isotopic composition calculations the five-group method for the use of two thermal groups. Indeed, the use of two thermal groups allows the local reaction-rate variations due to thermal-spectrum deformation to be determined for the two isotopes more accurately than one thermal group.

Figure 4-2 shows the results of the burn-up calculations with the BURSQUID code for all the rods of assembly A-106 at level C, while Fig. 4-3 gives the results obtained with the two-group BURNY code at level D.

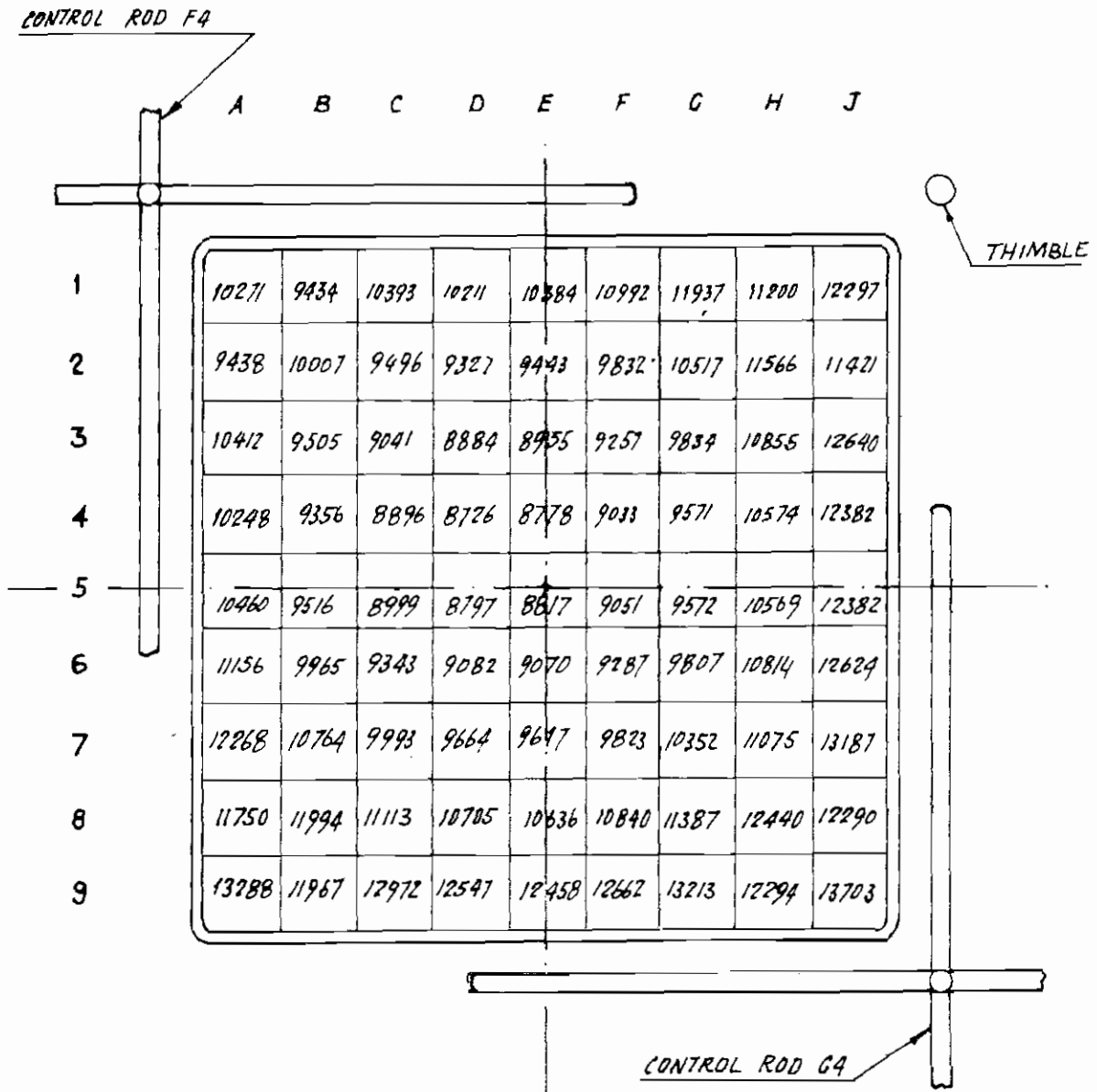


FIG. 4.2 BURN-UP OF SINGLE ROD AT DISCHARGE FOR LEVEL C AS CALCULATED BY 5-GROUP BURSQUID CODE (IN MWd/MTU)

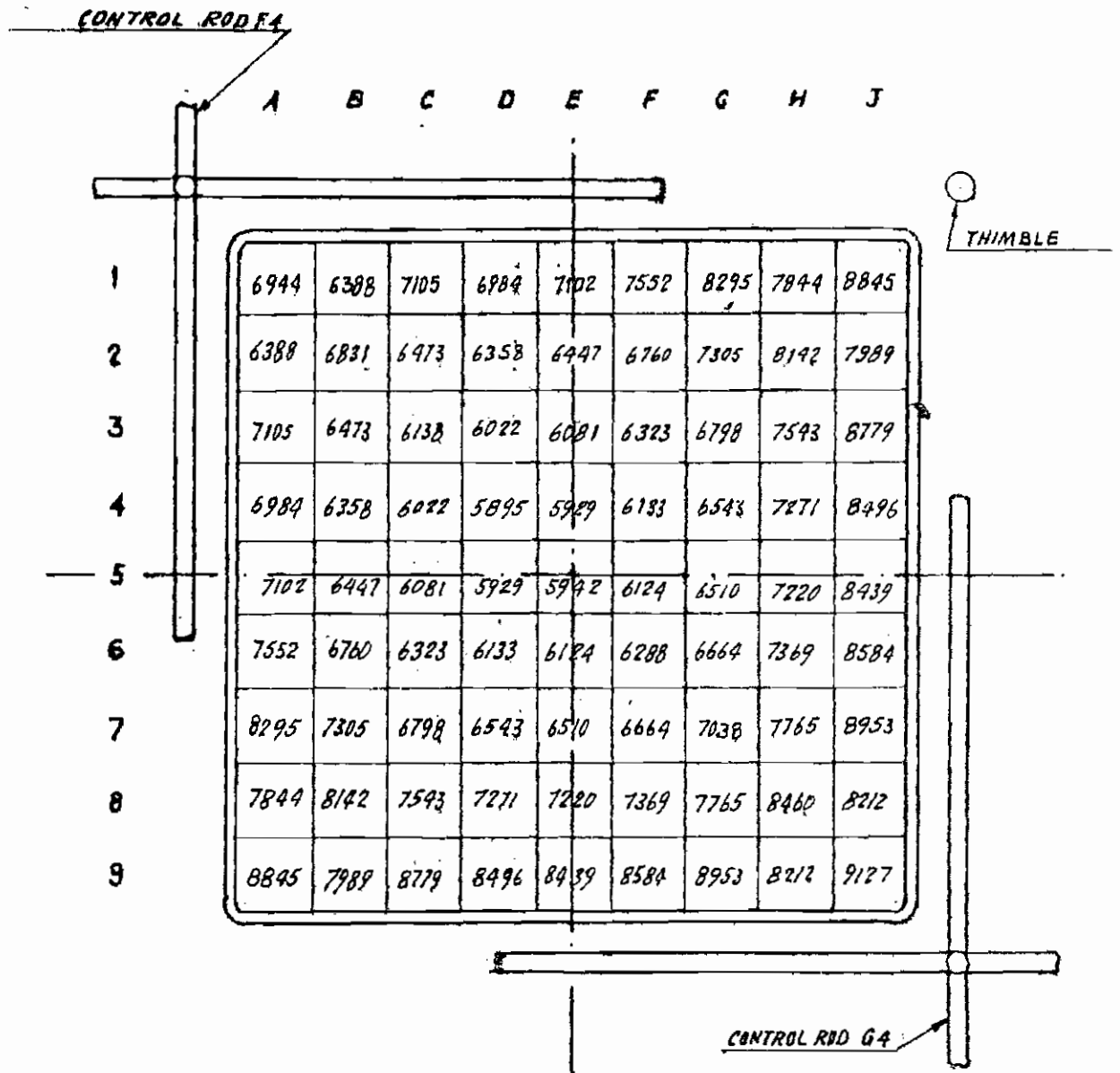


FIG. 4.3 BURN-UP OF SINGLE ROD AT DISCHARGE FOR LEVEL D AS CALCULATED BY 2-GROUP BURNY CODE (IN MWd/MTU)

## 5. POST-IRRADIATION ANALYSES

The selection of rods to be subjected to post-irradiation analyses was based on a compromise between the desire for a large measurement program and the transport requirements which limited the number of rods that could be transported in one container to only thirty-six half-rods. Of these, thirty-four were the upper halves of the full-length rods and comprise the measurement levels C and D. Two bottom half-rods were included in order to have some information on the lower part of the assembly. These lower halves were taken from a corner rod and a central one.

The program of analyses was broadly divided into non-destructive measurements for burn-up determination and destructive measurements for burn-up and heavy-isotope content determination.

From the flow diagram of the post-irradiation examination (Fig. 5-1) the sequence of each analyses can be seen.

After the non-destructive tests on all the mentioned fuel rods at two levels, pellet-size samples were cut from 18 rods at a position corresponding to level C. Figure 5-2 shows the orientation of the assembly and the position of these 18 rods inside it.

During dissolution of the samples, the isotopic composition of the fission gas was analyzed. The solutions were diluted sufficiently so that they could be handled outside the hot cells without danger. Portions of these solutions were then subjected to gamma and mass spectrometry. Gamma spectrometry was used to determine the concentrations of certain fission products from which the burn-up was derived; mass spectrometry was used to determine the concentrations of heavy isotopes and Nd-148. The Nd-148 concentration was then utilized for a separate evaluation of the burn-up.

### 5.1 Non-destructive gamma spectrometry

In order to determine the burn-up distribution in the fuel assembly at a fixed plane, the gamma activity over the whole emission spectrum (from a few keV to over 2 MeV) was monitored from each fuel rod at the



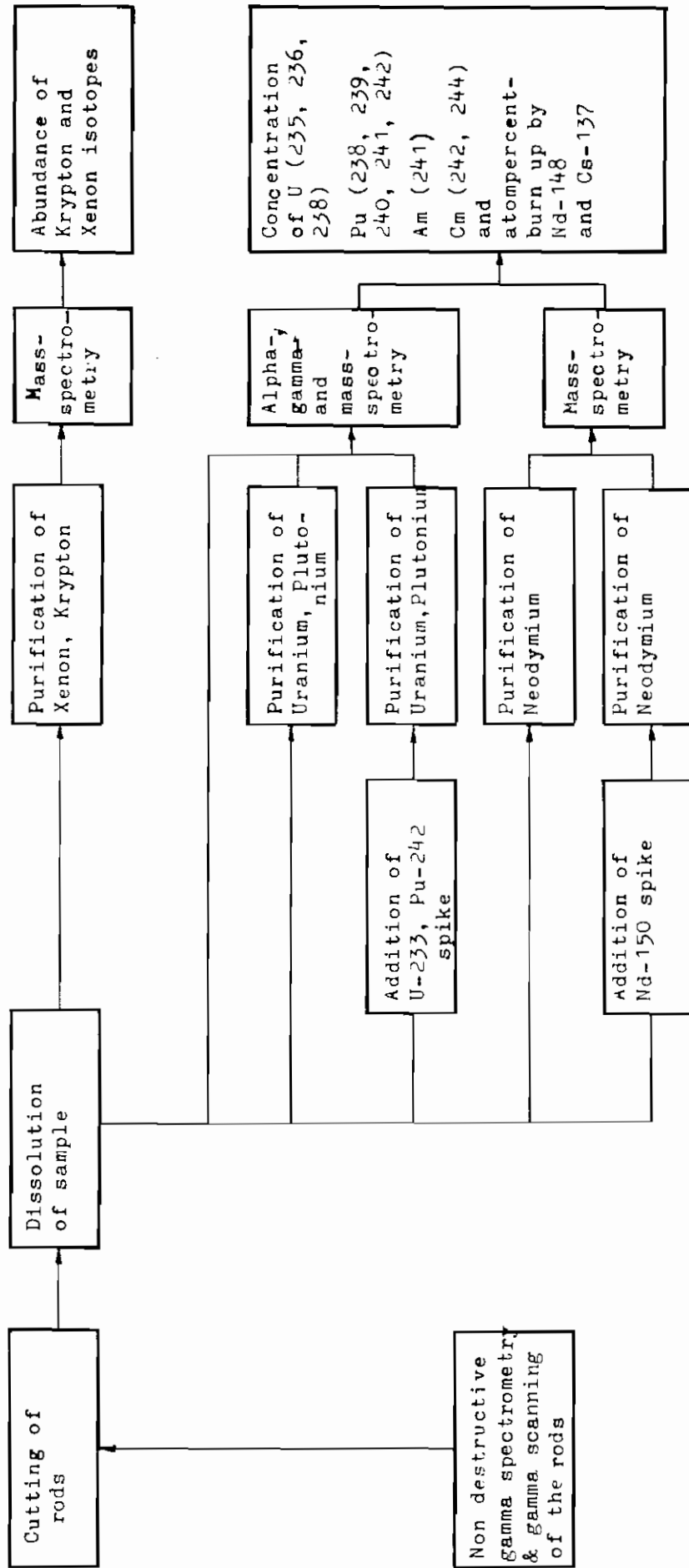
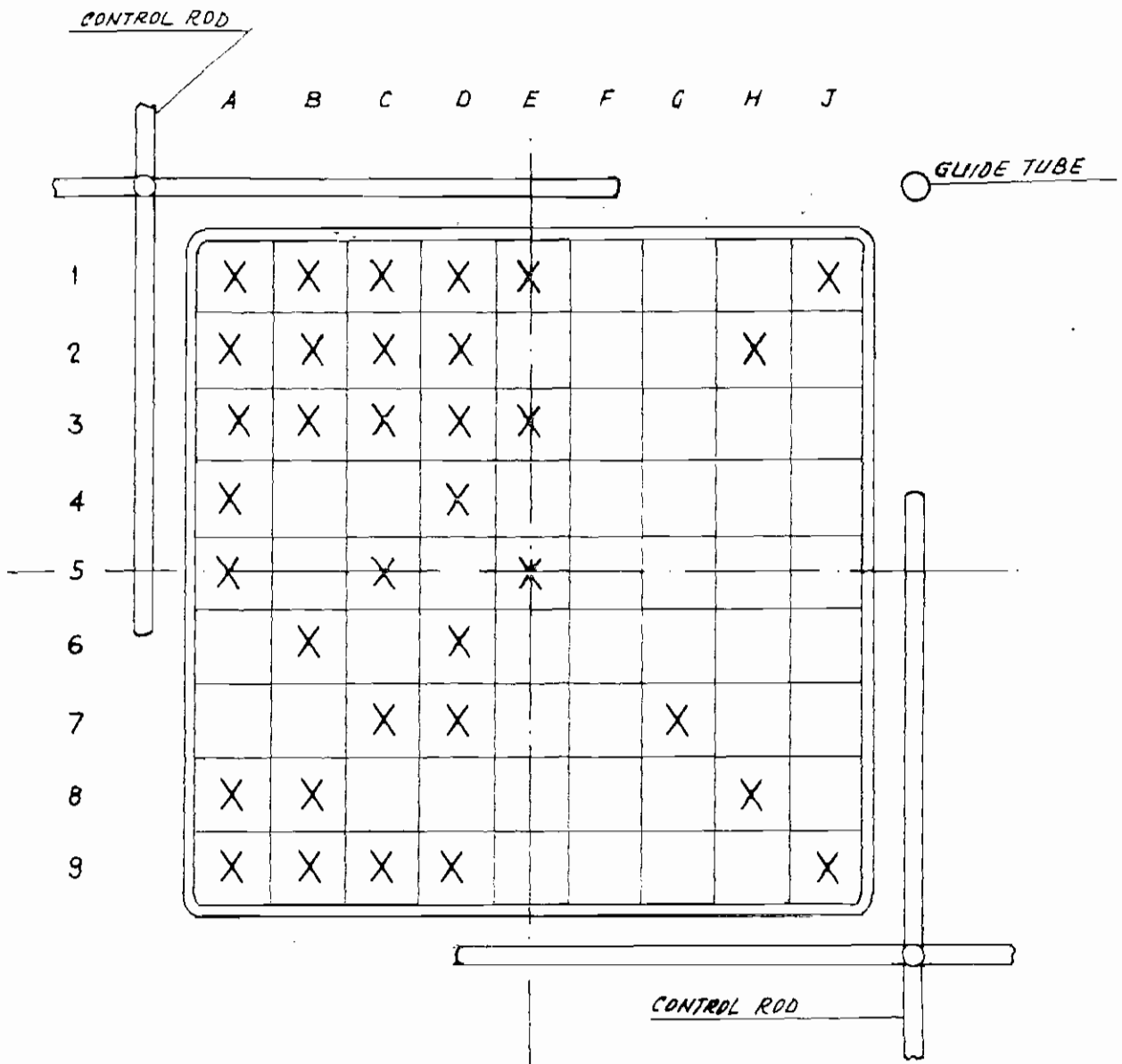


Fig. 5-1 : Flow diagram of post-irradiation examinations



ORIENTATION OF ASSEMBLY A-106

FIG. 5-2 RODS OF ELEMENT A-106 SELECTED FOR THE PROGRAM

same axial position, by high-resolution gamma spectrometry. This non-destructive technique is based on the possibility of correlating the gamma activity of a selected fission product to burn-up, so leading to a relative burn-up distribution. The reliability of this assumption depends on the extent to which the fission product satisfied the conditions for accurate burn-up monitors<sup>(3)</sup>.

The isotopes selected for these measurements were:

Isotope	Energy, keV	Half-life, yrs
Ru-106/Rh-106	512	1.008
Cs-137	662	30.60
Ce-144/Pr-144	2186	0.778

The activity of the relatively long-lived Cs-137 is proportional to the burn-up level reached, whereas the activities of Ru-106/Rh-106 and Ce-144/Pr-144 permit useful information to be obtained on the irradiation of the fuel element in the last period of residence in the reactor. For instance, owing to the different fission yields of U-235 and Pu-239 (0.38% versus 4.57% in the field of thermal fissions and 0.5% versus 6.4% for fast fissions), it is also possible to obtain information on plutonium burn-up in the preceding operating period from the activity of Ru-106/Rh-106<sup>(4)(5)</sup>. Although this report gives the results of the measurements on all three these isotopes, the analysis of the results was limited to the values of Cs-137, which can be correlated directly to the burn-up level calculated by means of the ENEL codes. To evaluate the information gathered from the other two isotopes, it is necessary to modify the calculation codes. This is being done, but at the time of this writing, the revised codes are not available yet for a complete analysis of the results.

The non-destructive technique adopted is based on the use of a Ge-Li monitor which gives a very high resolution of the gamma activity of the spectrum. This technique consists in monitoring the gamma activity

of a rod placed in front of a slit in the lead shield, whereby it is possible to collimate a very thin beam of radiations. The details of the technique are described in Appendix 2.

A typical spectrum obtained at the C level of a fuel rod is shown in Fig. 5-3. The peaks due to the main fission products (Cs-137, Ru-106/Rh-106, Ce-144/Pr-144), to the main neutron capture products (Cs-134, Eu-154) and to the main activated corrosion product (Co-60) are clearly recognizable.

The first set of scans was completed in December 1968. During the setting of the instrumentation before the measurements at level D, a non-linearity was noted in the response of the electronic chain at different energies. Therefore all the electronic equipment was substituted. Then gamma scanning at level D was performed and completed towards the end of January 1969.

#### 5.1.1 Data processing

The calibration and calculation procedures required for the interpretation of the spectra were considerably simplified because for the selected isotopes it was only necessary to establish the relative activity of the rods.

Peak integration and Compton-background correction were done by measuring the net area of each peak from the spectrum printed out in numerical form. In the calculation of the relative activities of the three isotopes from the resulting spectra, a simple numerical method was used to assess the area of the peaks, that is, a constant amplitude of nine memory channels was assigned to each peak (Fig. 5-4). In addition, to take into account the Compton effect and background, the peak area was defined by the formula:

$$I = \sum_{m-4}^{m+4} i_m - \frac{9}{2} (i_{m-4} + i_{m+4}) \quad (1)$$

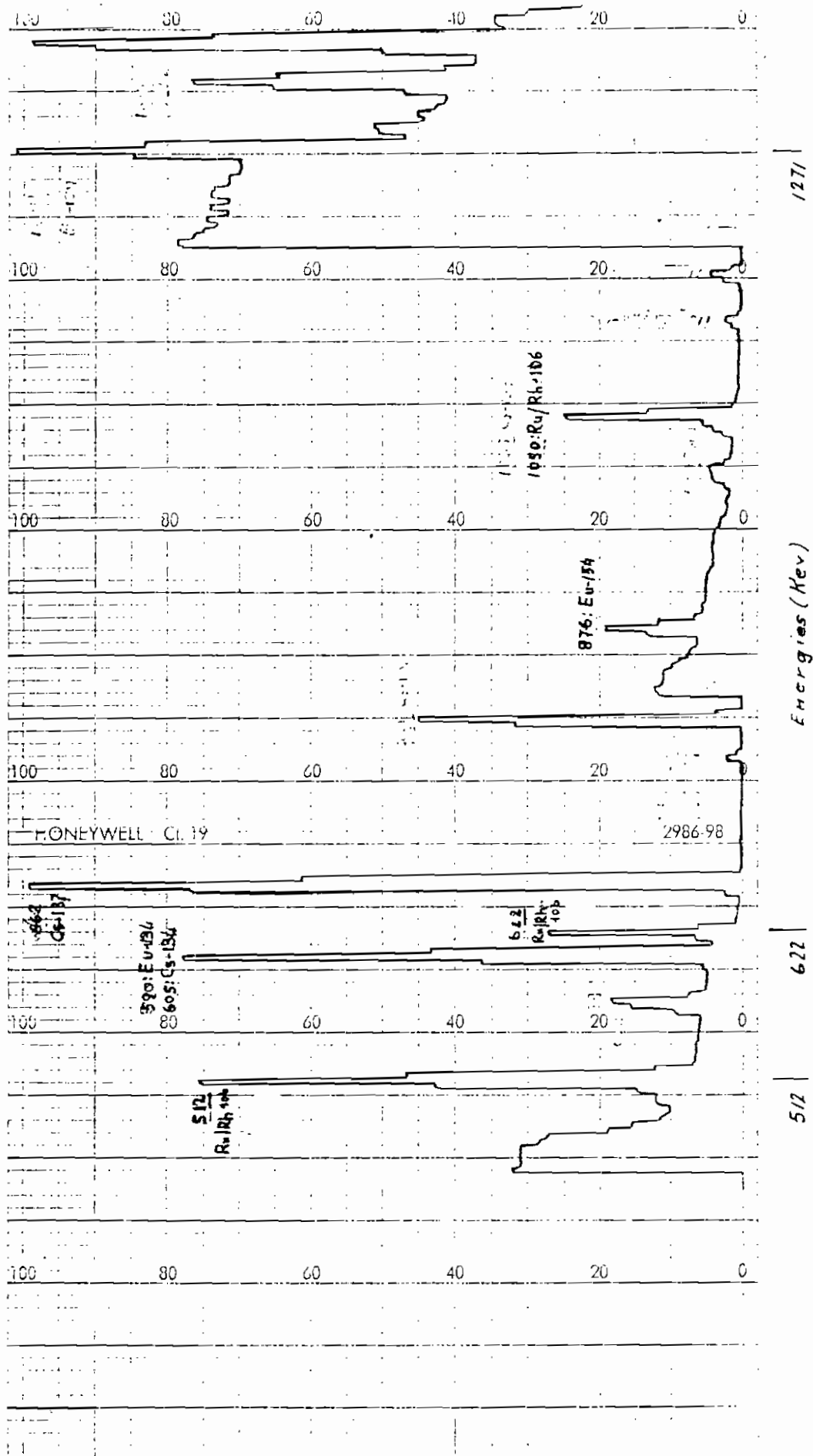


FIG. 5-3a - TYPICAL GAMMA SPECTRUM OBTAINED AT LEVEL "C"

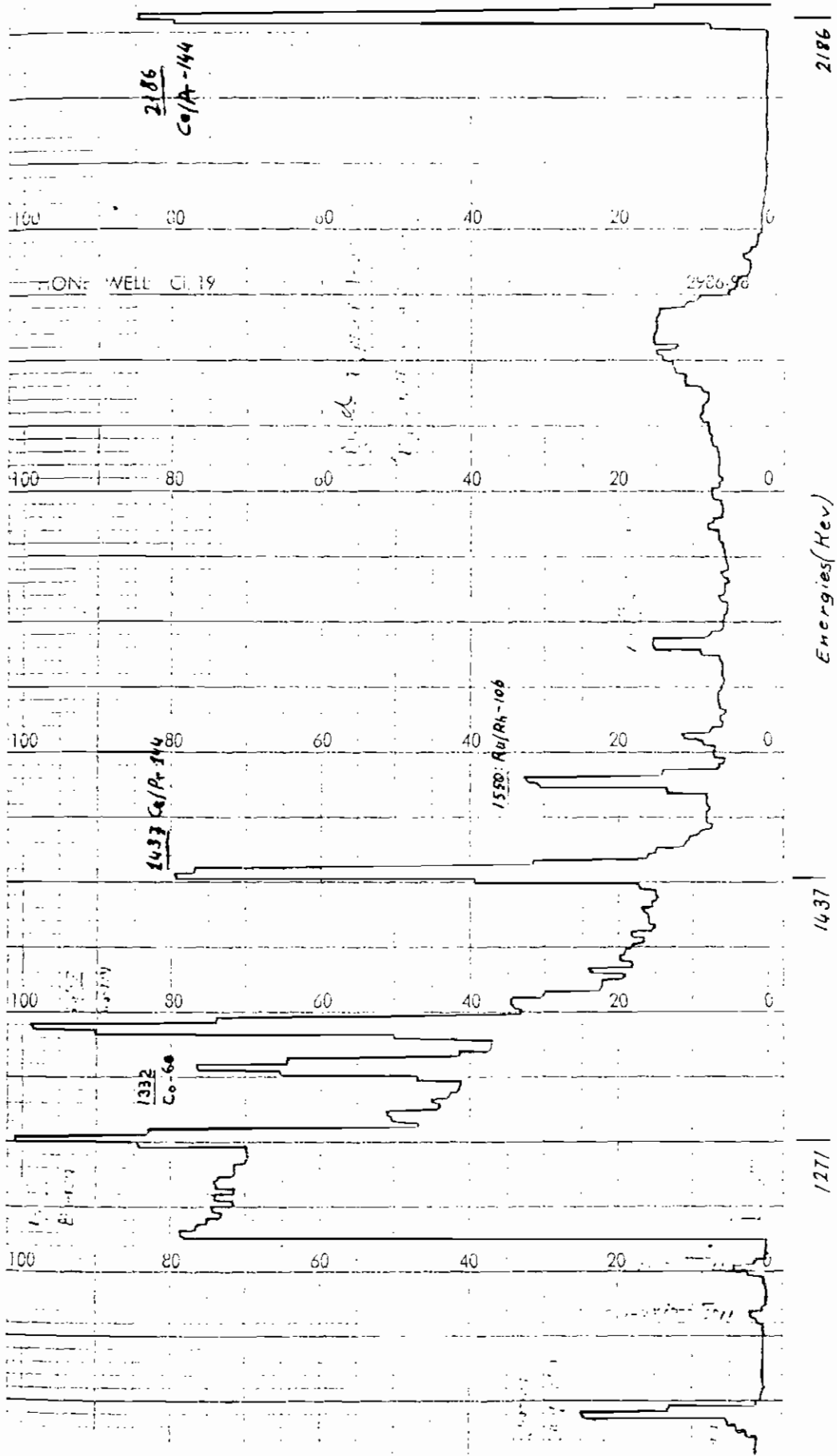


FIG. 5-3 b - TYPICAL GAMMA SPECTRUM OBTAINED AT LEVEL "C"

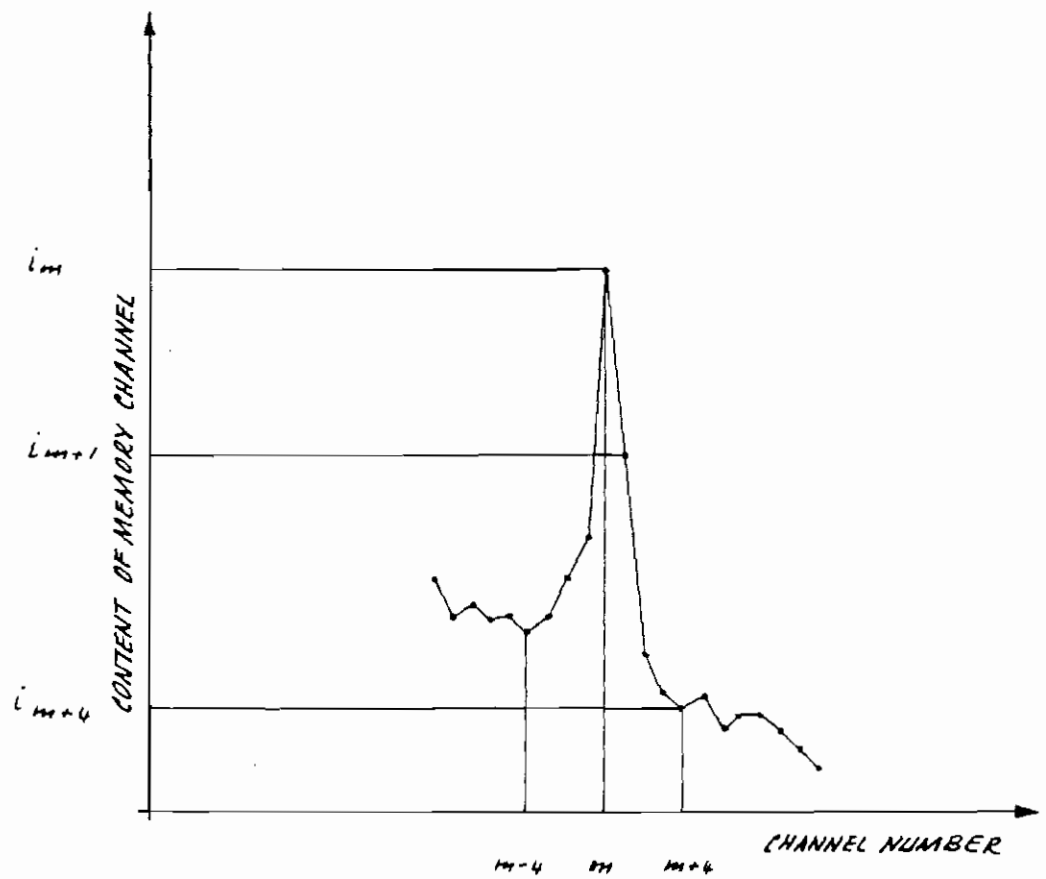


FIG. 5-4 - PEAK AREA ASSESSMENT

where:

i = memory channel content

m = channel index corresponding to the maximum value of the peak.

Tables 5-1 and 5-II list, for all the examined rods and for the two levels C and D, the measured activity values for the selected isotopes, namely, Ru-106/Rh-106; Cs-137, and Ce-144/Pr-144.

### 5.1.2 Precision of the measurements

During the measurements, a number of experiments were carried out for the dual purpose of developing a gamma-spectrometry technique and of evaluating the precision of the resulting data. One of these experiments consisted in establishing the effect of non-isotropic irradiation of the rod such as will generate a fission product distribution in the fuel which is not in circular geometry.

For this purpose, before beginning the measurements proper, the activity of Ru-106/Rh-106 was determined at the same level on one rod; since this isotope has the lowest peak energy (512 keV), it is the most sensitive to the rod self-shielding effect. It was observed that the deviation of the results was on the order of 5%, so that it was decided that the rods should be rotated manually during the measurements.

The reproducibility of the measurements was then checked by repeating the measurements on two rods (E-1 and E-5) several times on different days. The results for the three selected peaks are given in Table 5-III together with the experimental standard deviations ( $\sigma_{\text{exp}}$ ) and the theoretical statistical errors ( $\sigma_t$ ). It will be noted in this table that the theoretical statistical error for the measurement of Cs-137 activity (0.2%) is only a small fraction of the total error (1.8%). A larger contribution, though difficult to evaluate, is given by the error in positioning the rod in front of the collimator and by the probable displacement of the pellets or part of them inside the rod. To assess the magnitude of these errors



Table 5-I

Activities measured at level C

Rod	Counts, cps		
	(Ru/Rh) (★) 512 keV	Cs 662 keV	(Ce/Pr) (★) 2186 keV
A-1	75.12	164.90	1.453
B-1	67.08	148.29	1.357
C-1	60.43	158.59	1.388
D-1	63.08	159.29	1.465
E-1	64.36	164.15	1.470
J-1	92.45	196.24	1.661
A-2	63.17	146.33	1.339
B-2	60.66	159.68	1.435
C-2	55.61	148.30	1.352
D-2	55.69	143.65	1.306
H-2	68.50	179.60	1.586
A-3	61.23	158.14	1.424
B-3	56.16	146.55	1.356
C-3	53.23	141.37	1.302
D-3	52.99	139.24	1.286
E-3	54.17	139.43	1.240
A-4	61.72	160.16	1.455
D-4	50.48	131.67	1.209
A-5	66.38	165.99	1.549
C-5	55.55	143.77	1.322
E-5	43.03	112.82	0.996
B-6	61.80	157.38	1.412
D-6	53.94	142.98	1.278
C-7	59.41	155.26	1.416
D-7	47.45	124.71	0.861
G-7	62.21	160.87	1.459
A-8	95.11	187.15	1.636
B-8	72.03	185.16	1.716
H-8	74.50	190.79	1.680
A-9	102.98	214.39	1.827
B-9	88.27	185.92	1.638
C-9	81.02	201.91	1.842
D-9	79.77	191.18	1.827
J-9	88.19	175.51	1.533

(★) Counts referred to November 18, 1968

Table 5-II

Activities measured at level D

Rod	Counts, cps		
	(Ru/Rh) (★) 512 keV	Cs 662 keV	(Ce/Pr) (★) 2186 keV
A-1	37.69	94.48	0.774
B-1	35.30	96.12	0.815
C-1	32.54	101.75	0.856
D-1	32.05	101.03	0.839
E-1	33.41	96.56	0.785
J-1	46.48	119.68	0.989
A-2	33.71	92.84	0.744
B-2	30.35	98.10	0.796
C-2	28.05	89.50	0.707
D-2	27.76	89.04	0.736
H-2	33.05	106.11	0.882
A-3	31.74	99.65	0.731
B-3	28.04	89.21	0.785
C-3	28.26	88.57	9.717
D-3	25.73	83.11	0.647
E-3	26.20	82.35	0.648
A-4	30.83	96.81	0.794
D-4	25.58	81.28	0.657
A-5	32.59	100.51	0.827
C-5	26.12	82.31	0.667
E-5	25.26	78.70	0.654
B-6	27.96	89.22	0.705
D-6	26.59	81.51	0.671
C-7	28.10	89.72	0.735
D-7	27.81	85.74	0.688
G-7	29.74	92.20	0.749
A-8	41.72	109.01	0.893
B-8	34.62	110.70	0.915
H-8	36.18	114.74	0.940
A-9	49.57	125.45	0.958
B-9	44.39	11.12	0.914
C-9	39.32	118.97	1.032
D-9	37.70	113.46	0.936
J-9	51.44	123.17	1.011

(★) Counts referred to January 10, 1969

Table 5 -III

Total reproducibility measurements

	Date	Ru/Rh (512 keV)	Cs-137 (662 keV)	Ce/Pr (2186 keV)
Rod E 1/Level D	17/1/69	33.75	100.45	0.867
	21/1/69	34.48	96.81	0.748
	7/2/69	28.95	92.45	0.769
	7/2/69	31.05	93.92	0.795
	10/2/69	31.43	96.43	0.708
	Average	31.93	96.01	0.787
	$\sigma_{\text{exp}}$ %	6.95	3.19	6.30
$\sigma_t$ %	1.0	0.2	2.1	
Rod E 5 Bottom	15/11/68	80.52	168.61	1.549
	21/11/68	79.31	172.83	1.568
	25/11/68	75.98	166.10	1.466
	27/11/68	77.31	166.81	1.610
	3/12/68	78.92	166.18	1.546
	3/12/68	76.58	165.33	1.552
	3/12/68	77.08	164.95	1.556
	10/12/68	77.01	163.62	1.520
	Average	77.83	166.83	1.545
	$\sigma_{\text{exp}}$ %	2.00	1.80	2.60
$\sigma_t$ %	0.5	0.2	1.7	

it was decided that at least five rods should be given a "fine" axial gamma scan around a fixed position; the rods selected for this purpose were A-1, B-2, D-4, E-5 and J-9.

A gross gamma scan was started at level D, taken as a central datum, while the rod was moved in steps of 2 mm in either direction in order to cover a length equal to the height of a pellet. In addition, at each point, four measurements were taken at 90-degree angles around the rod. The errors of these measurements are given in Table 5-IV.

An examination of this table will reveal that the variation in the counts is generally on the order of 2% except for the case of rod A-1. For this rod, one must suppose that an axial dishomogeneity was present at level D.

Finally, from an analysis of the shape of the peaks it was observed that some of them presented an abnormal widening, which would appear to indicate instability in the counting chain. On the basis of this observation, the results relating to the following rods were considered of dubious reliability:

level C: E-5, D-7, J-9

level D: A-3, D-3, E-5, A-9.

## 5.2 Axial gamma scanning on rods A-1 and E-5

An axial gamma scanning was also carried out along the whole length of rods A-1 and E-5 for which both halves (bottom and top) were available. For this purpose a continuous advancing system was used and the individual activity of the selected isotopes was recorded. The rods were moved slowly and steadily in front of the slit by means of a motor-driven dolly; it should be noted that during the measurements it was not possible to ensure perfect constancy in speed.

Figures 5-5 and 5-6 give the normalized values of the activities of Ru-106/Rh-106 (512), Cs-137 (662) and Ce-144/Pr-144 (2186).

The two charts clearly show the diversity between the axial distribution of the corner rod (upwards tendency) and that of the central rod (tendency

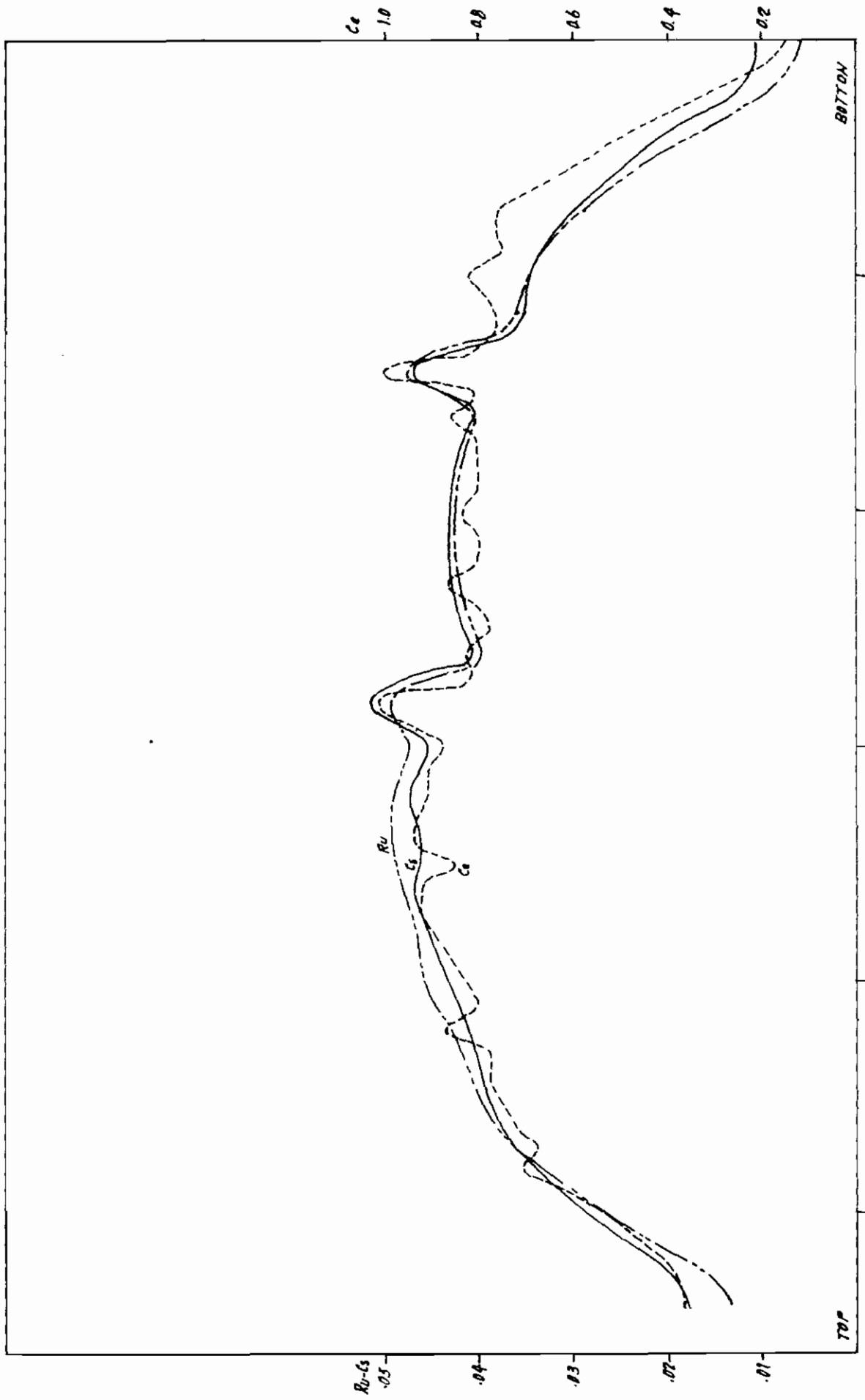


FIG. 5-5 AXIAL ACTIVITY DISTRIBUTION OF Ru(512), Cs(662) AND Co(2186) PEAKS IN ROD A-1

FIG. 5-5 AXIAL ACTIVITY DISTRIBUTION OF  $Ru(512)$ ,  $Cs(662)$  AND  $Co(2186)$  PEAKS IN ROD A-1

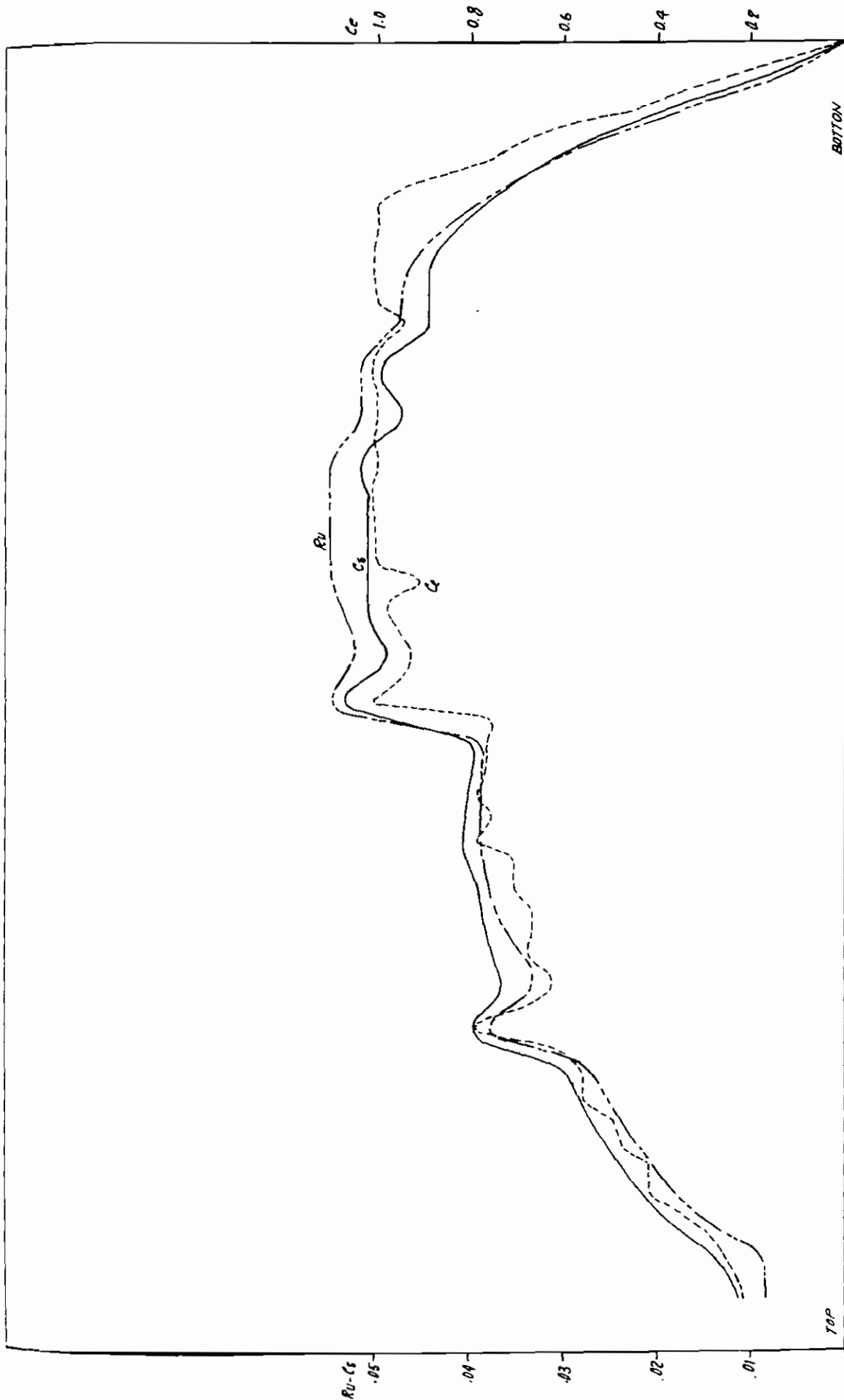


FIG. 5-6 AXIAL ACTIVITY DISTRIBUTION OF  $Ru(512)$ ,  $Cs(662)$  AND  $Co(2186)$  PEAKS IN ROD E-5

Table 5-IV

"Fine" axial gamma scan around level D

Rod	Average m (counts)	$\sigma$ %
A1	114970	13.1
A1'	118838	9.1
B2	101033	1.9
B2'	101480	1.3
D4	81711	1.8
D4'	82067	0.9
E5	80506	3.3
E5'	81333	1.4
J9	157351	2.3

Note: The primed values refer to the averages from which values exceeding the average by more than  $3 \sigma$  were discarded.

to shift toward the bottom of the core). This diversity is due to the combined effect of the voids and control rods.

The peaks due to the presence of the end connectors are fairly well identifiable in the reduced diagrams. On the contrary, some of the finer characteristics are visible only on the original recordings, on a wider scale. On these, for instance, it is possible to see the depressions due to the surfaces separating two adjacent pellets; in some points the depressions are so marked as to suggest the possibility that the whole pellet stack is separated. This is possible, at least in the case of the top half-rods where no spring is provided to compress the pellets together, but only a sleeve to ensure a plenum for collection of the fission gases. Thus, it is possible that there may be a few millimeters' clearance. The only way to avoid this trouble would have been to handle the rod in its normal position, that is, vertical.

### 5.3 Destructive gamma spectrometry

At the beginning of the destructive measurement program it was decided to take advantage of the availability of dissolved fuel slices to check the burnup level by determining the specific activity of some of the fission products in the fuel. Therefore, a portion of each solution was subjected to gamma spectrometry with an absolute-calibrated system. The solutions were diluted sufficiently to be handled outside the glove boxes and to avoid the use of shields.

The measured fission product isotopes were: Ru-106/Rh-106, Cs-137, Cs-134 and Ce-144/Pr-144, that is, the same isotopes selected for the non-destructive analyses plus Cs-134. The activity of the latter isotope can be correlated with the neutron flux to which the fuel was exposed<sup>(6)</sup>. For the same reasons given in Paragraph 5.1, although the experimental data are listed in this report, use was made only of the Cs-137 results. Once the specific activity of Cs-137 (defined as Cs-137 activity per gram of fuel) is known, it is possible to derive the burn-up by means of a conversion factor that takes into account the characteristics of this fission product and the reactor history.



Gamma spectrometry was performed on part of the solution prepared for the heavy-isotope analysis (Paragraph 5.3).

The sample was subjected to counting with the Ge-Li detector and multi-channels analyzer, as described in Appendix 2. The absolute efficiency of the monitoring counting system had been calibrated with standard sources over the desired range of energy.

Preliminary measurements were made to ascertain whether one sample of each solution was giving accurate results. For this purpose three samples of one gram each were counted with the same technique in respect of the 512 and 662 keV peaks. Since the observed experimental deviation (see Appendix 2) was very close to the statistical one, it was decided that only one sample should be used.

#### 5.3.1 Data processing

The measured spectra were processed in the same manner as described in Paragraph 4.1.1 by means of a similar formula to take into account the Compton effect and background, in peak integration. The resulting counting rate (cps) was corrected for decay since reactor shutdown (May 7, 1967).

For the calculation of the specific activity (Ci/g), the following formula for each selected isotope was employed:

$$A_i = \frac{S_i}{E_i} \cdot e^{\lambda_i T} \frac{R_i}{QPD_i} \frac{10^4}{3.7 \times 10^{10}} \quad (2)$$

where:

$i$  = isotope considered

$A_i$  = specific activity (Ci/g) at reactor shutdown (7 May 1967)

$S_i$  = counting rate of sample (cps), net of background and Compton effect

- $E_i$  = counting efficiency in percent
- $\lambda_i$  = decay constant ( $\text{sec}^{-1}$ )
- T = time lapse between 7 May 1967 and date of measurement ( $\text{sec}^{-1}$ )
- $R_i$  = self-absorption factor
- Q = weight of sample, (g)
- P = fuel concentration in the solution, (g/g)
- D = branching ratio, (%)

Table 5-V gives the parameters selected for the four isotopes with relevant references, and Table 5-VI lists the calculated values of specific activity (Ci/g) as of 7 May 1967.

Table 5-V

Parameters selected to calculate the fission product specific activity ( $C_i/g$ )

Isotope	Energy keV	$E_i$ %	$R_i$	$D_i$ %	$(T \frac{1}{2})_i$
Ru-106/Rh-106 <sup>(7)(8)</sup>	512	0.0958	1.063	20.5	368 d
Cs-137 <sup>(9)</sup>	662	0.0646	1.056	85.1	30.60 y
Cs-134 <sup>(10)</sup>	796	0.0510	1.050	97.0	2.04 y
Ce-144/Pr-144 <sup>(8)</sup>	2186	0.0140	1.080	0.73	284 d

Table 5 - VI

Specific activities of solutions (Ci/g)

Rod	Ru-106	Cs-137	Cs-134	Ce-144
A-1	0.146	0.0330	0.0218	0.291
A-3	0.111	0.0325	0.0191	0.308
A-5	0.119	0.0336	0.0210	0.296
A-9	0.203	0.0432	0.0343	0.343
B 1	0.126	0.0300	0.0187	0.272
B-2	0.104	0.0313	0.0186	0.284
B-8	0.135	0.0376	0.0242	0.316
C-1	0.118	0.0328	0.0203	0.288
C-3	0.102	0.0282	0.0163	0.260
D-2	0.102	0.0292	0.0172	0.262
D-4	0.098	0.0276	0.0160	0.251
E-1	0.137	0.0328	0.0213	0.297
E-5	0.096	0.0276	0.0164	0.245
G-7	0.122	0.0316	0.0195	0.286
H 2	0.130	0.0359	0.0238	0.306
H-8	0.129	0.0379	0.0252	0.320
J-1	0.167	0.0402	0.0205	0.343
J-9	0.204	0.0439	0.0352	0.358

5.3.2 Precision of the measurements

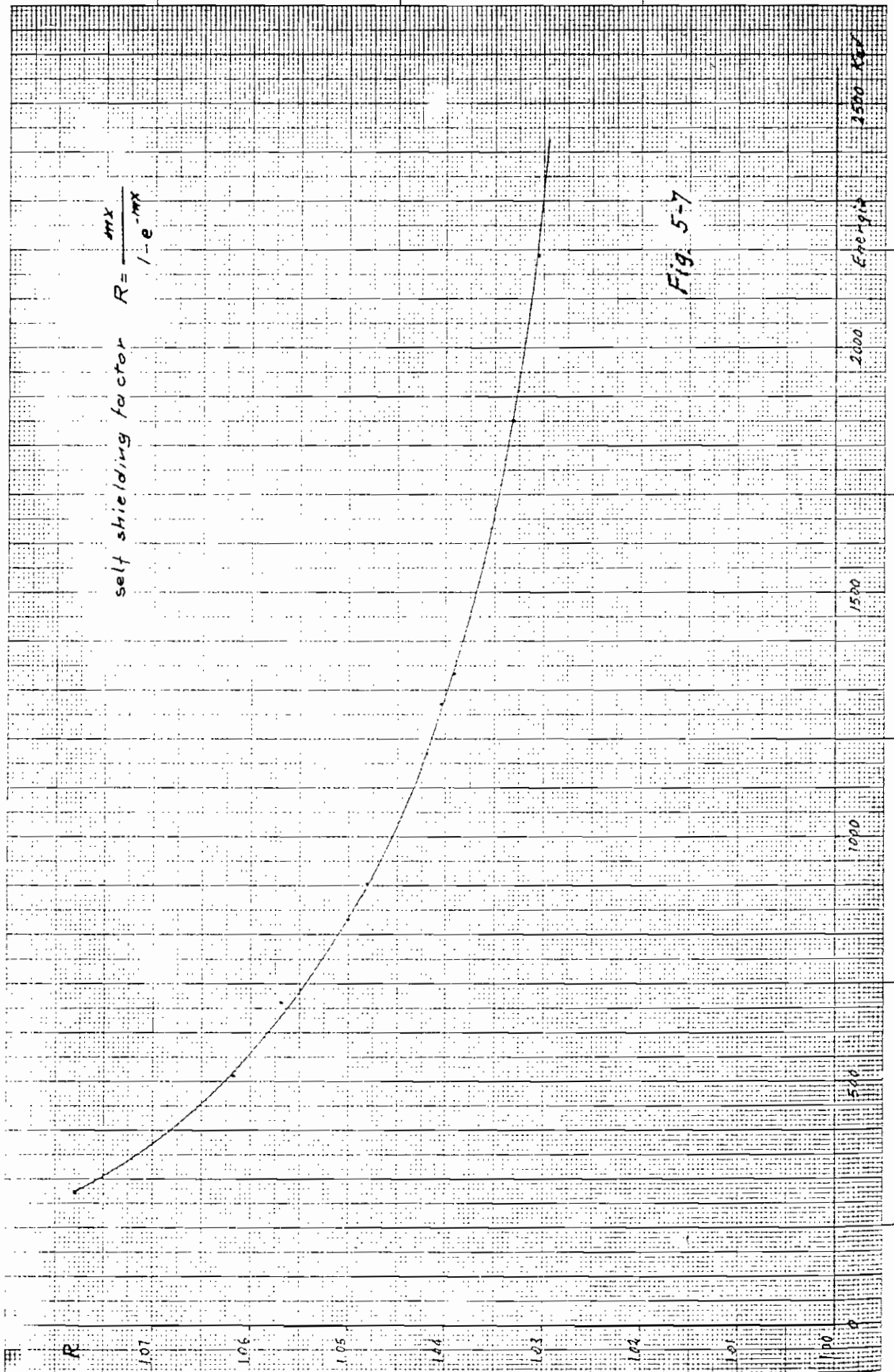
Since the parameters in the formula used for the calculation of the specific activity are multiplicative, the total coefficient of variation is the square root of the sum of each squared coefficient. Table 5-VII lists these values, calculated as explained below, for the four isotopes considered:

Table 5-VII  
Standard deviations % (o)

Isotope	Counting	Efficiency	Self-absorption	Concentration	Weight	Branching ratio	Total
Ru-106/Rh-106	1	2	0.4	0.1	0.1	5	5.49
Cs-137	0.3	2	0.4	0.1	0.1	0.5	2.12
Cs-134	1.2	2	0.4	0.1	0.1	2	3.10
Ce-144/Pr-144	1.3	2	0.4	0.1	0.1	5	5.55

The values in this table were obtained on the basis of the following considerations:

- (a) the error in integrating the peaks was calculated according to the formula in Appendix 2;
- (b) the error in efficiency (about 2%) includes the standard source error indicated by IAEA (abt 1%), the statistical counting error (0.3%) and the source positioning error (0.5%);
- (c) the uncertainty of the self-absorption coefficient can be assessed from the chart in Fig. 5-7, in which the deviation between the experimental values and the best-fit curve is about 0.4%;
- (d) the error in concentration (P) and weight (Q) is given by the precision of the weighing method, that is, on the order of 1 mg/g,
- (e) the error of the branching ratio is the largest; in fact, published branching ratios differ greatly and are affected by great errors.



### 5.3.3 Burn-up determination from Cs-137 activity

The method (see Appendix 2) is based on the calculation of the fissions occurred in the fuel by measuring the specific activity of Cs-137 deriving the number of Cs-137 atoms present and dividing by its fractional fission yield. Since the Cs-137 fission yield varies slightly with the fissile isotopes, an appropriate average was taken. The number of fissions was then converted into burn-up expressed in MWd/MTU, by multiplying by an energy transformation constant.

For the purpose of these calculations the following equation was derived:

$$B = K \frac{A \bar{T}}{\bar{Y}_{\text{Cs-137}} \sum (1 - e^{-\lambda T_i}) e^{-\lambda \tau_i}} \quad (3)$$

where:

- K = energy transformation constant
- A = Cs-137 specific activity (Ci/g)
- $\bar{T}$  = total time of residence in the reactor (days)
- $\bar{Y}_{\text{Cs-137}}$  = average Cs-137 fission yield (%)
- $\lambda$  = Cs-137 decay constant (days<sup>-1</sup>)
- $T_i$  = time of irradiation for any i-th period (days)
- $\tau_i$  = time of decay since any i-th period to the end of irradiation (days).

By using all the numerical values discussed in Appendix 2, the equation 3 is reduced to:

$$B = 3.086 \cdot 10^5 \cdot A \quad (4)$$

which permits the burn-up in MWd/MTU to be derived from the Cs-137 specific activity in Ci/g.

For the eighteen rods examined at level C, the burn-up so calculated is given in Table A.2-III of Appendix 2.

#### 5.4 Analysis of heavy isotopes

In order to determine the conversion of uranium atoms inside the fuel assembly, the abundance of heavy isotopes was measured by destructive analyses.

By means of isotope dilution and mass spectrometry techniques, the abundance were determined for all uranium and plutonium isotopes except Pu-238. This isotope, together with americium and curium isotopes, was analyzed by means of the alpha spectrometry technique.

The analyses have been performed in glove-boxes on diluted samples of about 0.2 mg of fuel per gram of solution.

##### 5.4.1 Mass spectrometry

The concentrations of U-235, U-236, U-238, Pu-239, Pu-240, Pu-241 and Pu-242 were determined by mass spectrometry combined with isotopic dilution techniques (11). For this purpose uranium and plutonium were separated from interfering material by washing the solution with 8 molar nitric acid and excessive uranium was removed from a single sample to get about the same quantities of uranium and plutonium (12). The techniques are described extensively in Appendix 3.

For isotopic dilution the U-233 and Pu-242 spikes were used after double calibration against standards of the National Bureau of Standards (N.B.S., U.S.A.). The results of the calibration were:

Spike	Calibration
Pu-242	$31.449 \cdot 10^{14}$ atoms per gram of solution $\pm$ 0.3%
U-233	$30.578 \cdot 10^{17}$ atoms per gram of solution $\pm$ 0.34%

These values were corrected for mass discrimination of the mass spectrometer as determined by N.B.S. standards (0.01% per mass unit).

Each mass spectrometry measurement was generally performed three times, only in a few cases it could be taken only twice. The experimental error, expressed as deviation from the mean value for a single analysis, are given in Appendix 4. On the average, the error is close to the calibration error.

### 5.4.2 Alpha spectrometry

Without any further chemical treatment, a portion of the dissolved sample containing about 0.01 mg of U was dropped onto a counting plate, and an alpha spectrum was taken. The alpha decay energies partly overlap, so that only the activity ratios (Pu-238 + Am-241)/(Pu-239+Pu-240), Cm-242/(Pu-239+Pu-240) and Cm-244/(Pu-239+Pu-240) can be determined. By measuring the (Pu-239+Pu-240)/Pu-238 activity ratio in the sample separate for mass spectrometry, and by use of the ratio Pu-239/Pu-240 determined by mass spectrometry, the concentration of the single nuclide can be computed.

The accuracy of the method is about 2-5%.

The technique used is described in Appendix 3.

### 5.4.3 Data processing

To compare the experimental data of the isotope analysis with the calculated values, they were related to the initial amount of the fuel. Use was made of the ratio of each heavy isotope  $N_i$  to the total of heavy isotopes  $N_i^0$  before irradiation, i.e. all initial uranium atoms. In this case the reduction of the measured data does not rely on any pre-irradiation data, as is clearly shown in the following equation:

$$\frac{N_i}{\sum N_i^0} = \frac{R_i}{\sum R_i + \sum \Delta} \quad (5)$$

where:

$R_i$  = is the ratio of each isotope to the post-irradiation amount of U-238 (i=U-234, U-235, U-236, U-237, U-238, Pu-238, Pu-239, Pu-240, Pu-241, Pu-242, Am-241, Am-242, Am-243, Cm-242, Cm-243, Cm-244)

$\sum \Delta$  = is the ratio of fissioned nuclides to the post-irradiation amount of U-238, that follows from the Nd-148 analyses.

The substitution of  $N_i$  and  $R_i$  is a simplification of the analysis where only the relative isotopic abundances are determined (see Appendix 3).

The results of the uranium and plutonium isotopes content are summarized in Table 5-VIII, while the radiometric and mass spectrometric measurement data are collected in Appendix 4.



TABLE 5-VIII  
Results of  $F_T$  determination and of the contents of uranium and plutonium isotopes

Sample	$F_T$ a/o	Uranium				Plutonium				$F_T \frac{\sum N_i}{\sum N_i^0}$
		$\frac{235}{\sum N_i^0}$	$\frac{236}{\sum N_i^0}$	$\frac{238}{\sum N_i^0}$	$\frac{238}{\sum N_i^0} \times 10^{-3}$	$\frac{239}{\sum N_i^0} \times 10^{-3}$	$\frac{240}{\sum N_i^0} \times 10^{-3}$	$\frac{241}{\sum N_i^0} \times 10^{-3}$	$\frac{242}{\sum N_i^0} \times 10^{-3}$	
A. 1	1.126	0.00777	0.00161	0.9739	0.01860	3.725	1.117	0.4394	0.0861	0.99993
A. 3	1.118	0.01235	0.00187	0.9693	0.01751	3.884	0.919	0.3722	0.0544	0.99995
A. 5	1.128	0.01185	0.00173	0.9697	0.01586	3.977	0.935	0.3847	0.0555	0.99993
A. 9	1.499	0.00555	0.00184	0.9720	0.02669	3.439	1.420	0.5496	0.1649	0.99998
B. 1	1.046	0.00851	0.00142	0.9742	0.01864	3.859	1.010	0.4030	0.0676	0.99995
B. 2	1.094	0.01231	0.00189	0.9696	0.01701	3.857	0.879	0.3506	0.0494	0.99989
B. 8	1.293	0.01050	0.00199	0.9693	0.02004	3.685	1.064	0.4036	0.0735	0.99997
C. 1	1.138	0.01225	0.00188	0.9692	0.01774	3.929	0.919	0.3761	0.0561	1.00001
C. 3	0.972	0.01348	0.00168	0.9697	0.01332	4.148	0.807	0.3360	0.0384	0.99992
D. 2	1.008	0.01297	0.00173	0.9698	0.01427	4.028	0.809	0.3383	0.0411	0.99981
D. 4	0.941	0.01332	0.00172	0.9701	0.01691	4.181	0.764	0.3311	0.0364	0.99988
E. 1	1.153	0.01204	0.00190	0.9690	0.01739	4.058	0.934	0.3909	0.0559	0.99993
E. 5	0.950	0.01335	0.00164	0.9701	0.01780	4.221	0.770	0.3336	0.0359	0.99997
G. 7	1.121	0.01199	0.00183	0.9693	0.01890	4.167	0.941	0.3894	0.0542	0.99990
H. 2	1.273	0.01096	0.00195	0.9690	0.01892	3.820	1.028	0.4130	0.0693	0.99999
H. 8	1.351	0.01036	0.00200	0.9685	0.02047	3.855	1.133	0.4360	0.0827	0.99990
J. 1	1.370	0.00631	0.00180	0.9725	0.02900	3.663	1.324	0.5497	0.1407	1.00002
J. 9	1.542	0.00541	0.00191	0.9714	0.03246	3.518	1.474	0.5840	0.1820	0.99993

### 5.5. Nd-148 analyses

The burn-up determination by means of the stable fission product Nd-148 has established advantages as a burn-up monitor over the other radioactive fission products (13). Again the isotopic dilution technique using a Nd-150 spike was applied. Chemical separation of neodymium is based on the selectivity of its complex with  $\alpha$ -hydroxyisobutyric acid on cation ion exchangers and is discussed extensively in Appendix 3. The unavoidable contamination of the sample by natural neodymium can be determined and corrected for by using the non-fission product Nd-142 as a monitor.

The determination of percent burn-up  $F_T$ , expressed as heavy atoms burnt per initial heavy atom, was calculated from the following equation (see Appendix 3):

$$F_T (\%) = \frac{R_{148}/Y_{148}}{\sum R_i + R_{148}/Y_{148}} \cdot 100 \quad (6)$$

where  $Y_{148}$  is the fission yield of Nd-148. A value of 1.695% was taken for  $F_T$  determination (see Paragraph 5.5.1 below).

The results of  $F_T(\%)$  are given in Table 5-VIII.

#### 5.5.1 Accuracy of $F_T$ derived from Nd-148 analyses

The calibration of the Nd-150 spike was performed against a natural neodymium standard which was supplied by the Central Bureau of Nuclear Measurement - Geel, Euratom. The error in calibration of Nd-150 is 0.6%.

Each analysis was performed at least twice. The error of a single analysis is given in Appendix 5 and on the average it is close to spike calibration error.

The Nd-148 fission yield was taken as the average between the values relevant to U-235 and Pu-239. From reference 14, these values are:

$$U-235 = 1.69 \pm 0.01\%$$

$$Pu-239 = 1.70 \pm 0.03\%$$

In the determination of burn-up as  $F_T$ , the error in fission yields prevails over all other errors and limits the accuracy of the burn-up analysis to about 1.5%.

## 6. DISCUSSION OF RESULTS

The results obtained can be divided into two categories: burn-up and isotopic composition data. Burn-up data were obtained with at least three different techniques; the relevant results were first compared with one another to evaluate the spread of experimental values. A correlation between the results of the destructive and non-destructive analysis was then developed in order to obtain the burn-up for the rods subjected only to non-destructive gamma spectrometry. The isotopic content data instead were checked for consistency with correlation criteria developed from additional measurements available. After having estimated the validity of the experimental data, a comparison with the theoretical calculations was performed.

### 6.1 Evaluation of burn-up analysis

For the various rods, the burn-up distribution was determined by non-destructive gamma spectrometry, whereas the irradiation level was determined by destructive techniques from the Cs-137 activity and from the Nd-148 concentration.

From all parallel burn-up analysis carried out it was possible to make a comparison of the burn-up distribution among rods at level C. Therefore, the integration of Cs-137 peak gamma activities (cps) based on the non-destructive measurement, the gamma activities (Ci/g) of Cs-137 in the solutions and the heavy atoms burned  $F_T$  (%) were normalized and compared. The normalization was made for the eighteen rods by referring each single measurement to the total value of that particular type of measurement. This comparison is shown in Table 6-1.

The agreement among these results was satisfactory (less than 2% deviation) and confirmed the discrepancy in some of the values of Cs-137 activity obtained from non-destructive gamma spectrometry (see Paragraph 5.1.2). Since the results for rods E-5 and J-9 showed a large deviation only in comparison with the destructive measurements, the values obtained from

TABLE 6-I  
Comparison of the burn-up distribution obtained  
with three different techniques

Rod	B <sup>1</sup> <sub>rel</sub>	B <sup>2</sup> <sub>rel</sub>	B <sup>3</sup> <sub>rel</sub>	Rod	B <sup>1</sup> <sub>rel</sub>	B <sup>2</sup> <sub>rel</sub>	B <sup>3</sup> <sub>rel</sub>
A-1	0.991	0.982	0.967	D-2	0.863	0.870	0.866
A-3	0.950	0.968	0.960	D-4	0.791	0.822	0.808
A-5	0.997	1.000	0.969	E-1	0.986	0.977	0.990
A-9	1.288	1.287	1.287	E-5	0.688	0.816	0.809
B-1	0.891	0.892	0.898	G-7	0.966	0.941	0.963
B-2	0.959	0.931	0.940	H-2	1.079	1.069	1.093
B-8	1.112	1.119	1.111	H-8	1.146	1.128	1.160
C-1	0.953	0.978	0.977	J-1	1.179	1.196	1.177
C-3	0.849	0.839	0.835	J-9	1.070	1.298	1.314

B<sup>1</sup><sub>rel</sub> from cps of Cs-137

B<sup>2</sup><sub>rel</sub> from Ci/g of Cs-137

B<sup>3</sup><sub>rel</sub> from % FT

$$\sigma \sqrt{(B_{rel}^2 - B_{rel}^1) / B_{rel}^1} = \pm 1.8\%$$

$$\sigma \sqrt{(B_{rel}^3 - B_{rel}^1) / B_{rel}^1} = \pm 1.5\%$$

TABLE 6-II

Comparison between the burn-up values obtained with the two  
destructive techniques based on Cs-137 activity and Nd-148 concentration

Rod	B <sup>1</sup>	B <sup>2</sup>	(B <sup>1</sup> - B <sup>2</sup> ) / B <sup>2</sup> x 100	Rod	B <sup>1</sup>	B <sup>2</sup>	(B <sup>1</sup> - B <sup>2</sup> ) / B <sup>2</sup> x 100
A-1	10,355	10,183	+1.66	C-3	8,939	8,702	+2.65
B-1	9,619	9,252	+3.81	D-4	8,653	8,517	+1.57
C-1	10,465	10,138	+3.12	A-5	10,373	10,369	+0.04
E-1	10,603	10,125	+4.51	E-5	8,736	8,517	+2.51
J-1	12,599	12,403	+1.56	G-7	10,309	9,752	+5.40
B-2	10,060	9,659	+3.98	B-8	11,890	11,597	+2.46
D-2	9,270	9,017	+2.73	H-8	12,424	11,696	+5.86
H-2	11,706	11,081	+5.34	A-9	13,785	13,344	+3.20
A-3	10,281	10,039	+2.35	J-9	14,180	13,547	+4.46

B<sup>1</sup> obtained from FT in MWd/MTU

B<sup>2</sup> obtained from Ci/g of Cs-137 in MWd/MTU

the gamma spectrometry on the two rods were excluded from all the subsequent comparisons.

The rod burn-up obtained from destructive techniques were compared in order to find the relative merits of the two methods. The comparison is shown in Table 6-II. From the examination of these results a systematic deviation of the values will be noted, being the burn-up from Cs-137 activity constantly lower than the corresponding values from  $F_T$ . The calculated standard deviation is  $\pm 3.5\%$ , which is well consistent with the error analysis carried out to evaluate the burn-up obtained from the two different methods.

With the burn-up results at level C it is possible to obtain a correlation with the non-destructive measurements of Cs-137 activity in order to obtain the burn-up of these rods which were submitted only to non-destructive gamma spectrometry. This correlation is presented in Table 6-III for the measurements taken at level C.

A mean correlation factor for sixteen rods (that is, excluding E-5 and J-9) of 64.33 MWd/MTU per cps was applied to the remaining sixteen rods (measured at level C only by non-destructive gamma spectrometry).

The burn-up values which are compared with the theoretical ones derived from the 18 destructive Nd-148 measurements and for the above-mentioned rods from this correlation.

It was not possible to extend the correlation to level D because, owing to the instrumentation replacement (see Para 5.1), the gamma spectrometry results at this level were not comparable with those at level C and no results are available from level D destructive measurements.

## 6.2 Correlations between isotope ratios and burn-up parameters

The formation and burn-up of isotopes exposed to neutron flux are related together and correlations between different isotope ratios can be predicted<sup>(15)</sup> and were experimentally observed<sup>(16,17)</sup>. During this study the correlations were used in the first place to check the consistency of experimental results, but some of the correlations, especially those based on fission gas nuclides, may be of general interest. Their potential will be discussed separately.

TABLE 6-III

Correlation of burn-ups as obtained from  $F_T$  (%)  
with Cs-137 (cps) non-destructive gamma spectrometry

Rod	$F_T$ (%)	B from $F_T$ (MWd/ MTU)	Cs-137 (cps)	$\frac{B}{Cs-137}$	B from Cs-137 (MWd/ MTU)	Rod	Cs-137 (cps)	B from Cs-137 (MWd/ MTU)
A-1	1.126	10,355	164.90	62.796	10,608	D-1	159.29	10,248
B-1	1.046	9,619	148.29	64.866	9,540	A-2	146.33	9,414
C-1	1.138	10,465	158.59	65.988	10,202	C-2	148.30	9,541
E-1	1.153	10,603	164.15	64.593	10,560	B-3	146.55	9,428
J-1	1.370	12,599	196.24	64.202	12,625	D-3	139.24	8,958
B-2	1.094	10,060	159.68	63.001	10,273	E-3	139.43	8,970
D-2	1.008	9,270	143.65	64.532	9,241	A-4	160.16	10,304
H-2	1.273	11,706	179.60	65.178	11,554	C-5	143.77	9,249
A-3	1.118	10,281	158.14	65.012	10,174	B-6	157.38	10,125
C-3	0.972	8,939	141.37	63.231	9,095	D-6	142.98	9,198
D-4	0.941	8,653	131.67	65.717	8,471	C-7	155.26	9,988
A-5	1.128	10,373	165.99	62.492	10,679	D-7	124.71	8,023
G-7	1.121	10,309	160.87	64.083	10,349	A-8	187.15	12,040
B-8	1.293	11,890	185.16	64.215	11,912	B-9	185.92	11,961
H-8	1.351	12,424	190.79	65.119	12,274	C-9	201.91	12,989
A-9	1.499	13,785	214.39	64.299	13,792	D-9	191.18	12,299

mean value 64.333

$\sigma = \pm 1.548\%$

### 6.2.1 Consistency of experimental results

A systematic study of the experimental results revealed several linear correlations, which are illustrated by the following plots. The consistency between independently obtained sets of data is proved by the correlations, too.

In Fig. 6-1 the post-irradiation isotopic ratio  $R_6$ , i. e. U-238/U-235 determined by mass spectrometric analysis, is plotted versus  $F_T$  (a/o), total atom percent burnt as determined by Nd-148 analysis. The observed linear correlation is slightly sensitive to initial U-235 enrichment. This fact explains the deviation for the corner rods for which the initial enrichment was, as already mentioned, lower than in other rods.

The sensitivity to the initial fuel enrichment is also apparent on the plot in Fig. 6-2, in which the  $R_6$  isotopic ratio is correlated to another isotopic ratio  $R_5$  from which the U-235 fractional depletion,  $D_5$ , defined as the ratio  $(U^O-235 - U-235)/U^O-235$ , and the fractional U-235 burn-up, can be deduced.

The consistency of the experimental results for the plutonium isotopic composition is clearly demonstrated by the plot in Fig. 6-3. The Pu-240/Pu-239 atom ratios plotted against the corresponding U-235/U-238 values result in two straight lines depending on the two different fuel enrichments.

The experimental data concerning burn-up parameters can also be correlated to the formation and depletion of selected fission products. We found experimentally that from the fission gas isotopes depleted by neutron capture, the stable Kr-83 isotope is the best to check burn-up parameters. For instance in Figs. 6-4 and 6-5 Kr-83/Kr-86 and Kr-84/Kr-83 atom ratios are plotted versus  $F_T$ ,  $F_5$  and  $D_5$ . In this case the correlations are not sensitive to initial fuel enrichment. Moreover the correlation Kr-84/Kr-83 versus  $D_5$ , shown in Fig. 6-5, can be described by an equation of the type:

$$(U^O-235 - U-235)/U^O-235 = a \text{ Kr-84/Kr-83} - b \quad (6)$$

For the analytical experimental data a least square fit gives for a and b the following values

$$a = 0.94; \quad b = 1.58$$

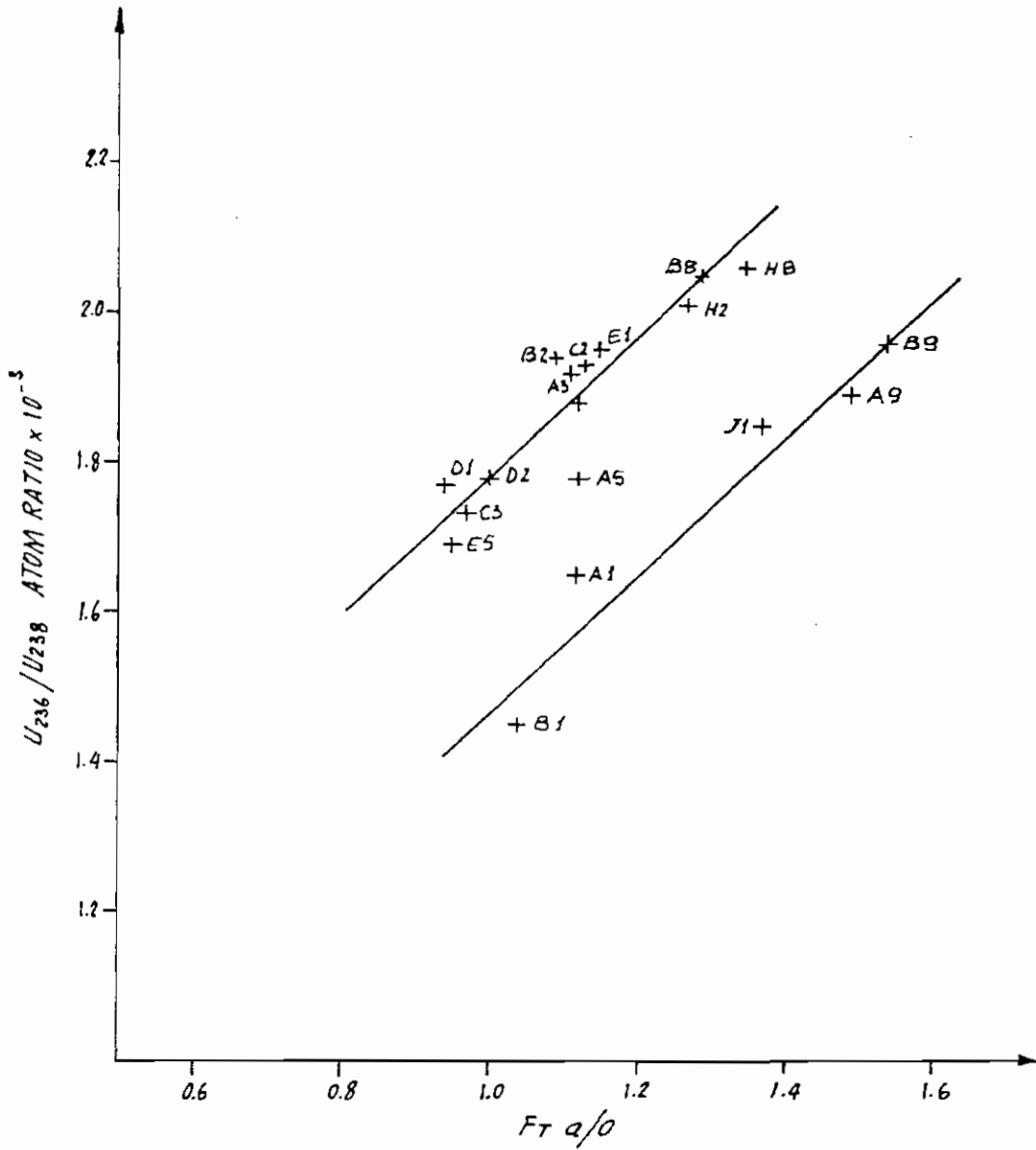


FIG.6-1 CORRELATION BETWEEN  $U_{236}/U_{238}$  AND BURN-UP EXPRESSED AS  $F_T$



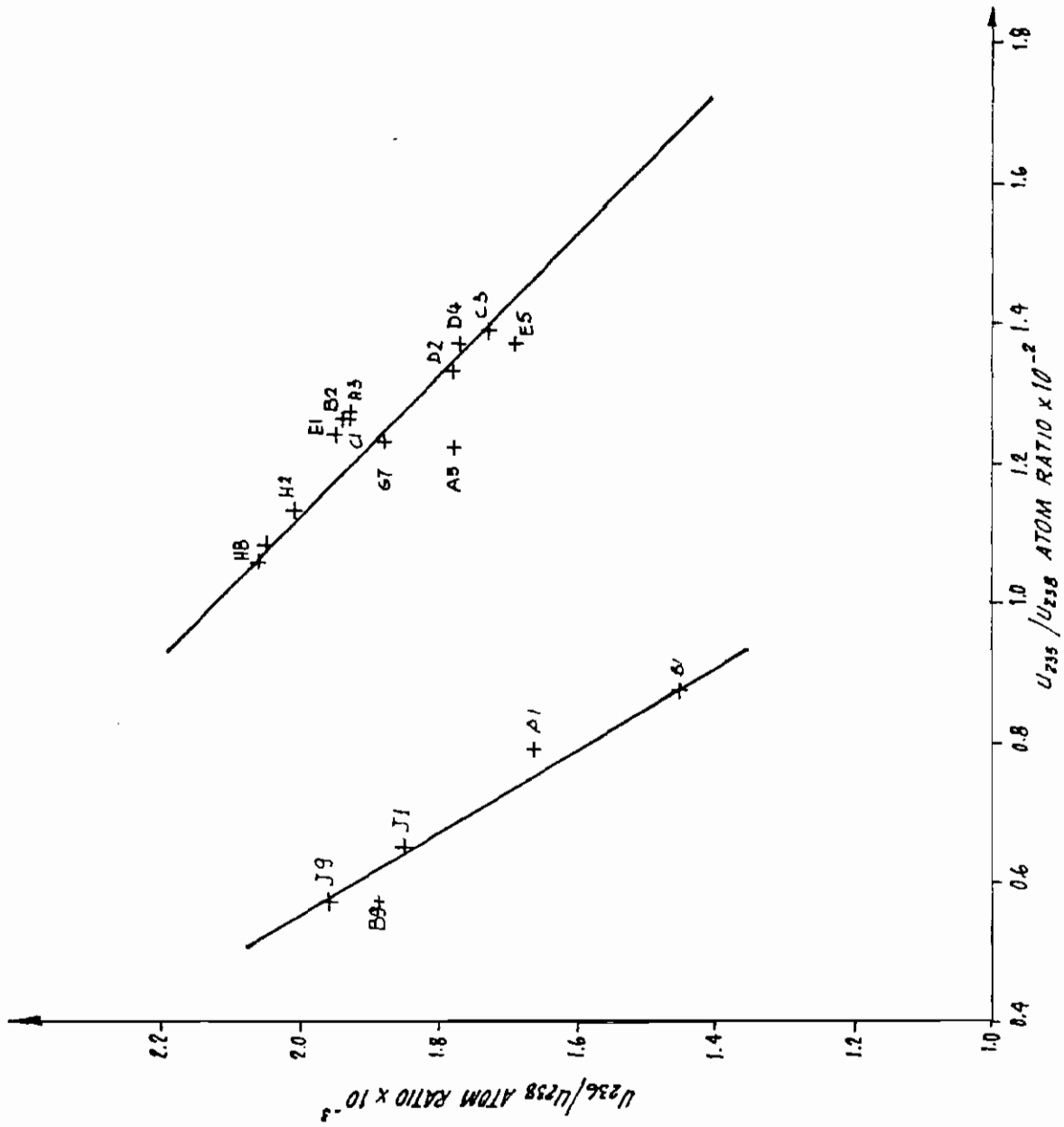


FIG. 6-2 CORRELATION BETWEEN  $U_{236}/U_{238}$  AND  $U_{235}/U_{238}$

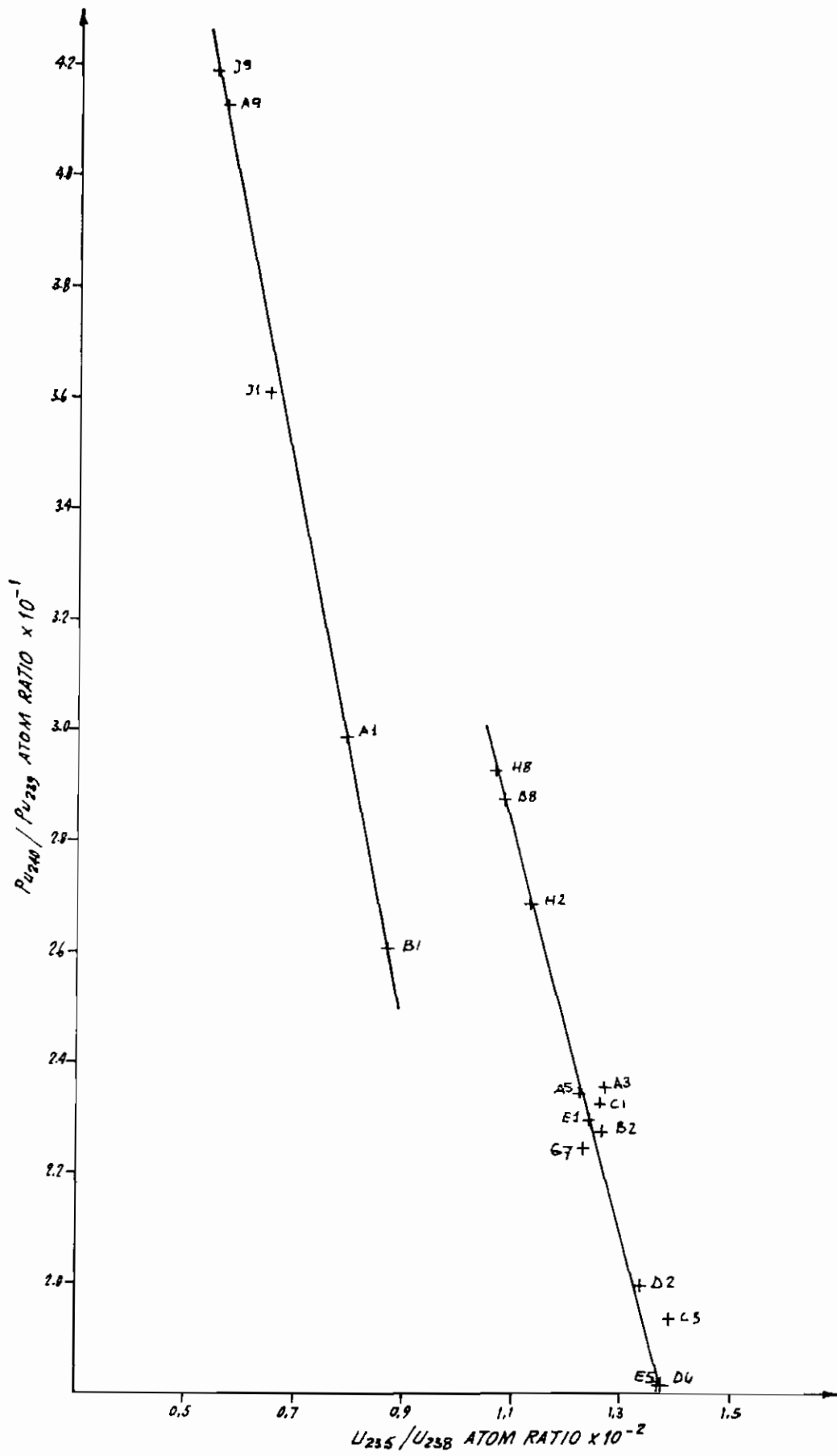


FIG. 6-3 CORRELATION BETWEEN  $Pu_{240}/Pu_{239}$  AND  $U_{235}/U_{238}$

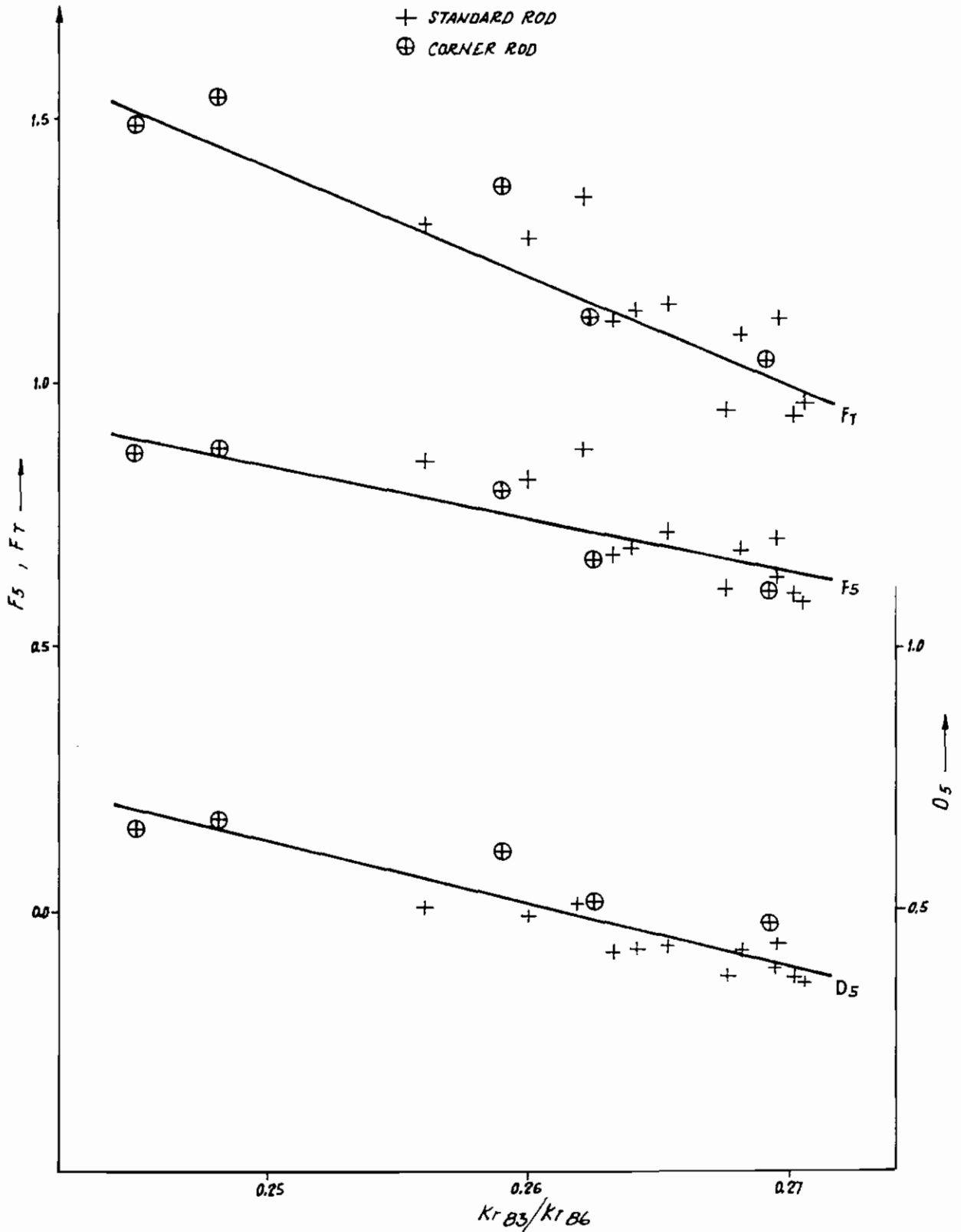


FIG. 6-4 CORRELATION OF  $U_{235}$  ATOMS BURNT ( $F_S$ ), HEAVY ATOMS BURNT ( $F_T$ ), AND FRACTIONAL  $U_{235}$  DEPLETION ( $D_S$ ) VERSUS KRYPTON ISOTOPE RATIO ( $Kr_{83}/Kr_{86}$ )

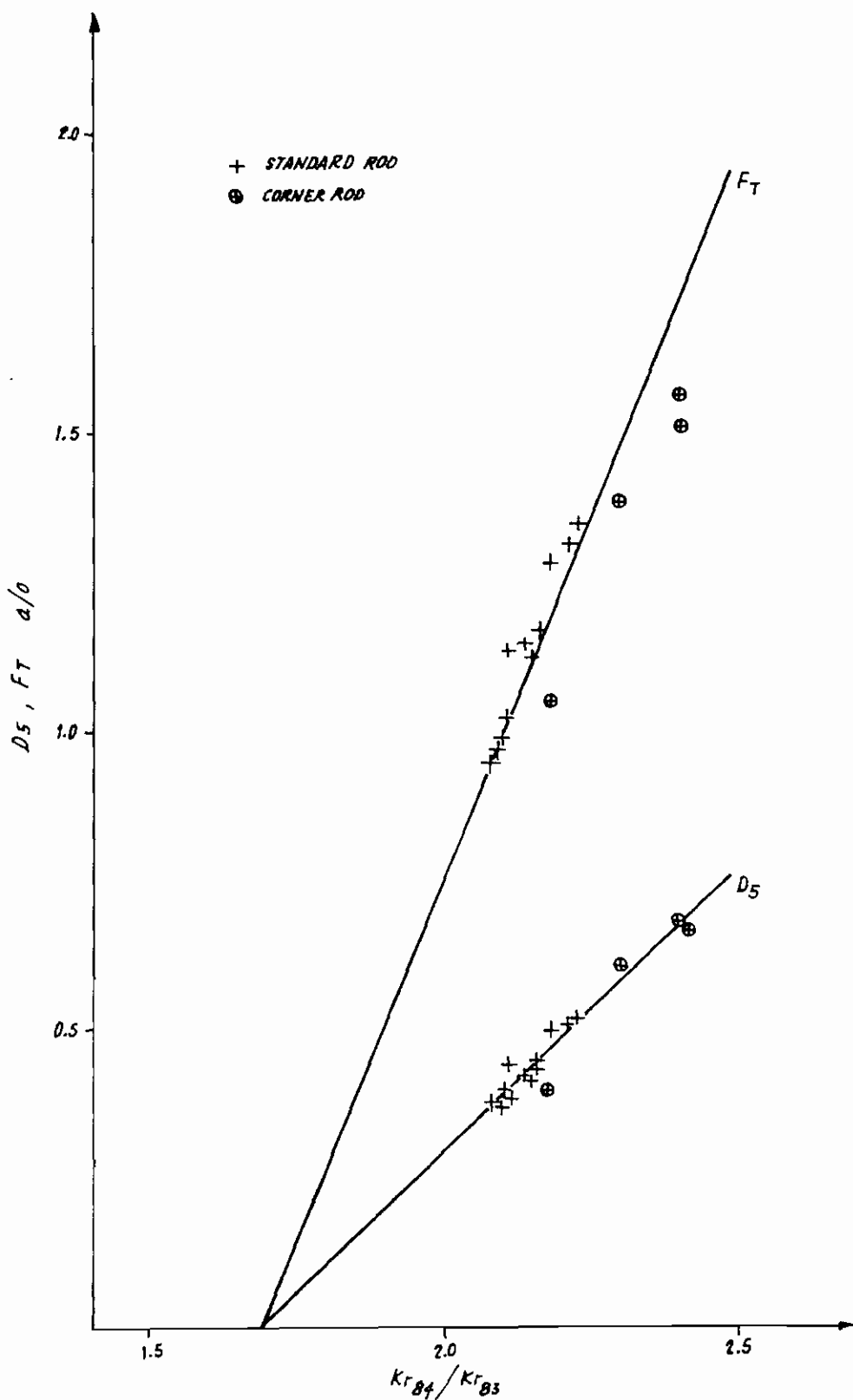


FIG.6-5 CORRELATION OF FRACTIONAL  $U_{235}$  DEPLETION ( $D_5$ ) AND HEAVY ATOMS BURNT ( $F_7$ ) VERSUS KRYPTON ISOTOPE RATIO ( $Kr_{84}/Kr_{83}$ )

From theoretical considerations it derives that the term 1.58 corresponds to the effective fission yield ratio of the two Krypton isotopes. A practical application of correlation (6), for instance, is the possibility of calculating the final amount of U-235, provided the initial one is known.

### 6.2.2 Discussion of correlations

The change of the amount of a nuclide,  $N$ , in a reactor depends on the integrated neutron flux,  $\Phi t$ , and on the neutron energy distribution, which is represented by the effective cross-section,  $\bar{\sigma}$ , for the considered reaction of the nuclide with neutrons. Hence the formation rate of a nuclide,  $dN/dt$ , can be described by:

$$\frac{dN_i}{dt} = \bar{\sigma}_{i-1}^c N_{i-1} \Phi \quad (7)$$

$$\frac{dN_f}{dt} = Y_f N_j \bar{\sigma}_j^f \Phi \quad (8)$$

The differential equation (7) stands for the build-up of a nuclide with a mass  $i-1$  by neutron capture. Equation (8) describes the formation of the fission product,  $N_f$ , with the fission yield,  $Y_f$  ( $\bar{\sigma}^c$  is the effective capture cross-section and  $\bar{\sigma}^f$  is the effective fission cross-section). The depletion rate due to neutron capture of the considered nuclide follows from equation:

$$\frac{dN_i}{dt} = \bar{\sigma}_i^c N_i \Phi \quad (9)$$

For the following discussions it is not necessary to account for the radioactive decay of the nuclides.

The burn-up of the fuel is directly proportional to the formation of fission products (equation 8). The formation and depletion of nuclides (equations 7 and 9) are functions of the neutron flux,  $\Phi$ , just as the burn-up. This may be considered an explanation for the correlations. A thorough explanation in the

frame of this report is impossible; besides it requires additional burn-up calculations.

### 6.3 Comparison between theoretical and experimental data

#### 6.3.1 Burn-up

In Fig. 6.6 are indicated the experimental values of burn-up (E) together with the percent deviations in comparison with theoretical values (T) calculated with two-group BURNY and five-group BURSQUID codes.

The results of the two calculation techniques are well consistent with the experimental data, larger deviations being observed for the two-group BURNY calculation ( $\sigma = \pm 3.1\%$  against  $\pm 1.5\%$ ).

By analyzing the deviations for the two-group BURNY calculation, it will be noted that the greater deviations occur in proximity of the areas where the enrichment differs and that the control rod effect on the corner rod is overrated because of the inadequate representation of the control rod blade intersection (see Para 4).

As for the comparison with the five-group theoretical results, no systematic concentration of the error is observed also because this calculation incorporated the modification relating to the control rod representation referred to in Para 4.

Fig. 6-7 shows the comparison at level D between theoretical data, obtained by two-group BURNY with the modified control rod representation, and the experimental data relating to non-destructive Cs-137 gamma spectrometry. Since no absolute burn-up values for this level are available, the experimental data were expressed normalized in respect of their average. The same method was applied to the theoretical data in order to evaluate the percent deviations between calculated and experimental values. The bias for the corner

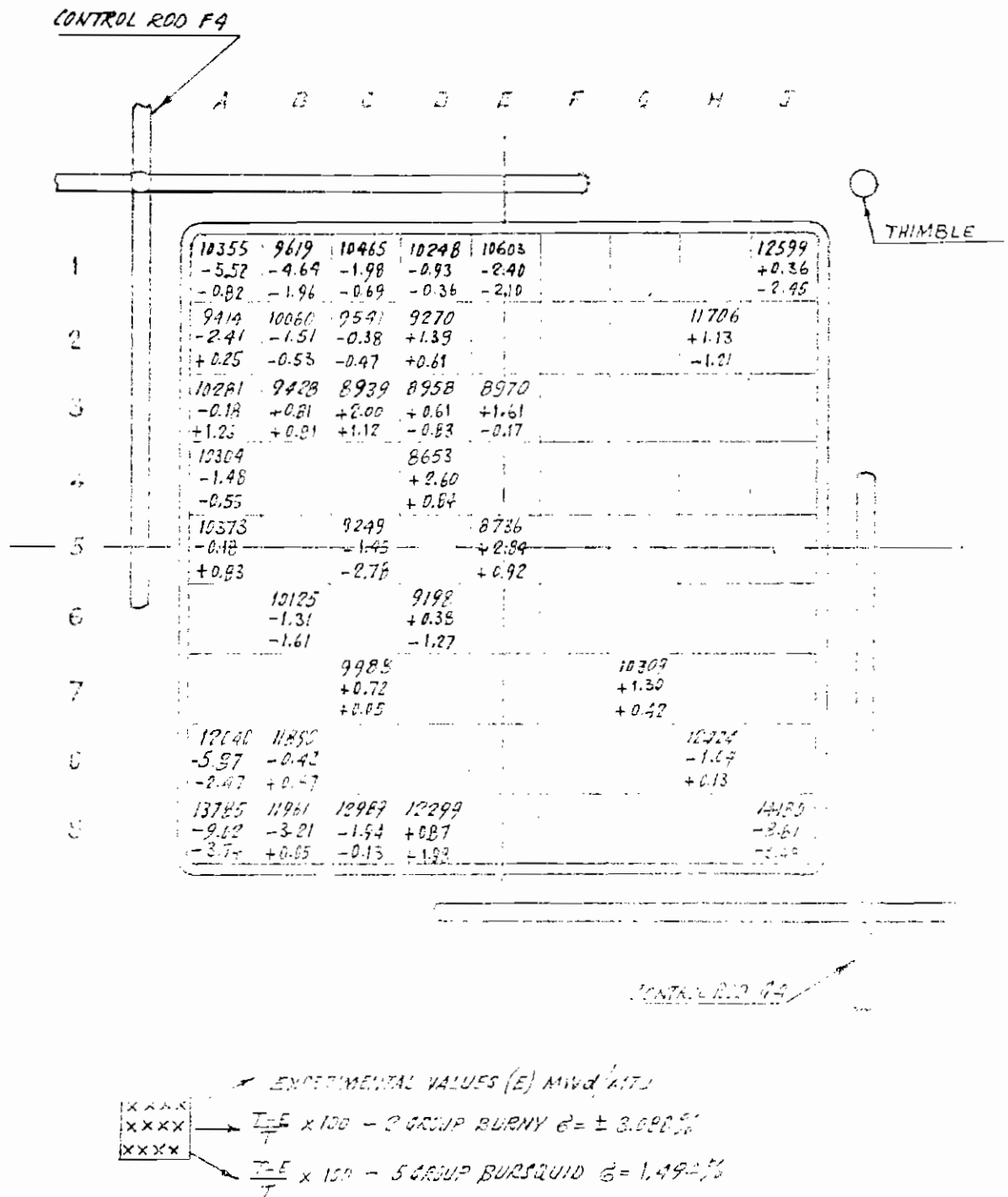
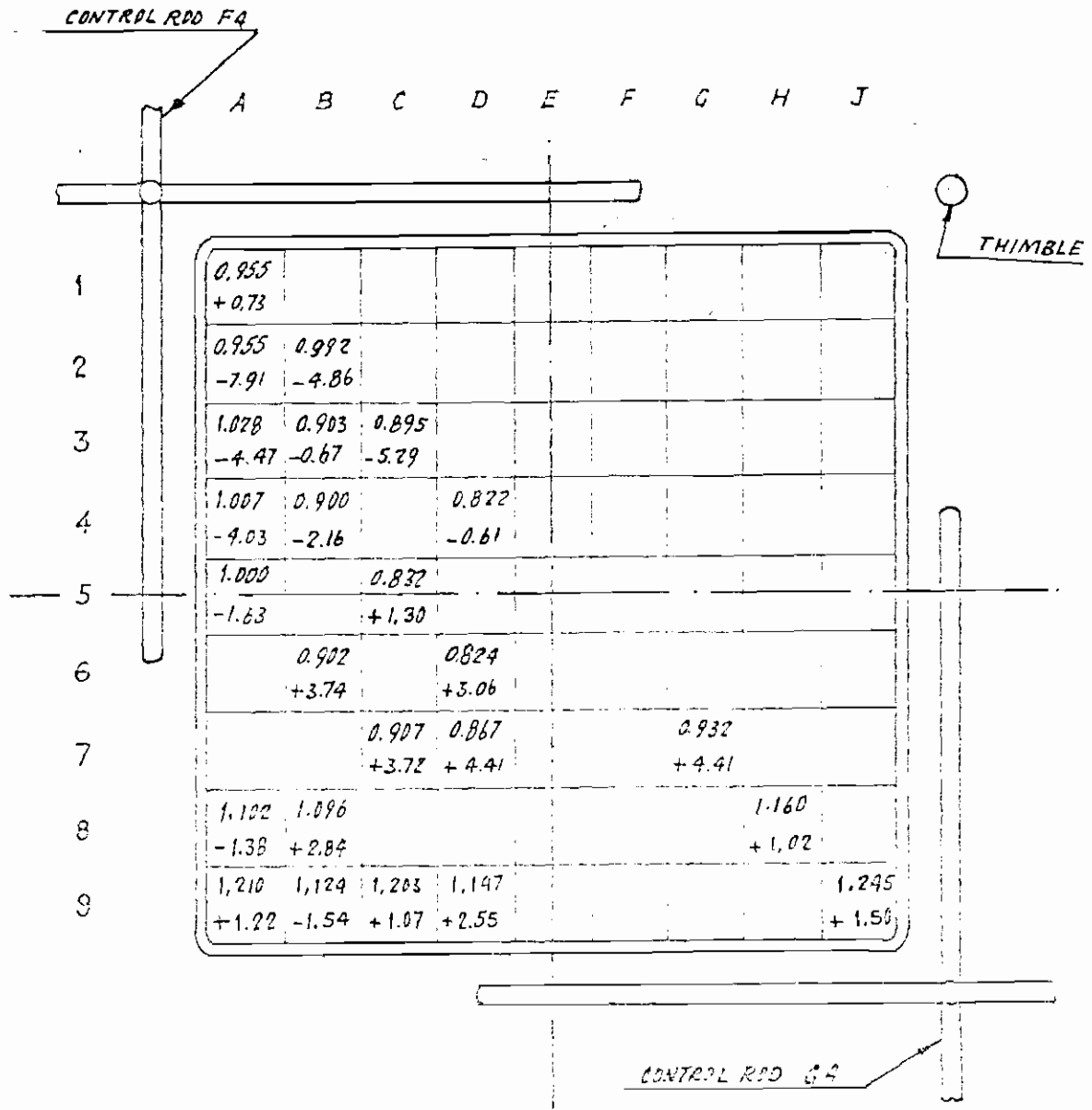


FIG. 6-6 THEORETICAL EXPERIMENTAL COMPARISON OF LEVEL C BURN-UP DATA



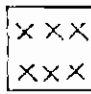

 EXPERIMENTAL VALUES (E) MWd/MTU  
 $\frac{T-E}{T} \times 100 - 2$  GROUP BURNUP  $G = \pm 3.37\%$

FIG. 6-7 THEORETICAL EXPERIMENTAL COMPARISON OF LEVEL D BURN-UP DATA



rods disappeared.

With regard to the peripheral rods facing the black area of the control rod blades, the deviations were greater at level D than at level C. This is probably imputable to the fact that for a certain period of irradiation the terminal part of a control rod was positioned right in front of level D. In the two-dimension irradiation calculation, it was assumed that the control rod was inserted beyond level D throughout the period considered, whilst in practice the effect of the control rod should have been smaller, because that level was actually between a controlled and non-controlled area.

### 6.3.2 Isotopic content

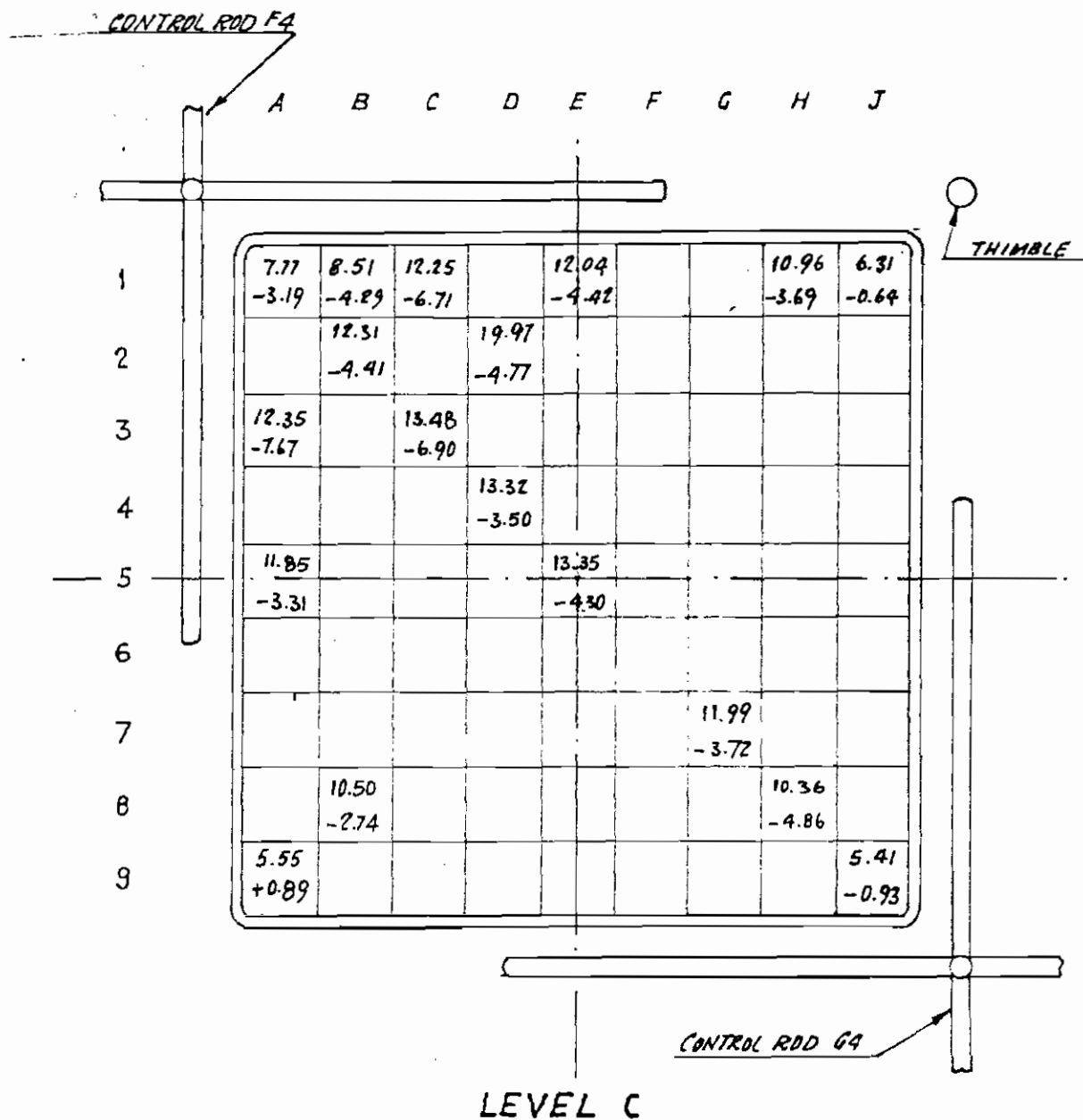
In Figs. 6-8 to 6-14 are collected the results of isotopic abundance measurements as percent of the post-irradiation number of atoms to the initial uranium atoms. These data are compared with the theoretical values calculated by two-group BURNY and five-group BURSQUID codes and reported as percent deviation.

Table 6-IV gives for each isotope the average deviation of the results of the two-group BURNY calculation. The deviations are given as arithmetical averages of  $\frac{T - E}{E} \times 100$  for the uranium isotopes and Pu-239 and Pu-240 where there appears to be a clear systematic error. For Pu-241 and Pu-242 the deviation seems to be erratic, so  $\sigma = \sqrt{\frac{(T-E/T)^2}{N}}$  was calculated.

The two-group BURNY calculation appears unsatisfactory in particular for what concerns Pu-239 concentration which is systematically underestimated by 25% on the average.

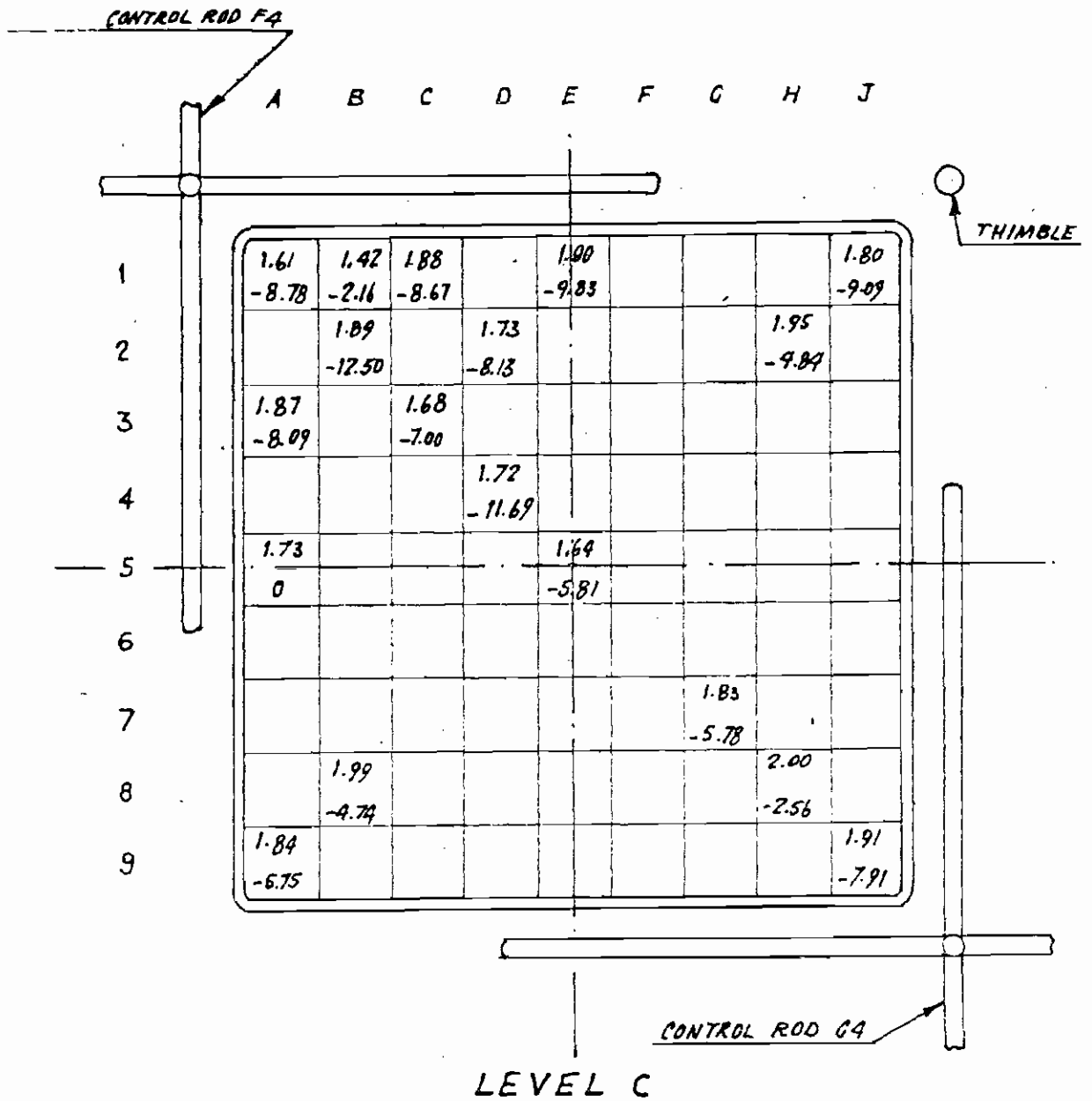
By observing the deviation distribution, it may be noted that the deviations above the average are in correspondence of corner and peripheral rods. From this it may be assumed that the difference is to be imputed to an inadequate representation of the thermal spectrum and to the library data used in BURNY 2.

This consideration seems to be confirmed by the results obtained by BURSQUID, which provides a more adequate representation of the thermal spectrum



XXX → VALUE OF  $U_{235} \times 10^{-3}$  REFERRED TO TOTAL INITIAL URANIUM  
XXX →  $\frac{T-E}{T} \times 100$  - 5 GROUP BURSQUID  $\epsilon = -3.94\%$

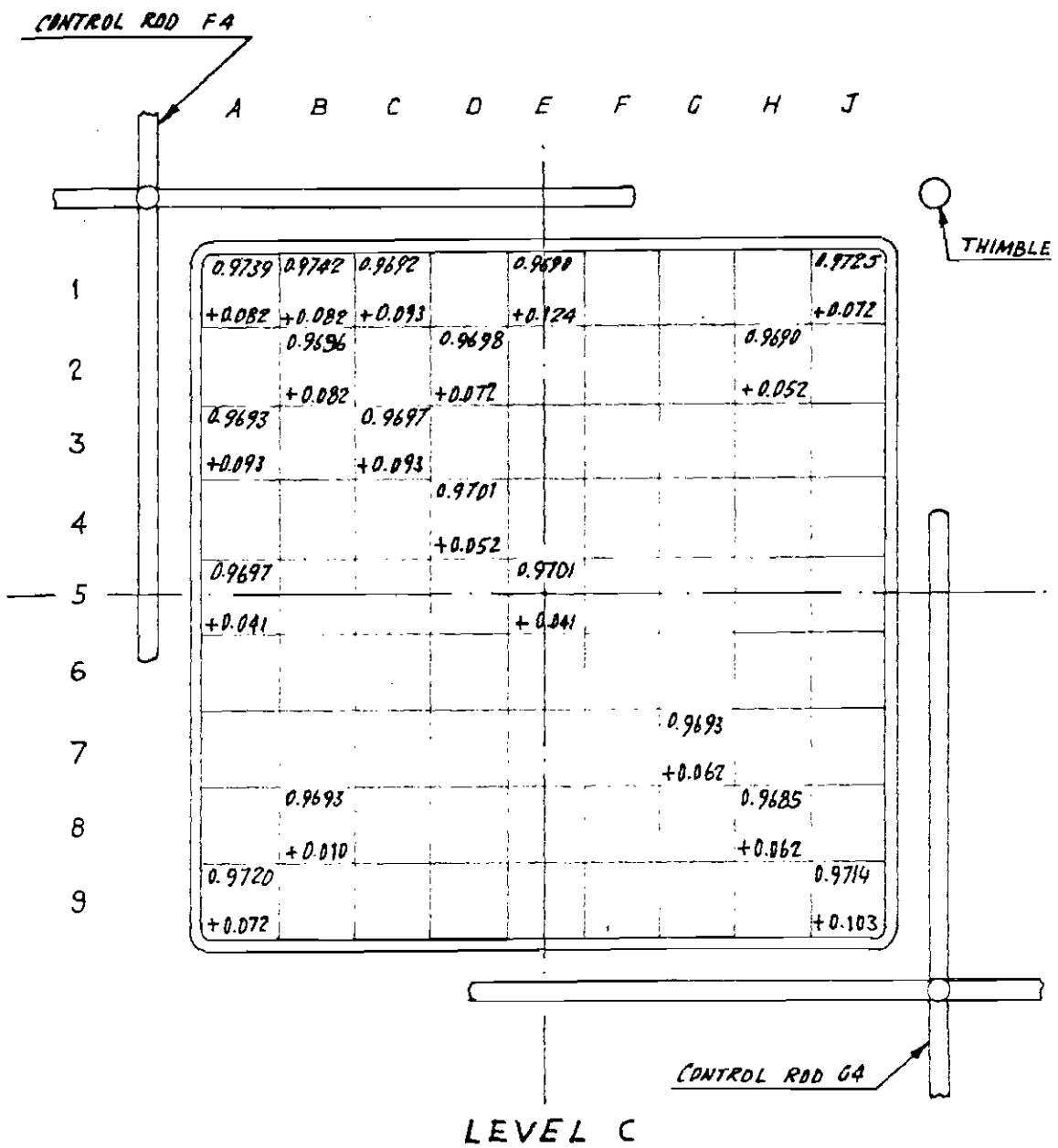
FIG. 6-8 THEORETICAL EXPERIMENTAL COMPARISON OF  $U_{235}$  CONTENT



x x x  
 x x x

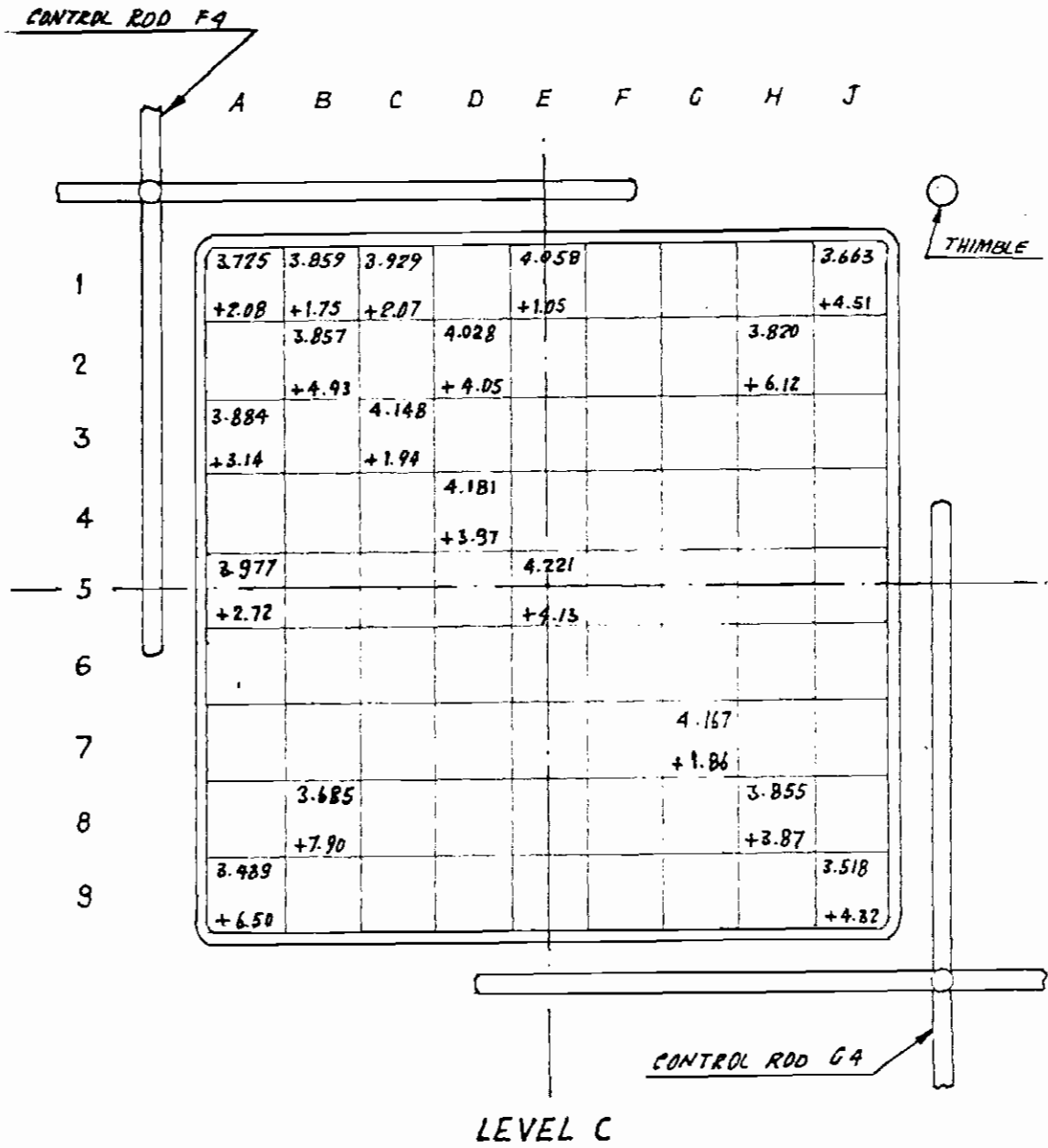
VALUE OF  $U_{236} \times 10^{-3}$  REFERRED TO TOTAL INITIAL URANIUM  
 $\frac{T-E}{T} \times 100$  - 5 GROUP BURSQUID  $\alpha = -6.85\%$

FIG. 6-9 THEORETICAL EXPERIMENTAL COMPARISON OF  $U_{236}$  CONTENT



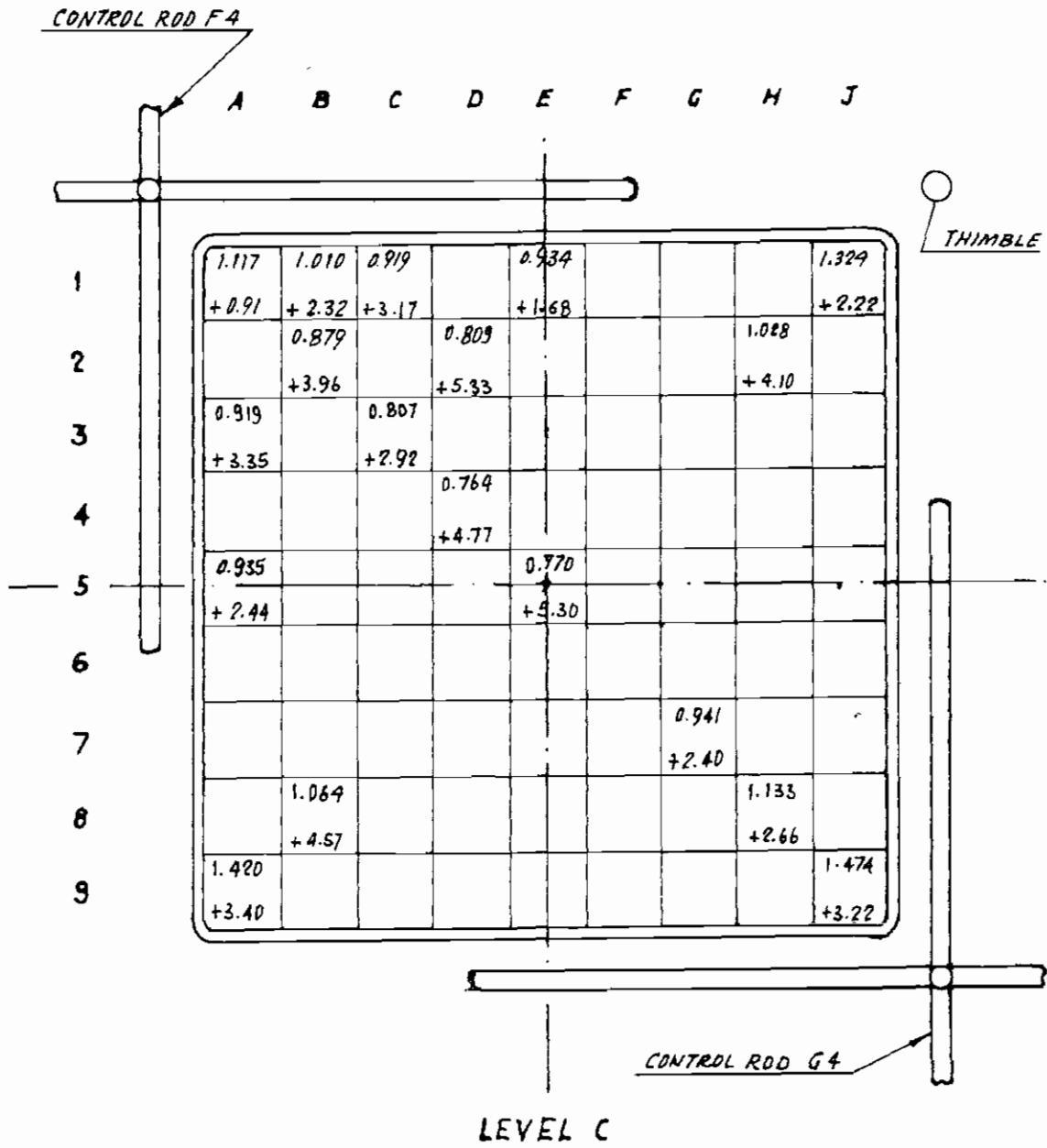
x x x → VALUE OF  $U_{238}$  REFERRED TO TOTAL INITIAL URANIUM  
x x x →  $\frac{T-E}{T} \times 100 - 5$  GROUP BURSQUID  $\epsilon = +0.0716\%$

FIG. 6-10 THEORETICAL EXPERIMENTAL COMPARISON OF  $U_{238}$  CONTENT



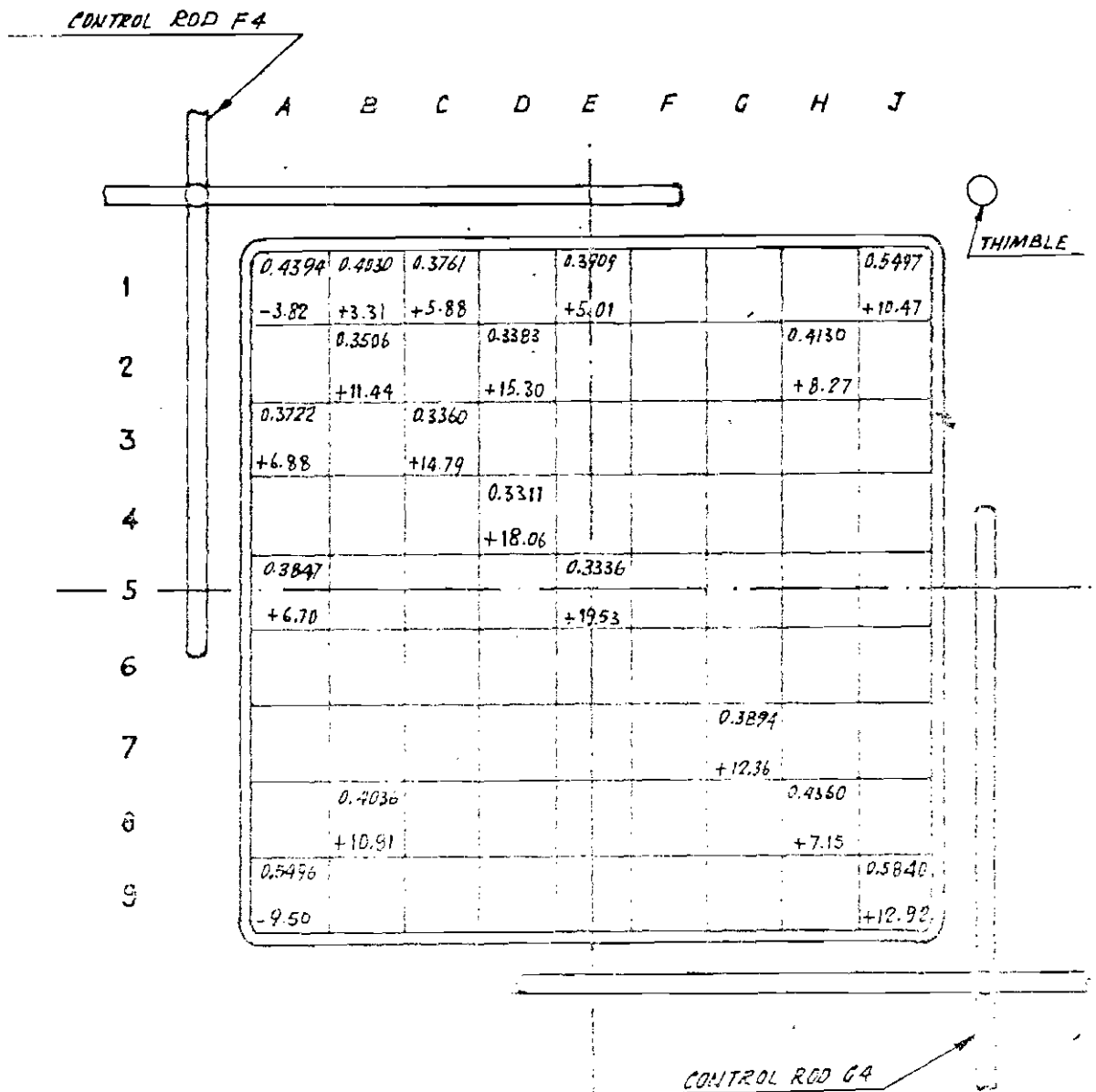
x x x → VALUE OF  $Pu_{239} \times 10^{-3}$  REFERRED TO TOTAL INITIAL URANIUM  
x x x →  $\frac{T-E}{T} \times 100$  - 5 GROUP BURSQUID  $\phi = +3.69\%$

FIG. 6-11 THEORETICAL EXPERIMENTAL COMPARISON OF  $Pu_{239}$  CONTENT



x x x → VALUE OF  $P_{U240} \times 10^{-3}$  REFERRED TO TOTAL INITIAL URANIUM  
x x x →  $\frac{T-E}{T} \times 100$  - 5 GROUP BRURSQUID  $\rho = + 3.26\%$

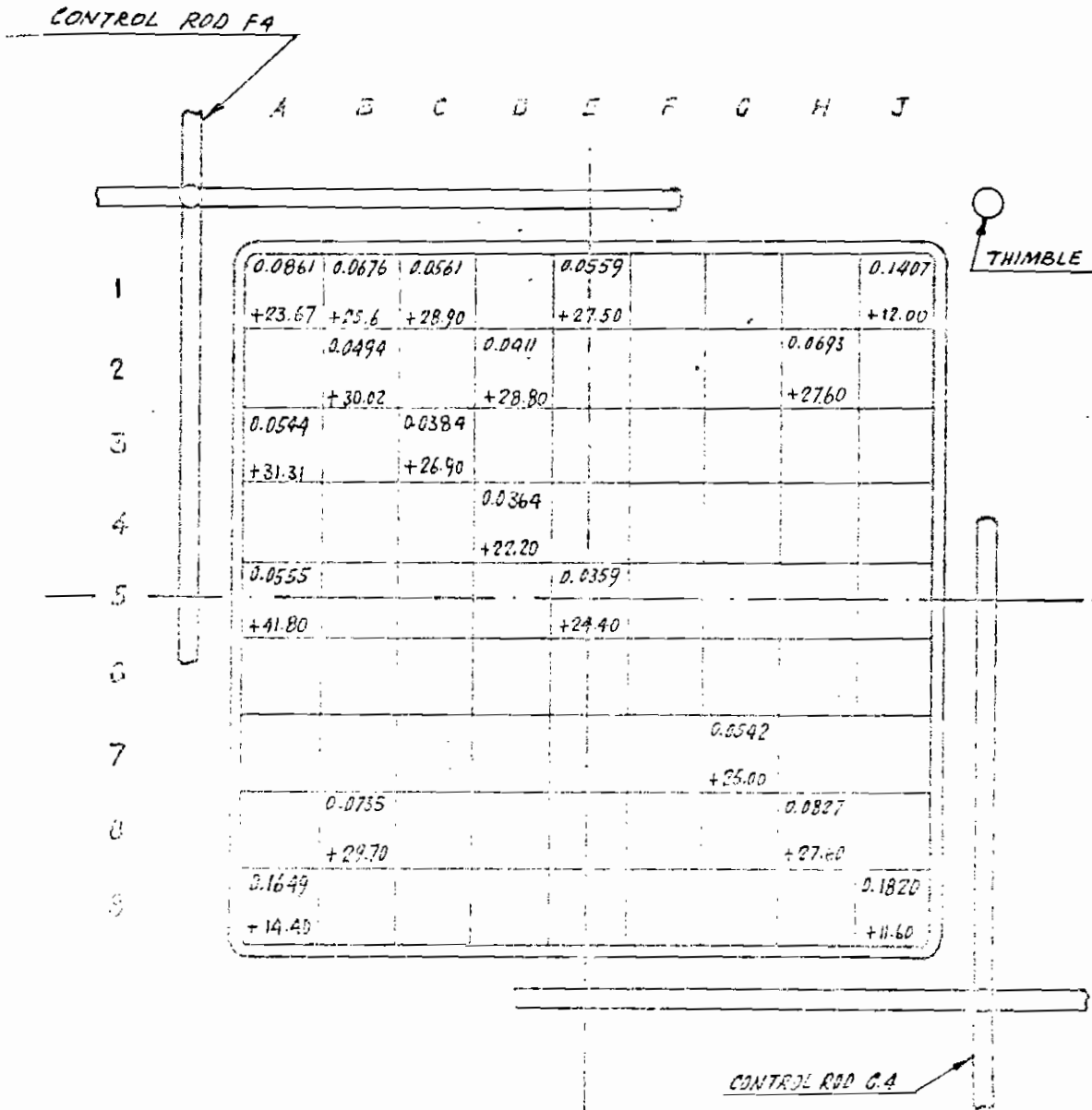
FIG. 6-12 THEORETICAL EXPERIMENTAL COMPARISON OF  $P_{U240}$  CONTENT



LEVEL C

x x x → VALUE OF  $Pu_{241} \times 10^{-3}$  REFERRED TO TOTAL INITIAL URANIUM  
x x x →  $\frac{T-E}{T} \times 100$  -5 GROUP BURSQUID  $\delta = + 10.12\%$

FIG. 6-13 THEORETICAL EXPERIMENTAL COMPARISON OF  $Pu_{241}$  CONTENT



LEVEL C

$\begin{matrix} \times \times \times \\ \times \times \times \end{matrix}$  → VALUE OF  $Pu_{242} \times 10^{-3}$  REFERRED TO TOTAL INITIAL URANIUM  
 $\frac{T-E}{T} \times 100$  - 5 GROUP BURSQUID  $\epsilon = +25.50\%$

FIG. 6-14 THEORETICAL EXPERIMENTAL COMPARISON OF  $Pu_{242}$  CONTENT



TABLE 6 - IV  
Theoretical-Experimental Comparison of Uranium and Plutonium Isotope Content

Sample	A1	A3	A5	A9	B1	B2	B8	C1	C3	D2	D4	E1	E5	G7	H2	H8	J1	J9
U-235 x 10 <sup>-3</sup>	7.70	12.35	11.85	5.55	8.51	12.31	10.50	12.25	13.48	12.97	13.32	12.04	13.35	11.99	10.96	10.36	6.31	5.41
	7.40	11.73	11.68	4.74	8.00	12.02	10.43	11.73	12.67	12.44	12.85	11.68	12.75	11.58	10.43	10.06	5.88	4.58
	-5.00	-5.29	-1.46	-17.09	-6.38	-2.41	-0.67	-4.43	-6.39	-4.26	-3.66	-3.08	-4.71	-3.54	-5.08	-2.98	-7.31	-18.12
U-236 x 10 <sup>-3</sup>	1.61	1.87	1.73	1.84	1.42	1.89	1.99	1.88	1.68	1.73	1.72	1.90	1.64	1.83	1.95	2.00	1.80	1.91
	1.48	1.68	1.69	1.70	1.40	1.64	1.86	1.68	1.56	1.59	1.54	1.69	1.55	1.72	1.86	1.91	1.70	1.72
	-8.78	-11.31	-2.37	-1.63	-1.41	-15.24	-6.99	-11.91	-7.69	-8.80	-11.69	-12.43	-5.81	-6.39	-4.84	-4.71	-5.88	-4.94
U-238	0.9739	0.9693	0.9697	0.9720	0.9742	0.9696	0.9693	0.9692	0.9697	0.9698	0.9701	0.9690	0.9701	0.9693	0.9690	0.9685	0.9725	0.9714
	0.9758	0.9715	0.9714	0.9736	0.9758	0.9715	0.9707	0.9715	0.9715	0.9715	0.9714	0.9714	0.9713	0.9709	0.9707	0.9705	0.9747	0.9735
	+0.19	+0.23	+0.18	+0.16	+0.16	+0.20	+0.14	+0.24	+0.18	+0.17	+0.13	+0.25	+0.12	+0.16	+0.18	+0.21	+0.23	+0.22
Pu-239 x 10 <sup>-3</sup>	3.725	3.884	3.977	3.439	3.859	3.857	3.685	3.929	4.148	4.028	4.181	4.058	4.221	4.167	3.820	3.855	3.663	3.518
	2.866	3.062	3.139	2.665	3.046	3.159	3.007	3.062	3.491	3.404	3.680	3.139	3.739	3.417	3.007	2.993	2.551	2.639
	-29.97	-26.84	-21.07	-29.04	-26.69	-22.10	-18.40	-22.07	-18.82	-18.33	-13.61	-29.28	-12.89	-21.95	-27.04	-28.80	-43.59	-33.31
Pu-240 x 10 <sup>-3</sup>	1.1170	0.9190	0.9350	1.4200	1.0100	0.8790	1.0640	0.9190	0.8070	0.8090	0.7640	0.9340	0.7700	0.9410	1.0280	1.1330	1.3240	1.4740
	1.2182	0.9887	0.9961	1.6063	1.1100	0.9444	1.1491	0.9887	0.8479	0.8815	0.8147	0.9461	0.8235	0.9943	1.1491	1.2022	1.4923	1.6400
	+8.29	+7.05	+6.13	+11.58	+9.01	+6.88	+7.40	+7.05	+4.82	+8.22	+6.22	+6.23	+6.50	+5.36	+10.54	+5.76	+11.28	+10.12
Pu-241 x 10 <sup>-3</sup>	0.4394	0.3722	0.3847	0.5946	0.4030	0.3506	0.4036	0.3761	0.3360	0.3383	0.3311	0.1909	0.3336	0.3894	0.4130	0.4360	0.5497	0.5840
	0.4119	0.3670	0.3806	0.5211	0.4071	0.3661	0.4171	0.3670	0.3745	0.3765	0.3869	0.3806	0.4006	0.4235	0.4171	0.4341	0.4411	0.5253
	-6.68	-1.42	-1.08	-5.47	+1.01	+4.23	+3.24	-2.48	+10.28	+10.15	+14.42	-2.70	+16.65	+8.05	+0.98	-0.44	-24.62	-11.17
Pu-242 x 10 <sup>-3</sup>	0.0861	0.0544	0.0555	0.1649	0.0676	0.0494	0.0735	0.0561	0.0384	0.0411	0.0364	0.0559	0.0359	0.0542	0.0693	0.0827	0.1407	0.1820
	0.0809	0.0533	0.0548	0.1430	0.0702	0.0495	0.0727	0.0533	0.0422	0.0450	0.0405	0.0548	0.0421	0.0577	0.0727	0.0801	0.1212	0.1515
	-6.43	-2.06	-1.28	-15.31	+3.70	+0.20	-1.10	-5.25	+9.00	+8.67	+10.12	-2.01	+14.73	+6.07	+4.68	-3.25	-16.09	-20.10

\* - Values calculated by two-group BURNY

\* Experimental value

\*\* Theoretical value

\*\*\* (T - E/T) x 100

and in addition employs an updated Pu-239 library<sup>(18)</sup>.

Table 6-V compares the average deviations for the two types of calculations and shows a satisfactory agreement between the BURSQUID data and the measured abundances of all isotopes having an average deviation less than 4%, except for Pu-241 (10%) and Pu-242 (25%). There still remains the fact that the errors have a bias; however, no high error concentration is noted for any of the rods.

TABLE 6-V

Comparison between the average deviations obtained with two-group BURNY and five-group BURSQUID calculations

Isotope	$\sigma\% (T - E/T)$	
	Five groups	Two groups
U-235	-3.94	-5.66
U-236	-6.85	-7.38
U-238	+0.072	+0.19
Pu-239	+3.69	-24.66
Pu-240	+3.26	+7.69
Pu-241	+10.12	+8.95
Pu-242	+25.50	+8.53

## 7. CONCLUSIONS

The main objectives of the program, i.e. the determination of the burn-up reached by each rod at given elevations and the determination of the concentration of heavy atoms, were substantially achieved. The resulting data were accurate and representative to permit a conclusive comparison with corresponding calculated data. Another objective achieved was that adequate measurement techniques were established, useful for measurements on fuels of nuclear power stations. These are high resolution gamma spectrometry with solid-state detectors, and mass spectrometry for isotope abundances of uranium, plutonium and neodymium.

Concerning the non-destructive gamma spectrometry technique on single rods, apart from a few initial difficulties, it proved to be relatively quick, simple and easy, and it provides abundant information. The main difficulties were encountered in adjusting the mechanical components in the hot cells and in maintaining the stability of the electronic equipment over long periods. Because of the latter point the time of future measurements should be kept to a minimum. Furthermore, for high resolution Ge-Li detectors it is necessary to work with large multichannel analyzer and therefore it is advisable to use on-line computers for data processing.

Similar considerations apply for the gamma spectrometry of the dissolved samples. This technique, however, can be used to calibrate the non-destructive gamma spectrometry of the rods. In this connection, it should be pointed out that the calibration of the results of non-destructive gamma spectrometry was done with those of Nd-148 mass spectrometric analysis, because the latter turned out to be more precise, although more time-consuming and painstaking. However, the determination of absolute gamma activity takes little effort and provides a fair number of data; it was used to cross-check the burn-up values obtained from Nd-148 concentration measurements and to identify possible experimental errors.

The experimental techniques employed for the destructive analyses proved to be adequate especially as regards the calculation methods used. The major obstacle was the possibility of cross-contamination of different samples. This can occur during the cutting of pellets out of the pins, the drilling of micro-samples, the chemical treatment of samples and the mass spectrometric measurement. In particular for the operations where small samples were to be taken from large amounts of fuel, i. e. microdrilling, mass spectrometry samples, etc., the danger of cross-contamination appeared to be enhanced. Only strict precautionary measures as the use of throw-away equipment, easy decontaminable hardware, etc., can cope with this problem. The techniques themselves are based more or less on known methods with minor changes, which proved to be useful.

The correlation between isotopic ratios and certain reactor parameters developed during this study may become a promising tool in the future. The accuracy demanded from the predictive methods can be met practically with the fission gas correlations. Some future studies will improve this technique, which may result in a sharp reduction of analytical efforts.

By comparing the experimental data with the values calculated according to the technique developed by ENEL, it is possible to obtain useful information for further refinement of the technique itself. First of all, it was possible to ascertain that the burn-up of single rods, including the corner rod and peripheral rods, i. e. rods in "difficult" positions, is well represented by both the two-group BURNY calculations ( $\sigma = \pm 3.1\%$ ) and the five-group BURSQUID calculations ( $\sigma = \pm 1.5\%$ ).

With regard to the isotopic abundance of fissile atoms, it was observed that two-group treatment of the neutron spectrum leads to a systematic under-rating of the plutonium content, particularly Pu-239. On the contrary, five-group treatment with the BURSQUID code, i. e. with the thermal group divided into two parts, gives a better evaluation of the Pu-239 content. This effect has already been noted in the measurements on the DIMPLE critical assembly with

plutonium-bearing fuel <sup>(2)</sup>. More specifically, an evaluation with the five-group BURSQUID improves the Pu-239 and Pu240 representation, but introduces for Pu-241 and Pu-242 higher systematic errors ( $\sigma = + 25\%$  for Pu-242). The U-235 content was slightly underestimated ( $\sigma$  ca.  $-5\%$ ) with both calculation techniques.

As a final comment, it should be pointed out that to obtain high precision with the BURSQUID calculations, it is necessary to use a more detailed calculation model and to take into account the irradiation history as close as possible.

#### 8. ACKNOWLEDGEMENTS

The authors wish to acknowledge the valuable help of Mr. De Meester and Mr. Heitz, TUI, for their work in the hot chemical laboratories, Mr. Rijkeboer and Mr. Molinet, TUI, for their work in the mass spectrometric laboratories, and Mr. I. Rosa, ENEL, for the preparation and adaptation of the codes used for the calculations.

Furthermore, they appreciate the help of Mr. Cottone, TUI, for handling and evaluating the analytical data and of Miss. M. Leonori, ENEL, for her assistance in the preparation of the English version.

## 9. REFERENCES

- (1) "Open-vessel experiments on plutonium prototype elements in the Gargliano reactor" - A. Ariemma, L. Bramati, V. Cammarota, M. Galliani, G. Lesnoni, M. Mirone, M. Paoletti, Gualandi, P. Peroni, B. Zaffiro, Doc. 4.811/17.
- (2) "Accuracy of power distribution calculation methods for uranium and plutonium lattices" - A. Ariemma, G. Lesnoni, M. Paoletti Gualandi, P. Peroni, B. Zaffiro, Nuclear Applications and Technology, Vol. 8, April 1970.
- (3) "Isotopic analysis of irradiated fuel and transplutonium elements", H.W. Geerling and L. Koch, EUR 3949.
- (4) "The non-destructive determination of burn-up by means of the Pr-144 2.18 MeV gamma activity", R.S. Forsyth and W.H. Blackadder, Non-destructive testing in nuclear technology, Proc. of the IAEA Symposium, Bucharest, May 1965. Vol. 2, IAEA, Vienna 1965, p. 399-411.
- (5) "Burn-up determination by high resolution gamma spectrometry: axial and diametral scanning experiments", R.S. Forsyth, W.H. Blackadder and N. Ronqvist, A.E. -267.
- (6) "The non-destructive measurement of burnup by gamma-ray spectroscopy", N.C. Rasmussen, J.A. Sovka and S.A. Mayman, Nuclear Materials Management, p. 829-849, UAEA, Vienna 1966.
- (7) B. Kahn and W.S. Lyon - Physics Review 92, p. 902 (1953).
- (8) Nuclear Data Sheet - National Bureau of Standards.
- (9) Data recommended by IAEA, Division of Research and Laboratories for a set of calibrated gamma sources, Vienna 1969.
- (10) Table of Isotopes, Lederer, Hollander and Perlman, J. Wiley Inc., N.Y. 1967.

- (11) Atompraxis 15, L.Koch, p. 27, 1969
- (12) Radiochimica Acta 12, L.Koch, p.160, 1969
- (13) Radiochimica Acta 10, L.Koch, G. Cottone and M.W.Geerlings, p. 122, 1968.
- (14) IN 1277, F. L. Lisman et al., 1969.
- (15) "Proposed determination of nuclear fuel burn-up based on the ratio of two stable fission products of the same element", W.J. Maeck, Report IDO-14642, April 1965.
- (16) "A summary of results obtained from the first MIST experiment at nuclear fuel services", D.E.Christensen et al., West Valley, New York. Paper SM-133/54 presented to IAEA Symposium on Progress in Safeguards Techniques, Karlsruhe, 6-10 July 1970.
- (17) "Some correlations between isotopes of Xe, Kr, U, Pu and burn-up parameters for different thermal and fast reactors", L.Koch, H.Braun, A.Cricchio, Paper SM-133/25 presented to the IAEA Symposium on Progress in Safeguards Techniques, Karlsruhe, 6-10 July 1970.
- (18) "RIBOT - A Physical Model for Light Water Lattices Calculations", P. Loizzo, BNWL-735, February 1978.
- (19) "Il Programma RIBOT", G. Buffoni and S. Lopez - CNEN, DOC. LFCR (66)26 1966
- (20) "FLARE - A three-dimensional boiling water reactor simulator", D. L. Delp, L. Fisher, J.M. Marriman and M. J. Stedwell, GEAP-4589, July 1964.
- (21) "Burn-up of pressurized or boiling water reactors", G. Buffoni, P. Loizzo, S. Lopez and M. Petilli, Symposium on Advances of Reactor Theory, Karlsruhe, June 1966.

- (22) "SQUID-360, a multigroup diffusion program with criticality searches for the IBM-360", A. Danesi, B. Gabutti and E. Salina, EUR-3882, 1968.
- (23) EUR-3619 f, M. Coquerelle, 1967.
- (24) Analytical chemistry, Vol. 40 N13, November 1968.
- (25) "Experimental and theoretical methods used for burn-up analyses at Battelle Northwest", L.C. Schmidt et alia, p. 30, The Physics Problems in Thermal Reactor Design, London, 1967.
- (26) Radiochimica Acta, L. Koch and R. De Meester (to be published).
- (27) "Physics design aspects of plutonium recycle", F.G. Dawson, BNWL-232, May 1966.



## APPENDIX 1

### BURN-UP CODES USED IN THE CALCULATIONS

This Appendix summarizes the main features of the codes used for the calculations of the burn-up and isotopic content of the fuel. A more detailed description of the codes, together with their verification and trimming, is contained in another topical report (2).

The burn-up calculations were performed with the FLARE code to represent the history of the whole core during the irradiation cycles and to determine the operating conditions in which the assembly was irradiated.

The irradiation distribution and the isotopic content of each rod of the assembly at the designated levels have been carried out with either the two-group BURNY code or the five-group BURSQUID code.

A brief description of FLARE, BURNY and BURSQUID codes follows.

#### A.1-1 FLARE code (20)

The three-dimension FLARE code permits a fairly approximate calculation of reactivity, power distribution and burn-up, and also the representation of the control rod configuration during the periods in which the life of a BWR is subdivided for the purpose of the calculations. Since this code is fairly quick, it was used to simulate the behaviour of the Garigliano core.

The FLARE code is characterized by:

- a) a three-dimension calculation technique;
- b) a representation of the effects of flow rate, power and void content, and their mutual interactions;
- c) the feasibility of considering each control rod separately at different insertion levels;
- d) the feasibility of considering the effects of irradiation on each individual element;
- e) a relatively small number of meshes so as to lead to acceptable computer running times.

This code permits a fairly rapid and accurate evaluation of the variation in macroscopic power distribution over the fuel cycle, and the optimization of the corresponding control rod withdrawal sequences.

The code represents every type of material by means of the multiplication constant for an infinite medium  $K_{\infty}$  and of the migration area  $M^2$ , and it is therefore necessary to furnish to the program those coefficients which, when introduced into appropriate analytical expressions, take into account the variations of these two parameters with irradiation, void content, rod density, and local power.

The program also requires parameters relating to the thermohydraulic part, such as those that represent the correlation between steam quality and enthalpy.

Local power sharing is controlled analytically by means of  $K_{\infty}$  and of two distinct expressions, conventionally called "kernels", one of which is axial and the other radial. Both kernels are a function of the  $M^2$  of the material and of an adjustment parameter  $g$ , which has no real physical significance. The kernel  $W_{lm}$  is a neutron balance term representing the fraction of neutrons born at node  $l$  and absorbed at node  $m$ , and is given by:

$$W_{lm} = (1 - g) \frac{\sqrt{M^2_i}}{2 r_{lm}} + g \frac{M^2_i}{r_{lm}^2} \quad (\text{A.1-1})$$

where  $r_{lm}$  is the distance between the  $l$  and  $m$  nodes.

The neutron leakage into the reflector from one of the peripheral fuel nodes is represented by:

$$L_1 = S_1 W_{lm} (1 - \alpha_1) \quad (\text{A.1-2})$$

where  $S_1$  is the source term. Considering this relation, it can be inferred that the parameter  $\alpha_1$ , conventionally called "albedo", has no real physical meaning, but constitutes only a simple means of adjusting the neutron balance at the nodal points located on the active core boundary.

With reference to a given reactor, both the  $g$  and  $\alpha$  parameters are practically derived from correlations between calculated and experimental power-distribution data.

#### A.1-2 BURNY code (21)

The BURNY code performs calculations of diffusion and lifetime in the  $x, y$  and  $r, z$  dimensions, utilizing a two-group scheme with energy cut-off at 0.625 eV. The calculation of the neutron constants is performed by means of the RIBOT code incorporated in the BURNY code.

The thermal constants are calculated by means of a correlation of the cross-sections based on the Wigner-Wilkins spectrum as a function on the following characteristic parameters:

1. Absorption  $1/v$  per atom of H
2. U-235 concentration per atom of H
3. Pu-239 concentration per atom of H
4. Absolute moderator temperature.

This correlation was carried out with recourse to the TEMPEST code. The cell disadvantage factors were calculated by means of the Amouyal-Benoist method

With regard to the determination of the constants of the fast group, the method used is still quicker than the one used for the thermal constants, even though as accurate. To define Ombrellaro type microscopic cross-sections, the fast group is in turn subdivided into three sub-groups, the lower limits of which are 183 keV, 5.5 keV and 0.625 eV respectively. The cross-sections of the three sub-groups are then condensed in one fast group.

The values of these microscopic cross-sections are obtained by correlating the results of a series of calculations performed with the MUFT-IV code for a variety of water lattices. Instead, the resonance integrals relating to Sub-Group 3 were calculated case by case as a function of the characteristics of the lattice being considered.

Making use of the RIBOT technique which permits the neutron constants to be calculated in a relatively short time (about 0.1 sec), the BURNY code has the specific characteristic of calculating the constants of the individual regions after each irradiation interval.

#### A.1-3 BURSQUID code

This code is a link of the five-group RIBOT (19) and SQUID (22) codes and was prepared by ENEL in the framework of this Contract.

The five-group RIBOT code retains the main features of the calculation model of the two-group calculation method described earlier; the modifications involve only the subdivision of the thermal spectrum into two groups. In addition, the condensation of the fast groups is no longer carried out, and therefore the division in groups is the following:

Group 1	over 183 keV
Group 2	183 to 5.5 keV
Group 3	5.5 keV to 0.625 eV
Group 4	0.625 eV to 0.2 eV
Group 5	less than 0.2 eV

The macroscopic transfer cross-sections of Group 3 ( $\sum_{R3,4}$  and  $\sum_{R3,5}$ ) are obtained from  $\sum_{R3}$  on the assumption that the scattering is elastic and isotropic and due only to atoms of H.

With regard to downscattering phenomena of Group 4 and those of upscattering from Group 5 to Group 4, it is assumed that these phenomena are due only to hydrogen according to the Wigner-Wilkins theory. The values of  $\sum_{R4,5}$  and  $\sum_{R5,4}$  were obtained by the TEMPEST code for a wide variety of water lattices.

For the diffusion calculation, use was made of the 15,000 mesh-point SQUID code which accepts a complete matrix of transfer cross-sections.

## APPENDIX 2

### GAMMA SPECTROMETRY TECHNIQUES

#### A.2-1 Non-destructive gamma spectrometry

For the non-destructive gamma spectrometry, the half rods were placed horizontally on two fork-shaped supports and rested against a shoulder; both the fork supports and the shoulder were rigidly attached to a lathe saddle that advanced automatically or was moved manually by means of the counting equipment.

Correct axial positioning of the rods in front of the counting equipment was ensured by standing a rule of calibrated length next to the rod and sighting by means of a mirror. Use of a mirror was necessary because the counting equipment was placed between two windows of the cell and could not be seen from outside.

The described equipment had not been designed especially for this type of measurement and thus there was some uncertainty on the reproducibility of the positioning and proper rotation of the rods (25).

The gamma rays from the rod were collimated and measured by a detector outside the cell. The width of the collimator could be varied, and it was fixed at 1 mm for these measurements. The detector was constituted of a semi-conductor Ge-Li crystal connected to an amplification and counting chain, according to the sketch in Fig. A.2-1.

The Ge-Li monitor used, manufactured by Nuclear Diodes, Inc., had the following characteristics:

Operating voltage	1600 V
Shape	Trapezoidal
Active area	10.6 cm <sup>2</sup>
Length	37.5 mm

SIZE OF SLIT 1x200 mm

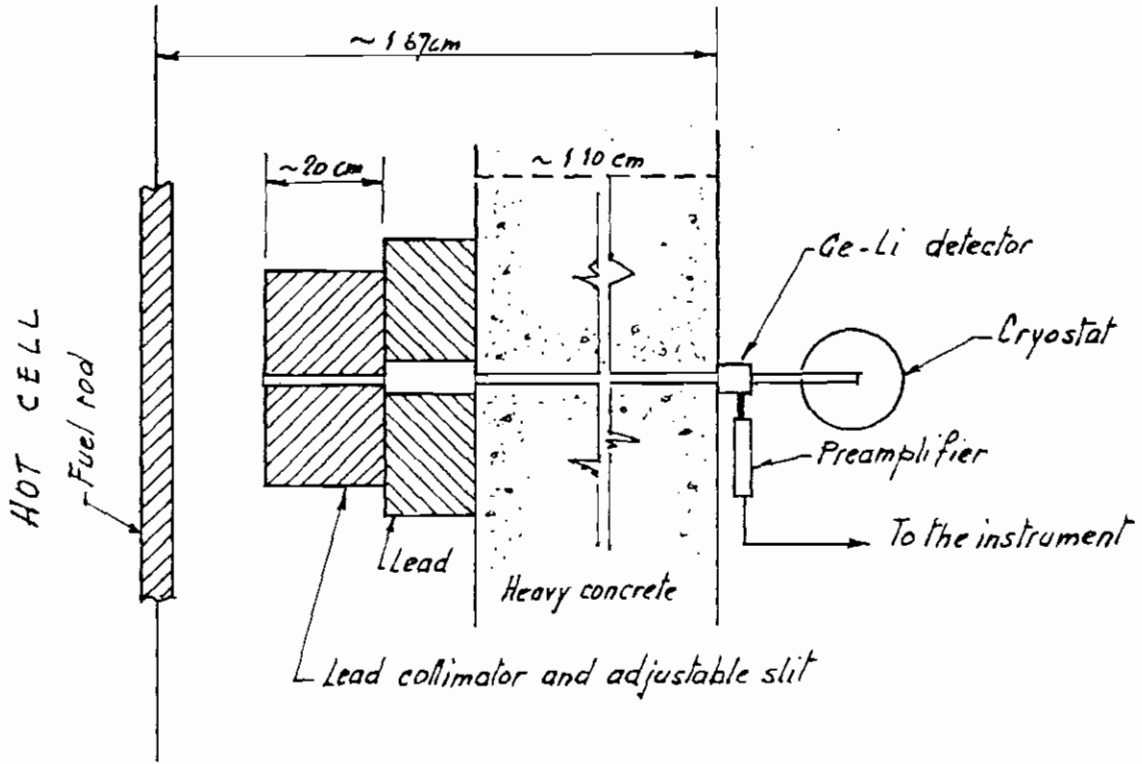


FIG.A2-1 SKETCH OF THE MEASUREMENT GEOMETRY SET UP FOR GAMMA SPECTROMETRY.

Relative efficiency at peak (1.33 MeV)	3.3%
Resolving power (1.33 MeV)	3.2 keV
Peak/Compton ratio (1.33 MeV)	12/1

The monitor was connected to a pre-amplifier-linear amplifier system with RC-pulse-shaping networks; the output signal passed via bias amplifiers and pulse stretchers to a 400-channel RIDL analyzer which recorded the spectra both in digital and analogic forms.

Fig. A.2-2 shows the block diagram of the circuit used for the gamma spectrometry.

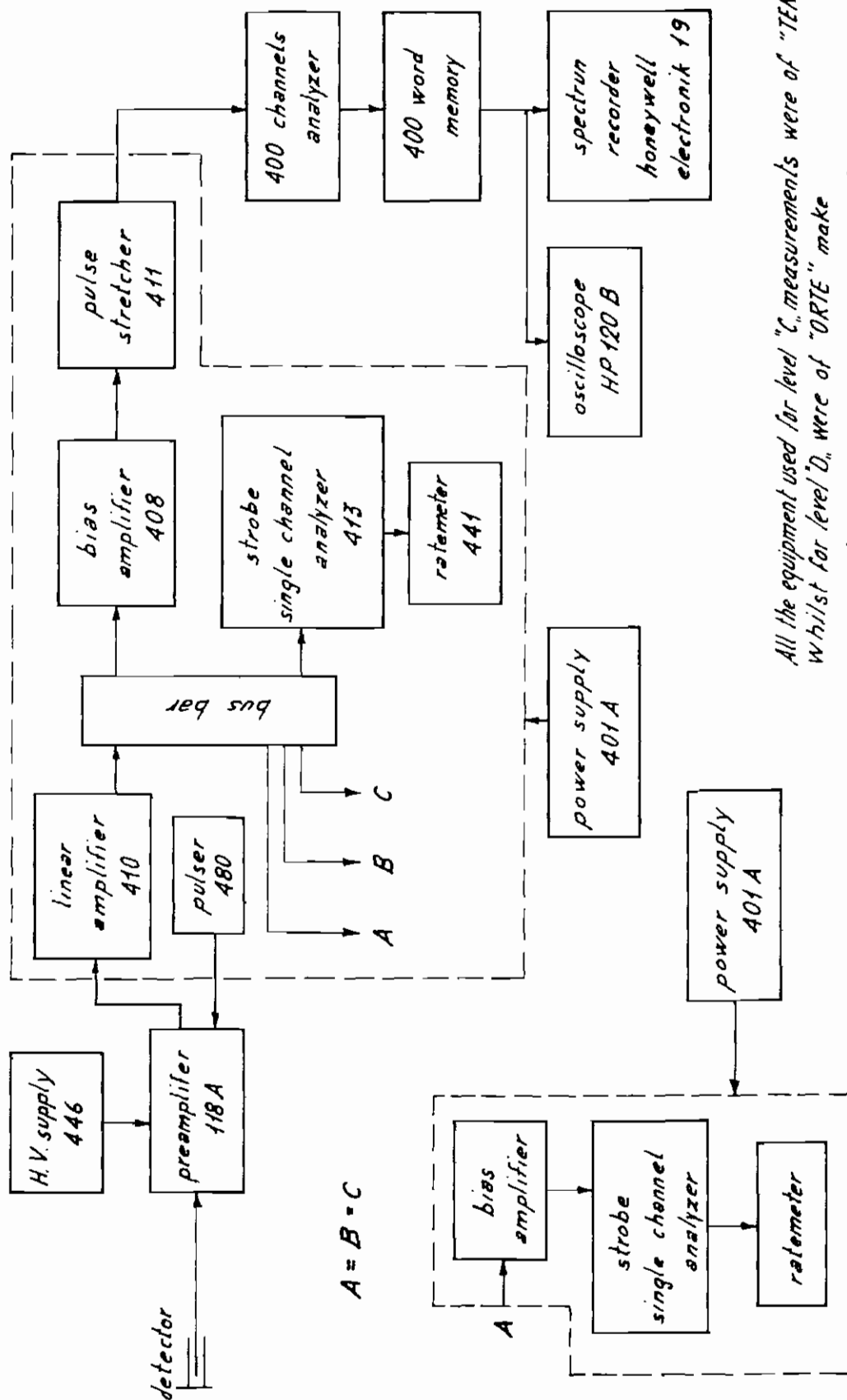
Since the spectrum to be analyzed ranged from 400 keV to 2300 keV, it was subdivided in about 5 keV per channel. The resolving power, at mid-height of the peaks, was in practice 8 keV, i.e. about four channels per peak.

Rather than take the gamma spectrum at a fixed distance from the shoulder of each rod, it was considered advisable to search around the preset point for the position that corresponds to a pellet center. The purpose was to avoid that, when the collimator slit was open 1 mm, any gap between pellets or inside a pellet in the measuring area might lead to erroneous results. Therefore, before each measurement, a gamma scan was performed in steps of one millimeter around the selected position.

This set-up was also used to perform the axial scan by means of a number of single channels each calibrated for one peak, and of potentiometric records to record the related intensities.

#### A.2-2 Gamma spectrometry of the solutions

The solutions obtained by dissolving the slices of rods at level C (see Appendix 3) were taken to a specially equipped laboratory for the gamma-spectrometry measurements. The equipment used for this purpose included a 14-cm<sup>3</sup>



All the equipment used for level "C" measurements were of "TENNELEC" make.  
Whilst for level "D", were of "ORTE" make  
The 400 channels analyzer was of RIDL (nuclear Chicago) make

FIG. A2-2 - BLOCK DIAGRAM OF THE GAMMA SCANNING CIRCUIT



Ge-Li detector, cryostat, TC 130 pre-amplifier, 446 Ortec HT unit, TC 200 amplifier, 4096-channel analyzer LABEN comprising an input and conversion unit, programming unit, printing unit and printer, punching unit and puncher, XY recorder, and visual display unit. The voltage setting was 1600 V.

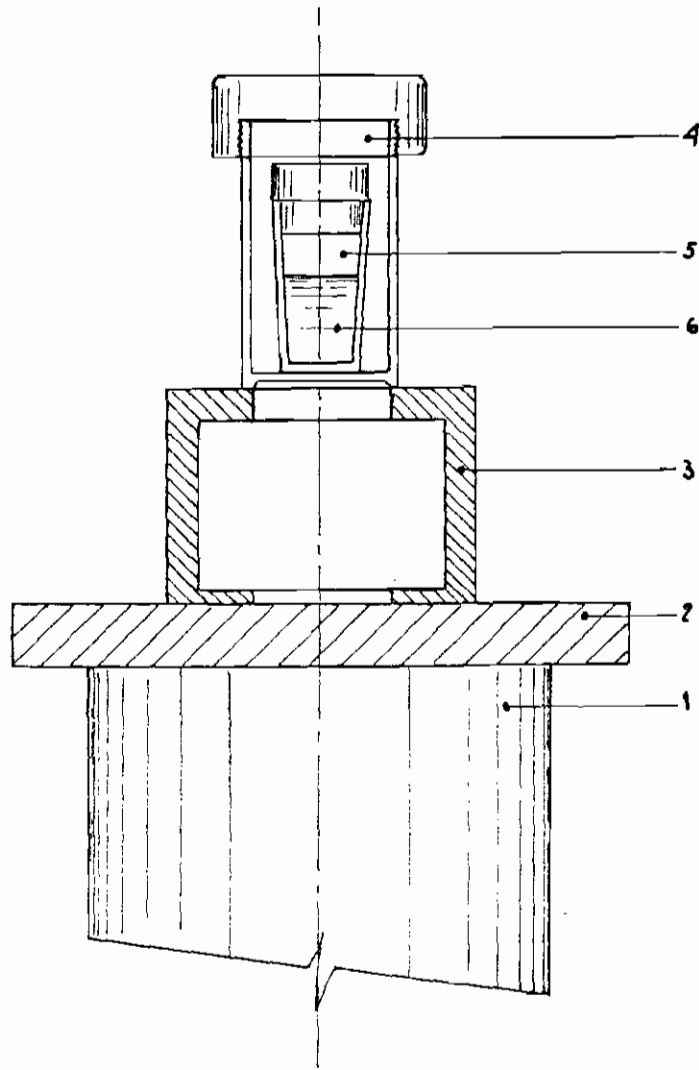
For these units, 2048 memory channels were used so as to have 1.4 keV/channel to cover the spectrum from 200 keV to about 3 MeV.

The upper face of the detector was used as a support and a 7.8-mm plexiglass shim was inserted to reduce the Bremsstrahlung. A hollow PVC cylinder was laid on the plexiglass shim, and the container with the sample or standard source was rested on top of it (Fig. A.2-3). The center of the solution was thus at 45 mm from the detector.

Considering its low efficiency, the monitoring system was not shielded; the natural background producing a uniform spectrum that decreased with energy was subtracted according to the integration technique described further on.

The measurement of each sample was carried out in two stages; the first lasted 1000 seconds and was repeated three times for the determination of the peaks at 512, 662 and 796 keV, whereas the second lasted 20,000 seconds and was also repeated three times for the lesser intense peak at 2186 keV (0.4 cps). While the 1000-second measurements led to very good statistics, the 20,000-second measurements for the Ce-144 peak are hardly sufficient. However, this time interval was maintained, because with a longer duration of the measurement the fluctuations of the instruments would have offset the advantage of better statistics.

To ascertain the number of solutions to be used, preliminary measurements were carried out on three samples of one gram each with the same technique. The results for the 512 keV peak of Ru-106/Rh-106 and for the 662 keV peak of Cs-137 are given in Table A.2-I.



- 1 - DETECTOR Ge-Li
- 2 - PLEXIGLASS SHIELD
- 3 - PVC SUPPORT
- 4 - OUTER PLEXIGLASS CONTAINER
- 5 - INNER PLEXIGLASS CONTAINER
- 6 - SOLUTION

*FIG. A. 2-3 SET-UP FOR GAMMA SPECTROMETRY MEASUREMENTS*

TABLE A.2-1

Measurements on different samples of the same solution

Isotope	Energy keV	cps/g, sample A1/1	cps/g, sample A1/2	cps/g, sample A1/3	Avg cps/g	Theor. $\sigma$ , %	Exper $\sigma$ , %
Ru-106/ Rh-106	512	58.2	57.3	57.8	57.76	1	0.8
Cs-137	662	157.0	155.5	155.7	156.06	0.32	0.52

The theoretical  $\sigma$  was calculated with the formula (24):

$$\sigma\% = \left[ \sum_{i=2}^{n-1} a_i + \left(\frac{n-2}{2}\right)^2 (a_1 + a_n) \right]^{0.5} \cdot \left[ \sum_{i=1}^n a_i - \frac{n}{2} (a_1 + a_n) \right]^{-1} \quad (A.2-1)$$

where:

i = number of the channel

a = counting of channel i

n = number of integration channels.

Since the experimental deviation was very close to the statistical one, only one sample was used.

#### Calculation of the intensity of the photoelectric peaks

Fig. A.2-4 shows a typical photoelectric peak produced by the counting system employed. It will be noted that it is asymmetrical in respect of the peak channel; therefore, an integration technique, asymmetrical to the peak, was selected. In choosing the channels to be used, the following requirements were met:

- 1) The largest number possible of channels should be considered to reach the energy zone in which the gamma radiation due to the Compton effect is nearly constant; in this manner instrumental variations of the peak width have little influence.
- 2) The number of channels should be limited to avoid the inclusion of smaller peaks due to other isotopes.

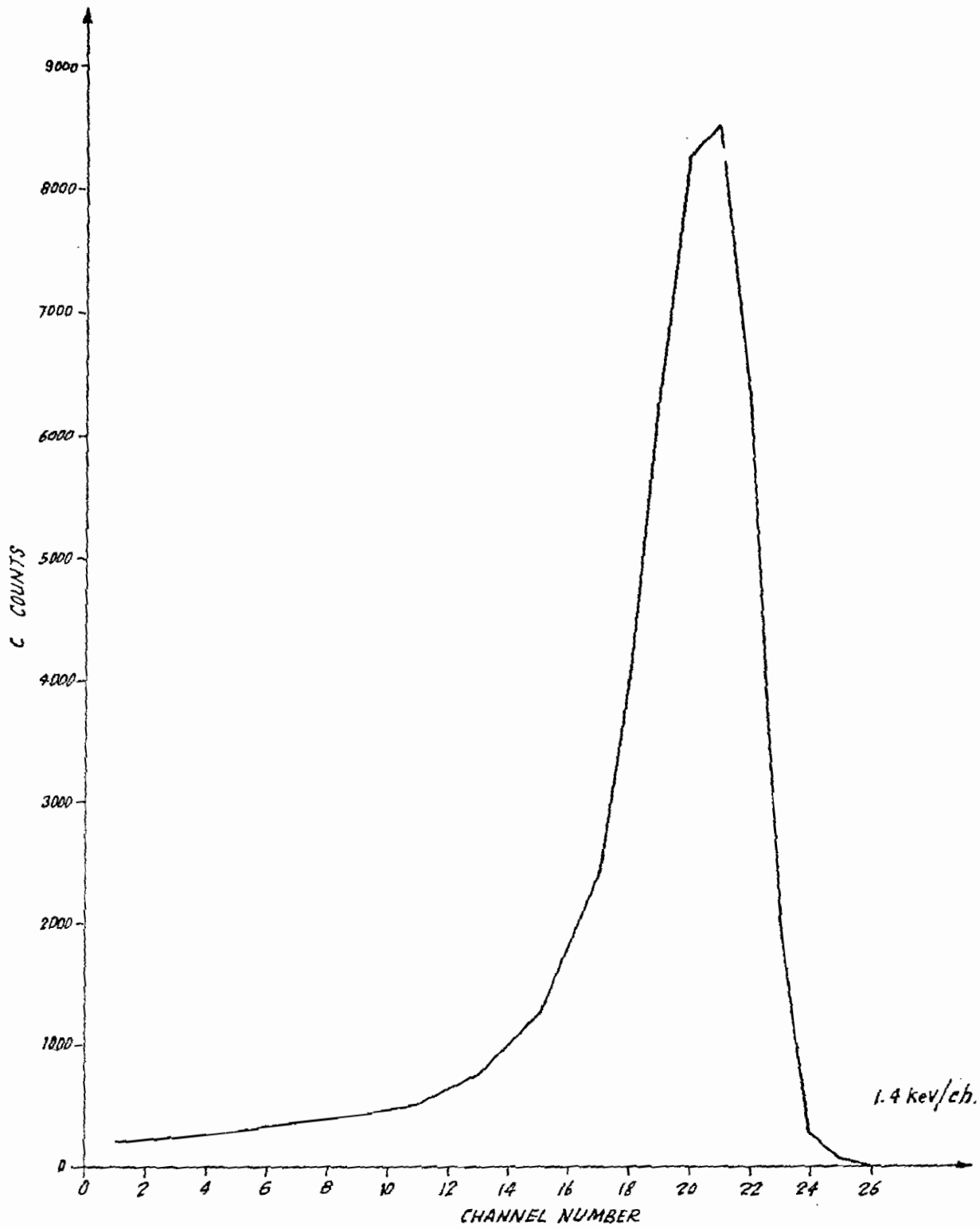


FIG. A.2-4 662 keV  $\text{Cs}_{137}$  PEAK

Since these requirements are conflicting, it is necessary to reach a compromise. It was therefore decided that the number of channels should be such that the variation of one channel determined a 2% variation in the integral. Fig. A.2-5 shows the variation of this integral as a function of the number of channels, for the peak of Fig. A.2-4.

#### Description of system calibration

Standard sources supplied by IAEA were used to obtain the equipment efficiency curve in the geometry described above.

The sources were placed on the PVC support at a height corresponding to the center of the solutions, between two aluminum disks, each 1 mm thick. This aluminum thickness was chosen to simulate the 2.3-mm thickness of the plastic at the bottom of the sample containers.

Table A.2-II provides, for each calibrating source, the results of the measurements, the parameters, the values corrected for decay, and the resulting efficiency. The efficiency data are plotted in Fig. A.2-6, and the value relating to the 2.186-MeV peak of Ce-144/Pr-144 was extrapolated from 1.850 MeV.

Since the thickness of the solutions was finite, it was necessary to calculate the effect of self-absorption as a function of the energy of the gamma rays. This effect was presented by the factor R, ratio between the measured activity and actual activity, as expressed by the equation

$$R = \frac{mx}{1 - e^{-mx}} \quad (\text{A.2-2})$$

where  $m$  is the absorption coefficient in  $\text{cm}^{-1}$  and  $x$  the thickness of the source.

The self-absorption factors so calculated at the energies of interest are given in Fig. 5.7

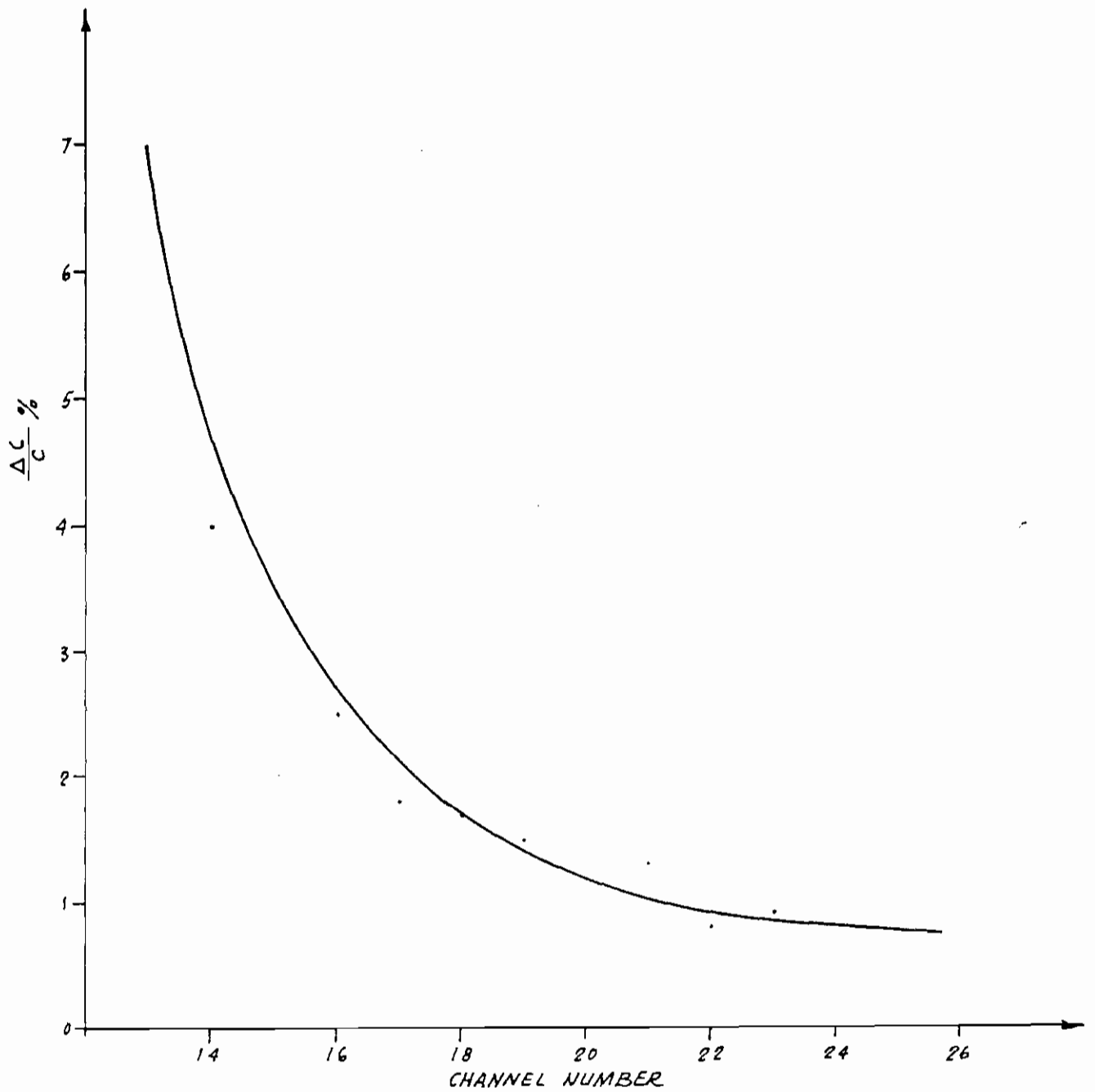


**FIG. A.2-5 PERCENT VARIATION IN COUNTS AS A FUNCTION  
OF THE NUMBER OF INTEGRATING CHANNELS  
662 keV  $Cs_{137}$  PEAK  
1.4 keV/ch.**

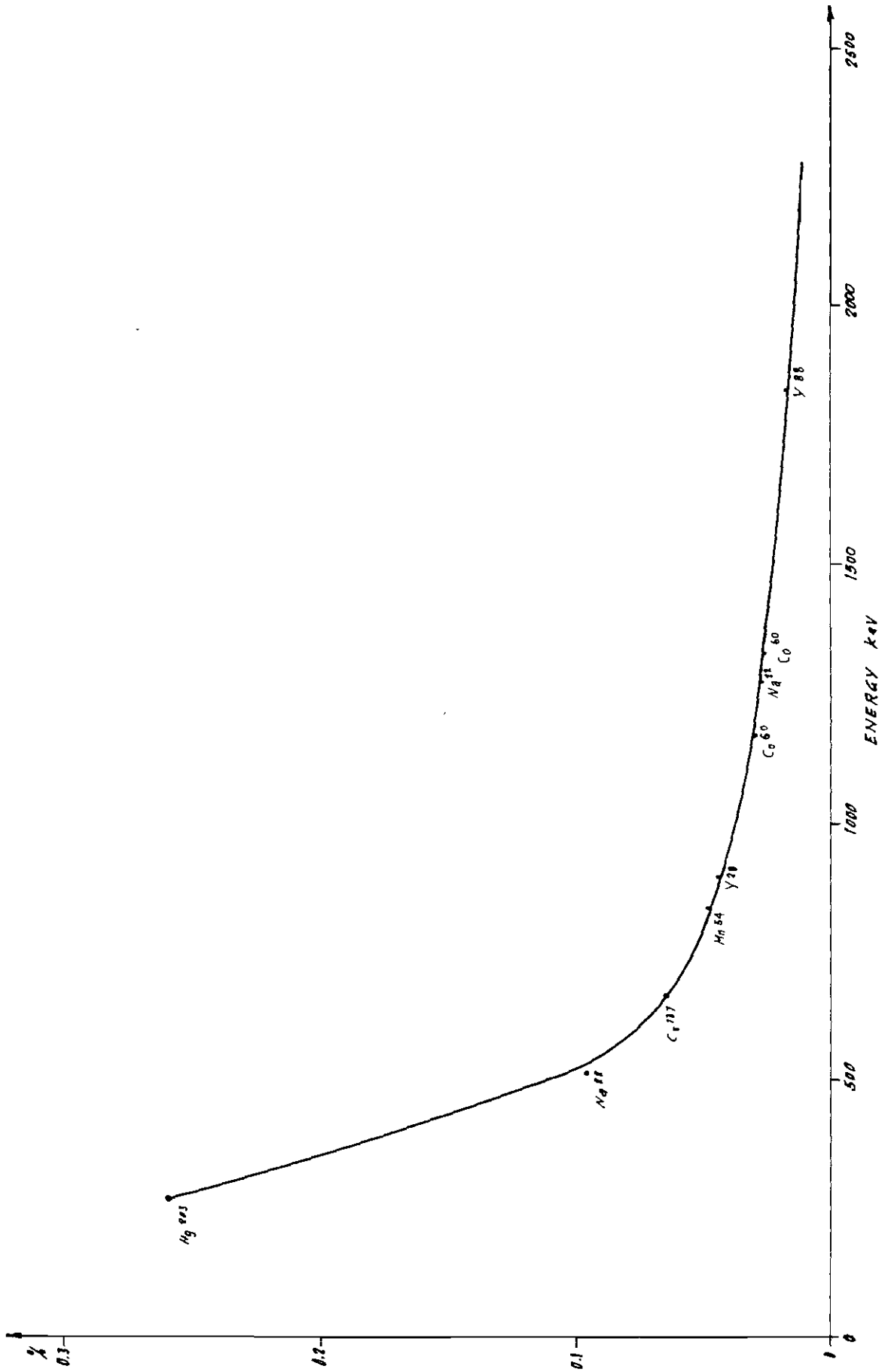


FIG. A.2-6 DETECTING SYSTEM EFFICIENCY IN PERCENT

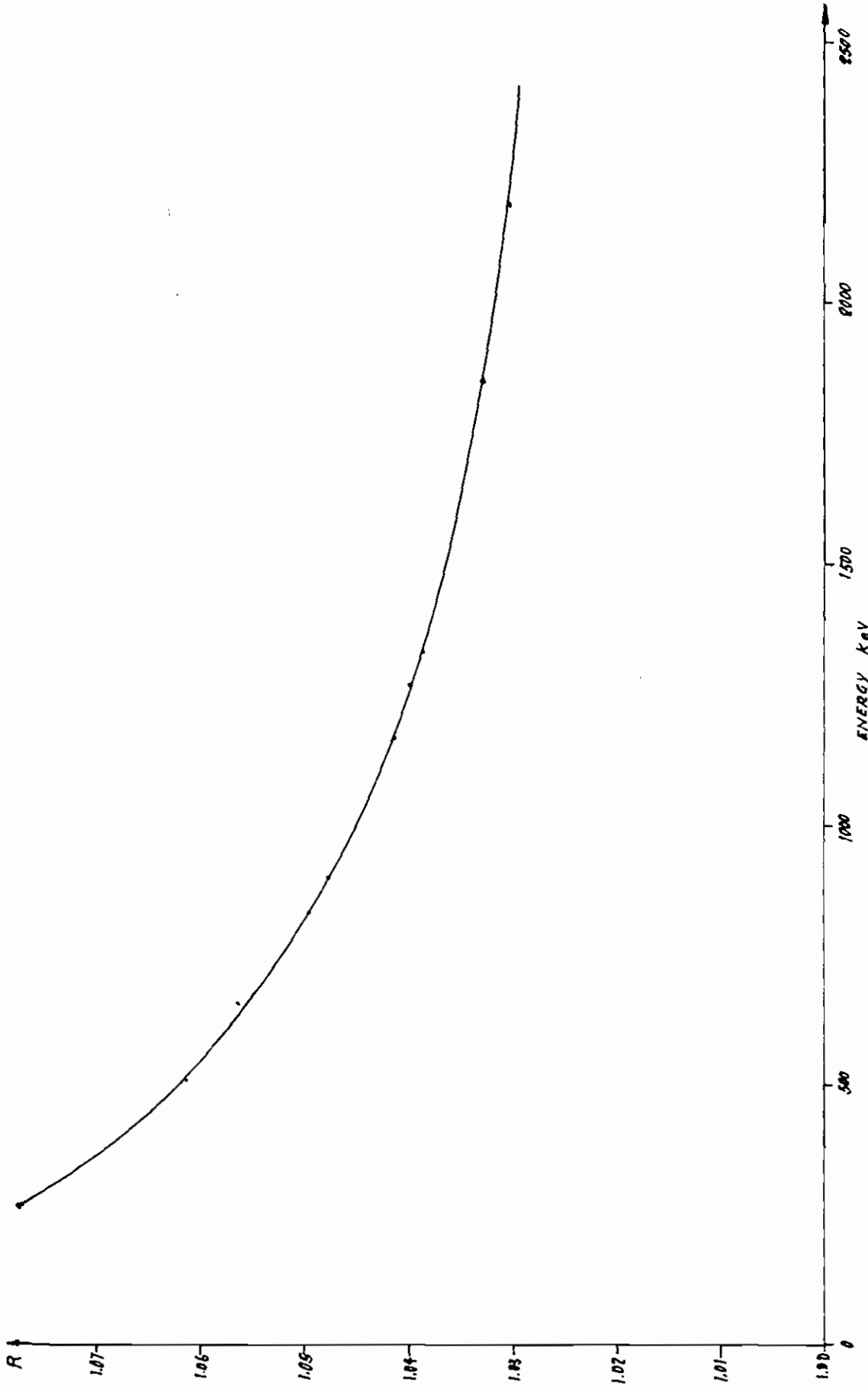


FIG. A.2-7 SELF-SHIELDING FACTOR  $\frac{m \times}{1 - e^{-m \times}}$



TABLE A. 2-II  
Efficiency of the monitoring system

Isotope	Energy	Activity on 1. 1. 69 ( $\mu$ Ci)	Activity on day of measurement ( $\mu$ Ci)	Gamma activity on peak (dps)	Pulses on peak (cps)	Efficiency % (cps/dps)
Hg-203	279.2	21.94	1.34	$4.04 \times 10^4$	104.6	0.259
Na-22	511	9.67	8.43	$5.60 \times 10^5$	536.3	0.0958
Cs-137	661.6	10.98	10.85	$3.41 \times 10^5$	220.7	0.0646
Mn-54	834.8	10.50	6.91	$2.56 \times 10^5$	124.3	0.0486
Y-88	898	10.77	3.19	$1.079 \times 10^5$	48.41	0.0448
Co-60	1174	10.99	10.26	$3.786 \times 10^5$	113.06	0.0298
Na-22	1274.5	9.67	8.43	$3.12 \times 10^5$	84.10	0.0269
Co-60	1332	10.99	10.26	$3.79 \times 10^5$	98.89	0.0261
Y-88	1836	10.77	3.19	$1.173 \times 10^5$	20.07	0.0171

A.2-3 Burn-up determination from Cs-137 activity

To determine the burn-up from Cs-137 activity it was necessary to know the irradiation history of the A-106 assembly. This history was introduced in the definition of the energy produced per tonne of fuel:

$$B = K \int_0^T \sum_f(t) \phi(t) dt \quad (A.2-3)$$

where,

B is the burn-up in MWd/MTU

K an energy transformation constant

T the total time of residence in the reactor ( $\text{sec}^{-1}$ )

$\phi(t)$  the neutron flux at time t ( $\text{cm}^{-2} \text{sec}^{-1}$ )

$\sum_f(t)$  the macroscopic fission cross-section of the fuel ( $\text{cm}^{-1}$ ).

To solve Eqn A.2-3 in a practical manner, it was necessary to introduce some approximations.

During irradiation, the fluxes and the macroscopic fission cross-sections vary in a way that it is difficult to establish; however, if it is legitimate to use an average flux  $\bar{\phi}$ , an arbitrary time T and an average uranium and plutonium fission cross-sections, we have

$$B = K \bar{\phi} T \left[ \sum_f^U + \sum_f^{Pu} \right] \quad (A.2-4)$$

On the other hand the specific activity of a fission product having a decay constant  $\lambda$  and a fission yield Y, will be at the end of irradiation:

$$A = \bar{\phi} (1 - e^{-\lambda T}) \left[ \sum_f^U \cdot Y^U + \sum_f^{Pu} \cdot Y^{Pu} \right] \quad (A.2-5)$$

If the values of Y do not differ much for the two isotopes, an average  $\bar{Y}$  may be used and the formula (A.2-5) becomes:

$$A = \phi \bar{Y} (1 - e^{-\lambda T}) \left[ \sum_f^U + \sum_f^{Pu} \right] \quad (A.2-6)$$

By combining (A.2-4) and (A.2-5) we obtain

$$B = K \frac{AT}{\bar{Y} (1 - e^{-\lambda T})} \quad (A.2-7)$$

which relates the burn-up with the specific activity of a fission product and a few parameters dependent on the reactor life.

It is now to be demonstrated that to get the expression in (A.2-7), the approximations made are valid for assembly A-106 and for the fission product Cs-137.

From the history of the reactor power for the period during which assembly A-106 was irradiated (see Chapter 3) we note the presence of five main intervals, three relating to the reactor at power and two to shutdowns:

(1) April 10 to August 30, 1964	At power: 174 days
(2) September 1 to November 3, 1964	Shutdown: 34 days
(3) Nov. 4 to September 24, 1965	At power: 324 days
(4) Sept 24, 1965 to April 27, 1966	Shutdown: 218 days
(5) April 28, 1966 to May 7, 1967	At power: 371 days.

Since the total reactor power remained practically constant throughout all the periods of operation, we may use an average value of the flux  $\phi$ .

The average value of the Cs-137 fission yield was determined by weighing the yields of the fissile isotopes over their respective macroscopic fission cross-sections in the A-106 assembly as a function of time, as calculated with the BURNY-2 code. The Cs-137 fission yields (Y) used for the different fissile isotopes were:

$$6.22 \pm 0.14\% \text{ U-235}$$

$$6.48 \pm 0.19\% \text{ Pu-239}$$

$$6.62 \pm 0.33\% \text{ Pu-241}$$

indicated in reference (25). As one may see, the difference for U-235, Pu-239 and Pu-241 is reduced to a few units per cent so that the uncertainty in the iso-

tope composition existing at any given time is of minor consequence. The average value  $\bar{Y}$  was thus calculated from

$$\bar{Y} = \frac{\sum_f^{235} 6.22 + \sum_f^{239} 6.48 + \sum_f^{241} 6.62}{\sum_f^{235} + \sum_f^{239} + \sum_f^{241}} \quad (\text{A.2-8})$$

For the three irradiation periods and for the two U-235 enrichments (1.6% the following values were found:

$$\begin{aligned} \bar{Y} \text{ I} & \left\{ \begin{array}{l} 6.23\% \\ 6.23\% \end{array} \right. \\ \bar{Y} \text{ II} & \left\{ \begin{array}{l} 6.26\% \\ 6.25\% \end{array} \right. \\ \bar{Y} \text{ III} & \left\{ \begin{array}{l} 6.37\% \\ 6.32\% \end{array} \right. \end{aligned}$$

These values were averaged by weighing them over the number of days of the three periods, thus obtaining:

$$\begin{aligned} & 6.28\% \text{ for } 1.6\% \text{ of U-235} \\ & 6.27\% \text{ for } 2.1\% \text{ of U-235.} \end{aligned}$$

Since the difference between these two values was minimal, in the calculations the value of 6.27% was used for all the rods.

In respect of time T, the following approach was adopted. A half-life of 30.6 years was used for Cs-137 and the three periods of operation at constant flux and two shutdown times were taken into account so that the formula A.2-7 became:

$$B = K \cdot \frac{AT}{Y \sum_1^3 (1 - e^{-\lambda T_i}) e^{-\lambda \tau_i}} \quad (\text{A.2-9})$$

where  $T_i$  denotes the days of irradiation for the i-th period and  $\tau_i$  the days of decay since the i-th period to the end of irradiation (May 7, 1967).

With the following values in days:

$T_i$	$\tau_i$
174	948
324	585
371	0

the exponential term at the denominator of (A.2-9) gives 0.0519.

Instead, by using a more sophisticated procedure to take into account the actual irradiation and decay periods, we get a value of the exponential term of 0.05218, which differs by 0.5% from the preceding figure. Therefore, the simplification of using only three irradiation periods appears to be acceptable.

Then, Eqn A.2-9 becomes:

$$B = \frac{K \cdot A \cdot 869}{6.27 \cdot 0.05218} \quad (\text{A.2-10})$$

For the calculation of K the following approach was adopted:

- 1) Each fission was taken to correspond to  $3.634 \cdot 10^{-22}$  MWd, based on an average value of energy released per fission of 196 MeV (cfr. Para A.3-6).
- 2) A factor of  $3.7 \cdot 10^{16}$  was introduced to convert A from Ci/g to dps/t.
- 3) A factor of  $10^2$  was introduced because the fission yield Y is expressed in percent.
- 4) T was converted from days into seconds.

Thus  $K = 1.162 \cdot 10^2$  and from Eqn A.2-9 we get:

$$B = 3.086 \cdot 10^5 A \quad (\text{A.2-11})$$

where B is expressed in MWd/MTU, and A in Ci/g.

The calculated irradiation for the eighteen rods examined at level C, based on the activity values of Cs-137, are given in Table A.2-III.

TABLE A.2-III  
Burn-up values as obtained from Cs-137  
activity measurements

Rod	B(MWd/MTU)	Rod	B(MWd/MTU)
A1	10,183	C3	8,702
B1	9,252	D4	8,517
C1	10,138	A5	10,369
E1	10,125	E5	8,517
J1	12,403	G7	9,752
B2	9,659	B8	11,597
D2	9,017	H8	11,696
H2	11,081	A9	13,344
A3	10,039	J9	13,547

ed

### APPENDIX 3

#### MASS AND ALPHA SPECTROMETRY TECHNIQUES

##### A.3-1 Dissolution of samples and analysis of fission gases (26)

###### Apparatus and Reagents

A mass spectrometer of the type CH-4, Varian MAT was used. Manometers and pumps were from Leybold - Heraeus. All reagents were from Merck with the exception of the titanium sponge (Serva) and the helium with 97.95% purity (Messer Griesheim).

###### Procedure (the apparatus is shown in Fig. A.3-1)

1. The weighed sample  $G_1$  is brought into the dissolution flask (C) and the apparatus cleaned by flushing with helium.
2. The collection flask (F) is evacuated to 1 Torr.
3. 100 ml of concentrated  $\text{HNO}_3$  are transferred into C and heated to boiling.
4. The fission gases are transferred by an helium stream to F. In order to avoid losses due to leakage no excess pressure is allowed to build up in the apparatus.
5. After complete dissolution of the sample the fission gases are forced through the washing bottles,  $G_1$ , ( $\text{KMnO}_4$  solution,  $\text{NaHSO}_3$  -  $\text{NaOH}$ ,  $\text{CaCl}_2$ ,  $\text{CuO}$ ) - furnace,  $\text{Mg}(\text{ClO}_4)_2$  + natronasbestos furnace with titanium sponge. With helium into absorption tubes, H, which are cooled by liquid nitrogen. The speed of dissolution is about  $12 \text{ mg/min.cm}^2$ .
6. The sample is separated from helium by adsorption on molecular sieves. The Xe and Kr isotopes are determined by mass spectrometry.
7. The solution of the samples is transferred into a weighing bottle and the weight  $G_2$  of the solution determined.
8. The undissolved ring of cladding of the fuel element is dried and the weight  $G_3$  determined.
9. An aliquot of solution is diluted to about  $0.2 \text{ mg/g}$  and the solution factor determined.

- A He bomb
- B Pump
- C Dissolution flask
- D HNO<sub>3</sub> inlet
- E Reflux condenser
- F Collection flask
- G Purification of gases
- H Adsorption tube

gh

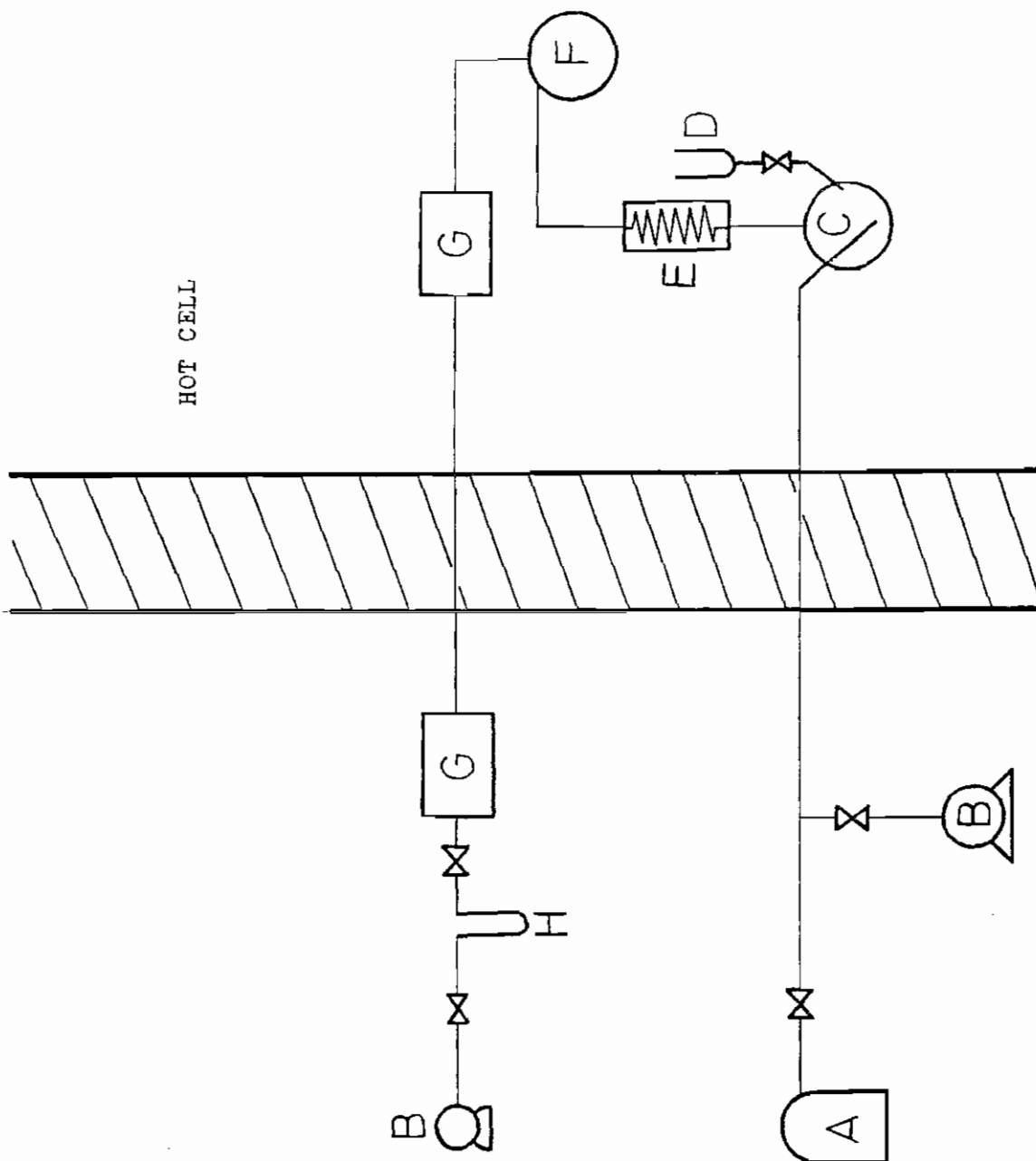


Fig. A.3-1- Apparatus for sample dissolution and fission gas collection



### Data Handling

Five scans of each mass spectrum of Kr and Xe isotopes are evaluated and the isotopic ratios R (Kr, Xe) are determined.

$$R (\text{Xe}) = \text{Xe-131}/\text{Xe-134}; \text{Xe-132}/\text{Xe-134}; \text{Xe-136}/\text{Xe-134}$$

$$R (\text{Kr}) = \text{Kr-83}/\text{Kr-86}; \text{Kr-84}/\text{Kr-86}; \text{Kr-85}/\text{Kr-86}$$

The weight of the dissolved sample G is calculated:  $G = G_1 - G_3$ .

The concentration of sample solution C is:  $C = G/G_2$ .

### A.3-2 Isotopic dilution analysis (11)

The isotopic dilution technique was used for the mass spectrometric analysis in order to determine the isotopic concentration. This technique is briefly described below.

In the ideal case this analysis is rather simple.

Let A be the isotope, the quantity of which has to be determined, and I the known quantity of the spike isotope which has been added to the sample to be analysed. After separation of the element from the sample (the separation yield need not be known), the isotopic ratio A/I is measured. The quantity of isotope A =  $\frac{A}{I} \cdot I$ .

Frequently, however, the sample already contains some amount of  $I_p$  of the spike isotope and it may be that some  $A_i$  of the isotope A to be determined is already in the spike. Therefore the isotopic ratio R in the sample ( $A/I_p = R_p$ ) and in the indicator ( $A_i/I = R_i$ ) has to be determined.

The mixture of the spike solution and the sample consequently contains the quantity of the spike isotope  $I_m = I_p + I$  and the quantity of the isotope to be determined  $A_m = A_i + A$ .

The isotopic ratio in the mixture,  $R_m = A_m/I_m$  follows from considerations of  $R_p$  and  $R_i$ .

$$R_m = \frac{A + I \cdot R_i}{A/R_p + I} \qquad A = I \frac{R_m - R_i}{1 - R_m/R_p} \qquad (A.3-1)$$

that is, also in this case only isotopic ratios have to be determined. In most isotopic analyses only the isotopic concentration of the most abundant single isotope is determined. The concentration of the other isotopes in the sample follows from the corresponding isotopic ratio.

### A.3-3 Uranium and plutonium isotopic concentration (12)

#### Apparatus and Reagents

For the separation of uranium from plutonium the exchanger Dowex A x 8, 200-400 mesh, and quartz-distilled nitric acid diluted with bidistilled water was used. Uranium and plutonium standards were supplied by the NBS and U-233 and Pu-242 spikes by the Isotopes Sales Department, ORNL. The mass spectrometer was a model CH-4 (Varian, Bremen). The samples are measured in terms of  $Me^+$  ion with the two-filament technique.

#### Procedure

1. About 0.25 g of the exchanger are placed together with 1 ml 8M  $HNO_3$  into disposable pipettes ( $\phi$  5 mm) of which the top has been plugged with glass wool. This column is washed with 1 ml of acid.
2. The sample, dissolved in 8M  $HNO_3$ , and containing about 0.1 - 1  $\mu g$  Pu is added to the column. According to the uranium content of the sample it is washed with n ml 8M  $HNO_3$ . Uranium and plutonium are eluted with 3 ml of 0.35 M  $HNO_3$ .
3. The plutonium concentration can be roughly determined by gross alpha counting and alpha spectrometry.
4. 1-5  $\mu g$  of plutonium are placed in the middle of the evaporation filament and the spectra of uranium and plutonium isotopes are recorded with the mass spectrometer.

5. To the same amount of the sample as cited under 2, a calibrated amount of spike mixture (U-233 and Pu-242) is added. The amount of U, Pu and the ratio U/Pu of the spike mixture must correspond to that of the sample.
6. To the solution of spike and sample about 0.3 ml of 1M  $\text{NH}_2\text{OH} \cdot \text{HCl}$  are added. The solution is heated to  $80^\circ\text{C}$ , cooled for 5 min. and then 0.7 ml 1M  $\text{NaNO}_2$  are added. After evolution of the gases the solution is mixed and slightly heated.
7. The solution is treated according to points 2-4.

#### Data Handling

Eight scans of the mass spectra are sufficient for evaluation and correction of possible changes in ion current. From the peak height the isotopic ratio R is calculated and related to the most abundant isotope:

$$R_5 = \text{U-235}/\text{U-238}$$

$$R_6 = \text{U-236}/\text{U-238}$$

$$R'_0 = \text{Pu-240}/\text{Pu-239}$$

$$R'_1 = \text{Pu-241}/\text{Pu-239}$$

$$R'_2 = \text{Pu-242}/\text{Pu-239}$$

The concentration of Pu-239 and U-238 in the sample is determined by isotopic dilution analysis according to equations (A.3-1). From the ratio  $\text{Pu-239}/\text{U-238} = R_9$  the corresponding ratios  $R = N_i/\text{U-238}$  ( $i = 240, 241, 242$ ) are computed. The further reduction of data to pre-irradiation conditions is described in Paragraph 5.4.3.

#### A.3-4 Determination of other transuranic isotopes

##### Apparatus and Reagents

Reagents are as in A.3-3. The alpha spectrometer consists of an ORTEC semiconductor detector type SBBJ 025, connected to ORTEC amplifiers 103, 203, and RIDL 400-channel analyzer, model 3412 B.

Procedure

1. About 50  $\mu$ l of the diluted sample solution are dropped onto the stainless steel counting plate and are dried. The plate is fired at about 800°C.
2. An alpha-spectrum counting time should be chosen such that the nuclide of lowest abundance is counted with at least 10,000 cpm.
3. An alpha spectrum is also taken from the purified uranium and plutonium solution (A.3-3).

Data Handling

The percentage I of the disintegration pertaining to a single alpha decay energy is calculated. I (64) and I (62) are the percentages of Cm-244 which can be calculated directly. For the determination of the percentages of Pu-238 and Am-241, chemical separation is necessary.

The comparison of the percentages I (8 + 51) (before separation) and I (8)' (after separation) which are related to the corresponding percentages of Pu - (239 + 240) - I (9 + 0)' and I (9 + 0)' follows:

$$I(8) = I(9 + 0) I(8)' / I(9 + 0)$$

$$I(51) = I(8 + 51) - I(8)$$

To split up the percentage I (9 + 0), the isotopic mass ratio Pu-240/Pu-239 = R<sub>9</sub> must be known:

$$I(9) = I(9 + 0) / 1 + (R'_9 \cdot A_9/A_0)$$

A<sub>i</sub> is the specific activity of the nuclide.

Ai	Dpm/mol
Pu-238	9.19.10 <sup>15</sup>
Pu-239	3.25.10 <sup>13</sup>
Pu-240	1.20.10 <sup>14</sup>
Am-241	1.83.10 <sup>15</sup>
Cm-242	1.77.10 <sup>18</sup>
Cm-244	4.47.10 <sup>16</sup>

The conversion of  $R_i$  values ( $R_i = N_i/\text{U-238}$  isotopic mass ratio) follows the equation:

$$R_i = \frac{A_9}{I(9)} \cdot \frac{I(i)}{A(i)} \cdot R_9 \quad (\text{A.3-2})$$

The further reduction of the measured values to the pre-irradiation conditions is described in Paragraph 5.4.3.

#### A.3-5 Nd-148 concentration analyses (13)

##### Apparatus and Reagents

The separation of neodymium was performed by chromatographic elution with  $\alpha$ -hydroxyisobutyric acid (purest, Serva Entwicklungslabor) Dowex 50 x 8, 200-400 mesh. All reagents are made with quartz-distilled water. Nd-150 for spiking was received from the Isotope Sales Department, ORNL. The experimental setup was simplified on purpose in order to permit easy replacement of components which have been contaminated by neodymium. Therefore, regulation of the flow rate in the column by air pressure was used. The alpha emitters Am-241, Cm-242 and Cm-244 were measured by using a drop counter (Frieske und Hoepfner). The mass spectrometer was a model CH-4 (Varian, Bremen). The samples are measured as  $\text{Me } 0^+$  and  $\text{Me}^+$  ions using the single-filament technique.

##### Procedure

1. About 0.5 g of the resin are placed into the column and washed with 12 M HCl. The size of the column is 6.5 cm x 0.3 cm. The column is subsequently washed with 3 ml 12 M HCl, 3 ml  $\text{H}_2\text{O}$ , 1 ml 12M  $\text{NH}_4\text{OH}$ , and with water until pH = 7. Then the column is treated with 2 ml 0.25 M  $\alpha$ -H IBS, pH = 4.6.
2. The sample solution, from which uranium and plutonium have been separated, is brought to dryness and dissolved in 100  $\mu\text{l}$  0.05M HCl, 200  $\mu\text{l}$  0.05 M HCl; the sample solution and 300  $\mu\text{l}$  0.05M HCl are then added to the column.

3. With 0.25M HIBS, pH 4.6, elution is carried out until the Am-241 activity disappears. Directly after this a neodymium fraction of 0.75 ml is taken.
4. The neodymium fraction is diluted with 70  $\mu$ l 15M  $\text{HNO}_3$  + 1 ml  $\text{H}_2\text{O}$  and added to a second column with the same ion-exchanger (the resin must be washed previously with 0.5M  $\text{HNO}_3$ ), and finally the neodymium is eluted with 2 ml 6M  $\text{HNO}_3$ . The neodymium solution is brought to dryness and dissolved in 50  $\mu$ l 1M  $\text{HNO}_3$ . The solution is placed on the evaporation filament of a sample holder for mass spectrometry.
5. To a known amount of the sample solution a calibrated amount of Nd-150 spike is added. This mixture is treated according to steps 2-4.
6. In the mass spectrometer, the samples are continuously heated until the neodymium isotopes can be measured as  $\text{NdO}^+$  ion. During the measurement, the absence of  $\text{CeO}^+$  and  $\text{SmO}^+$  ions of masses 156 (Ce-140 O-16), 168 (Sm-152 O-16), and 170 (Sm-154 O-16) is controlled.

#### Data Handling

Eight scans of each mass spectrum are sufficient for the evaluation and correction for possible changes in ionic current. From the peak height the isotopic ratio  $R''$  is calculated and related to neodymium-150:

$$\begin{aligned} R''_{142} &= \text{Nd-142/Nd-150} \\ R''_{148} &= \text{Nd-148/Nd-150} \end{aligned} \quad (\text{A. 3-3})$$

The  $\text{NdO}^+$  spike is measured, and correction for the heavy oxygen isotopes is not necessary because the neodymium isotopes are of similar abundances. Another correction, however, is unavoidable. Contamination by natural neodymium must be corrected for. This amount of neodymium can be calculated by the natural abundance  $^i\text{H}$  ( $i = 142, 148, 150$ ) and Nd-142 because this isotope is not formed during fission. The corrected ratio  $R'_{148} = \text{Nd-148/Nd-150}$  is calculated according to the equation:

$$R'_{148} = \frac{{}^{142}\text{H} - {}^{148}\text{H} R''_{142}/R''_{148}}{{}^{142}\text{H}/R''_{148} - {}^{150}\text{H} R''_{142}/R''_{148}} \quad (\text{A.3-4})$$

By isotopic dilution analysis according to equation (A.3-2) the concentration of Nd-148 can be determined and from the known U-238 concentration the ratio  $R_{148} = \text{Nd-148}/\text{U-238}$  is calculated.

#### A.3-6 Burnup determination from Nd-148 content

Nd-148 was selected as a burnup monitor because, of all the other fission products, it is the only one presenting the following main characteristics (3):

- Its cumulative fission yield  $Y_f$  is practically identical for uranium and plutonium and is independent of neutron energy.
- Neodymium and its chain members do not change location in the fuel by diffusion or other transport mechanisms during irradiation.
- It is stable and neutron capture by the chain members is practically negligible with respect to their beta decay. This characteristic is quite important since it is generally impossible to account for neutron flux changes and shutdown periods in the fuel irradiation.
- Its chemical separation and analysis by isotope-dilution mass spectrometry is relatively simple (see Para A.3-5).

In order to derive the burnup (B) in MWd/MTU, it is first necessary to determine the percentage of fissioned atoms referred to the initial heavy atoms,  $F_T$ . By indicating with  $Y_{148}$  the average value of Nd-148 fission yield, the ratio  $R_{148}/Y_{148}$  represents the number of heavy atoms fissioned referred to the U-238 atoms. Consequently, the number of initial heavy atoms is given by the sum of all the remainder heavy atoms, referred to U-238 atoms, and the fissioned ones,  $R_{148}/Y_{148}$ . Therefore, we shall have:

$$F_T = \frac{R_{148}/Y_{148}}{\sum R_i + R_{148}/Y_{148}} \quad (\text{A.3-5})$$

in which  $\sum R_i$  is the sum of all the uranium, plutonium, americium and curium atoms present in the fuel.

Since:

$$1 \text{ W. sec} = \frac{6.2419 \times 10^{12}}{E} \text{ fissions}$$

where E is the total energy released per fission in MeV, once  $F_T$  is known we have:

$$1 \text{ MWd} = \frac{5.393 \times 10^{23}}{E} \text{ fissions} \quad (\text{A.3-6})$$

and therefore

$$B(\text{MWd/MTU}) = \frac{F_T \times 10^4 \cdot N^0 / A}{(5.393 \times 10^{23})/E} = F_T \times 46.92 \times E \quad (\text{A.3-7})$$

where  $N^0$  is Avogadro's number and A is the average atomic weight of a heavy atom ( $A = 238$ ).

Assuming a total energy per fission of 194 MeV for U-235 and 200 MeV for Pu-239 (27), and that the U-235 fissions are on the average 70%, we obtain a mean value of  $E = 196$  MeV. As a result, Eqn A.3-7 becomes:

$$B = 9.196 \times 10^3 F_T \text{ MWd/MTU} \quad (\text{A.3-8})$$



APPENDIX 4  
ANALYTICAL RESULTS

The results of the radiometric and mass spectrometric measurements are collected in the following tables.

The tables A.4.1 and A.4.2 show the results of mass ratios for the isotopes of uranium, plutonium, americium, neodymium, krypton and xenon. For repeated measurements of a sample the mean value and the single standard deviation is given.

The same applies to the table A.4.3, which contains the percentage of alpha activity for the alpha emitting nuclides of plutonium, americium and curium and for table A.4.4, where the isotopic concentrations of Nd-148, U-238 and Pu-239 are given, as they are determined by the isotope dilution technique.



Table A. 4-1 Contd

Sample No.	Uranium		Plutonium				Americium		Neodymium
	R 5 (U-235/U-238)	R 6 (U-236/U-238)	R' 0 (Pu-240/Pu-239)	R' 1 (Pu-241/Pu-239)	R' 2 (Pu-242/Pu-239)	R' 242 (Am-242/Am-241)	R' 243 (Am-243/Am-241)		
D-2	0.01343 ± 0.25	0.00186 ± 1.20	0.2007 ± 0.15	0.0732 ± 0.31	0.0102 ± 0.82			2.2168 ± 0.32	
	0.01333 ± 0.36	0.00171 ± 1.40	0.2011 ± 0.22	0.0733 ± 0.25	0.0102 ± 1.20	0.00433	0.0541	2.1515 ± 0.41	
	0.01338 ± 0.40	0.00178 ± 1.60	0.2009 ± 0.20	0.0732 ± 0.30	0.0102 ± 1.30	0.00433 ± 2.10	0.0541 ± 0.90	2.1837 ± 0.70	
D-4	0.01372 ± 0.21	0.00176 ± 0.50	0.1828 ± 0.18	0.0714 ± 0.34	0.0089 ± 1.50			2.1860 ± 0.31	
	0.01374 ± 0.24	0.00179 ± 0.80	0.1826 ± 0.20	0.0710 ± 0.28	0.0085 ± 1.40	0.0585		2.2042 ± 0.25	
	0.01373 ± 0.30	0.00177 ± 0.80	0.1827 ± 0.20	0.0712 ± 0.40	0.0087 ± 1.80	0.0585 ± 1.70		2.2008 ± 0.30	
E-1	0.01225 ± 1.20	0.00192 ± 2.10	0.2304 ± 0.27	0.0844 ± 0.16	0.0139 ± 0.59	n. m.	n. m.	2.2095 ± 0.49	
	0.01261 ± 1.30	0.00201 ± 1.80	0.2300 ± 0.25	0.0840 ± 0.35	0.0137 ± 0.62			2.1978 ± 0.45	
	0.01243 ± 1.50	0.00196 ± 2.30	0.2302 ± 0.30	0.0842 ± 0.40	0.0138 ± 0.70			2.2036 ± 0.50	
E-5	0.01369 ± 0.37	0.00166 ± 1.01	0.1830 ± 0.25	0.0713 ± 0.31	0.0085 ± 0.73				
	0.01383 ± 0.40	0.00171 ± 1.15	0.1819 ± 0.18	0.0705 ± 0.15	0.0084 ± 0.68			2.2029 ± 0.25	
	0.01376 ± 0.32	0.00164 ± 1.09	0.1820 ± 0.28	0.0710 ± 0.16	0.0085 ± 0.76	0.00518	0.0584	2.2165 ± 0.35	
G-7	0.01376 ± 0.40	0.00169 ± 1.30	0.1825 ± 0.30	0.0709 ± 0.30	0.0085 ± 0.90	0.00518 ± 2.90	0.0584 ± 0.80	2.2097 ± 0.40	
	0.01241 ± 0.20	0.00192 ± 0.78	0.2254 ± 0.15	0.0843 ± 0.38	0.0129 ± 0.92	n. m.	n. m.	2.1564 ± 0.47	
	0.01234 ± 0.24	0.00187 ± 1.20	0.2262 ± 0.20	0.0848 ± 0.32	0.0132 ± 1.10			2.1590 ± 0.30	
H-2	0.01237 ± 0.30	0.00189 ± 1.20	0.2258 ± 0.20	0.0846 ± 0.40	0.0130 ± 1.20			2.1577 ± 0.40	
	0.01126 ± 0.77	0.00203 ± 1.00	0.2692 ± 0.23	0.0947 ± 0.18	0.0181 ± 0.64			2.2272 ± 0.31	
	0.01136 ± 0.79	0.00201 ± 1.60	0.2690 ± 0.15	0.0939 ± 0.35	0.0182 ± 1.10	0.00441	0.0827	2.2186 ± 0.43	
H-8	0.01131 ± 0.90	0.00201 ± 1.60	0.2691 ± 0.20	0.0943 ± 0.40	0.0181 ± 1.10	0.00441 ± 2.60	0.0827 ± 0.60	2.2229 ± 0.40	
	0.01070 ± 1.00	0.00199 ± 1.90	0.2943 ± 0.25	0.1029 ± 0.50	0.0215 ± 1.10	n. m.	n. m.	2.2150 ± 0.20	
	0.01062 ± 0.84	0.00208 ± 1.70	0.2933 ± 0.42	0.1020 ± 0.40	0.0214 ± 1.10			2.2005 ± 0.18	
J-1	0.01066 ± 1.10	0.00203 ± 2.20	0.2938 ± 0.40	0.1025 ± 0.60	0.0215 ± 1.30			2.2178 ± 0.30	
	0.00652 ± 0.28	0.00188 ± 0.90	0.3615 ± 0.11	0.1321 ± 0.40	0.0386 ± 0.84			2.1525 ± 0.20	
	0.00646 ± 0.34	0.00182 ± 1.20	0.3612 ± 0.18	0.1307 ± 0.42	0.0383 ± 0.72	0.1486		2.1437 ± 0.16	
J-9	0.00649 ± 0.40	0.00185 ± 1.30	0.3613 ± 0.20	0.1314 ± 0.50	0.0384 ± 1.00	0.1486 ± 1.50		2.1481 ± 0.30	
	0.00556 ± 0.50	0.00196 ± 1.31	0.4189 ± 0.21	0.1485 ± 0.20	0.0516 ± 0.42			2.1372 ± 0.29	
	0.00555 ± 0.61	0.00200 ± 1.20	0.4194 ± 0.19	0.1496 ± 0.31	0.0515 ± 0.34	n. m.	n. m.	2.1541 ± 0.16	
	0.00560 ± 0.45	0.00195 ± 1.25	0.4206 ± 0.19	0.1489 ± 0.18	0.0522 ± 0.38			2.1553 ± 0.30	
	0.00557 ± 0.60	0.00197 ± 1.50	0.4192 ± 0.20	0.1491 ± 0.30	0.1518 ± 0.50				

TABLE A. 4-2 Isotope mass ratios of Krypton and Xenon

Sample No.	Kr 83/86	Kr 84/86	Kr 85/86	Xe 131/134	Xe 132/134	Xe 136/134
A-1	0.2626 ± 0.15	0.5763 ± 0.25	0.1185 ± 0.21	0.3544 ± 0.15	0.6678 ± 0.20	1.4310 ± 0.10
A-3	0.2633 ± 0.63	0.5671 ± 0.89	0.1153 ± 1.13	0.3488 ± 0.30	0.6501 ± 0.18	1.3712 ± 0.34
A-9	0.2445 ± 0.22	0.5902 ± 0.43	0.1143 ± 0.52	0.3385 ± 0.28	0.6824 ± 0.13	1.5175 ± 0.17
B-1	0.2694 ± 1.52	0.5923 ± 0.72	0.1163 ± 0.77	0.3512 ± 0.38	0.6654 ± 0.29	1.4232 ± 0.24
B-2	0.2682 ± 0.39	0.5698 ± 0.17	0.1172 ± 0.10	0.3509 ± 0.33	0.6550 ± 0.28	1.3580 ± 0.25
B-8	0.2561 ± 1.19	0.5707 ± 0.49	0.1135 ± 0.59	0.3433 ± 0.49	0.6614 ± 0.64	1.4130 ± 0.29
C-1	0.2641 ± 0.28	0.5671 ± 0.39	0.1111 ± 0.78	0.3496 ± 0.30	0.6531 ± 0.37	1.3680 ± 0.62
C-3	0.2706 ± 0.40	0.5687 ± 0.40	0.1188 ± 0.50	0.3486 ± 0.50	0.6517 ± 0.40	1.3040 ± 0.20
D-2	0.2696 ± 0.75	0.5679 ± 0.36	0.1099 ± 0.78	0.3494 ± 0.53	0.6524 ± 0.39	1.3270 ± 0.27
D-4	0.2703 ± 0.50	0.5650 ± 0.40	0.1178 ± 0.80	0.3486 ± 0.30	0.6491 ± 0.40	1.2936 ± 0.30
E-1	0.2653 ± 0.60	0.5732 ± 0.40	0.1124 ± 0.90	0.3478 ± 0.50	0.6566 ± 0.60	1.3636 ± 0.40
E-6	0.2632 ± 0.46	0.5678 ± 0.14	0.1152 ± 0.30	0.3464 ± 0.37	0.6553 ± 0.23	1.3670 ± 0.18
G-7	0.2696 ± 0.40	0.5702 ± 0.30	0.1181 ± 0.30	0.3491 ± 0.40	0.6588 ± 0.20	1.3490 ± 0.20
H-2	0.2601 ± 0.72	0.5681 ± 0.28	0.1136 ± 0.84	0.3423 ± 0.35	0.6610 ± 0.22	1.3980 ± 0.29
H-8	0.2622 ± 0.60	0.5855 ± 0.30	0.1187 ± 0.70	0.3473 ± 0.30	0.6670 ± 0.20	1.4040 ± 0.20
J-1	0.2567 ± 0.92	0.5959 ± 1.57	0.1161 ± 1.63	0.3417 ± 0.24	0.6817 ± 0.17	1.4810 ± 0.24
j-9	0.2481 ± 0.70	0.5966 ± 0.50	0.1179 ± 0.80	0.3365 ± 0.30	0.6857 ± 0.20	1.5380 ± 0.20

Table A. 4-3 . Percent of activity per alpha-emitting nuclides of plutonium, americium and curium

Sample	Date of measurement	Before separation				After separation	
		Pu239 + 240 %	Pu238+Am241 %	Cm242 %	Cm244 %	Pu239 + 240 %	Pu240 %
A-1	06. 26. 69	26. 60	34. 00	34. 00	5. 00	54. 45	45. 55
		25. 90	33. 60	34. 85	5. 65	55. 00	45. 00
		26. 40	33. 80	34. 60	5. 20	54. 00	46. 00
		26. 30 ± 1. 3	33. 80 ± 0. 6	34. 62 ± 0. 6	5. 28 ± 6. 3	54. 48 ± 0. 9	45. 52 ± 1. 1
A-3	10. 09. 69	34. 80	41. 80	17. 20	6. 20	56. 55	43. 45
		34. 40	41. 50	17. 70	6. 40	56. 20	43. 80
		34. 70	42. 10	16. 70	6. 50	57. 00	43. 00
		34. 63 ± 0. 6	41. 80 ± 0. 7	17. 20 ± 2. 9	6. 37 ± 2. 4	56. 58 ± 0. 7	43. 42 ± 0. 9
A-5	02. 23. 70	36. 40	47. 10	11. 80	4. 20	57. 30	42. 70
		36. 60	47. 80	11. 50	4. 10	58. 10	41. 90
		36. 30	48. 00	11. 40	4. 30	57. 50	42. 50
		36. 43 ± 0. 4	47. 80 ± 0. 4	11. 57 ± 1. 8	4. 20 ± 2. 4	57. 63 ± 0. 7	42. 37 ± 1. 0
A-9	02. 23. 70	27. 80	46. 40	14. 90	10. 90	47. 90	52. 10
		28. 30	45. 60	15. 30	10. 80	47. 80	52. 20
		28. 10	45. 40	15. 10	11. 40	48. 10	51. 90
		28. 07 ± 0. 9	45. 80 ± 1. 1	15. 10 ± 1. 3	11. 03 ± 2. 9	47. 93 ± 0. 3	52. 07 ± 0. 3
B-1	09. 18. 69	34. 80	39. 00	20. 90	5. 30	55. 65	44. 35
		34. 40	39. 10	21. 60	4. 50	55. 05	44. 95
		34. 70	39. 40	20. 80	5. 10	55. 40	44. 60
		34. 63 ± 0. 6	39. 17 ± 0. 5	21. 10 ± 2. 0	5. 10 ± 3. 0	55. 37 ± 0. 5	44. 63 ± 0. 7
B-2	07. 15. 69	32. 43	38. 10	22. 89	6. 58	56. 20	43. 80
		32. 82	38. 51	22. 81	5. 86	55. 45	44. 55
		32. 95	38. 28	22. 56	6. 21	55. 84	44. 16
		32. 73 ± 0. 8	38. 30 ± 0. 5	22. 75 ± 0. 8	6. 22 ± 5. 7	55. 83 ± 0. 7	44. 17 ± 0. 8
B-8	09. 15. 69	31. 80	43. 40	18. 80	6. 00	54. 50	45. 50
		31. 60	43. 60	18. 60	6. 20	53. 80	46. 20
		32. 10	43. 30	18. 70	5. 90	53. 40	46. 60
		31. 83 ± 0. 8	43. 44 ± 0. 3	18. 70 ± 0. 5	6. 03 ± 0. 5	53. 90 ± 1. 0	46. 10 ± 1. 2
C-1	10. 08. 69	35. 10	41. 50	18. 00	5. 40	55. 55	44. 45
		35. 90	41. 50	17. 40	5. 20	55. 60	44. 40
		35. 50	41. 70	17. 50	5. 30	55. 55	44. 45
		35. 50 ± 1. 1	41. 57 ± 0. 3	17. 63 ± 1. 8	5. 30 ± 1. 9	55. 57 ± 0. 1	44. 43 ± 0. 1
C-3	05. 13. 69	36. 30	35. 30	25. 40	3. 00	63. 15	36. 85
		35. 90	35. 50	25. 50	3. 10	63. 00	37. 00
		36. 20	35. 45	25. 45	2. 90	62. 95	37. 05
		36. 13 ± 0. 6	35. 42 ± 0. 3	25. 45 ± 0. 2	3. 00 ± 3. 3	63. 03 ± 0. 8	36. 96 ± 0. 3

Table A. 4-3 Contd

Sample	Date of measurement	Before separation				After separation	
		Pu239 + 240 %	Pu238+Am241 %	Cm242 %	Cm244 %	Pu239 +240 %	Pu240 %
D-2	02. 17. 70	38.90	45.20	10.40	5.50	59.60	40.40
		39.70	44.40	10.40	5.50	59.40	40.60
		39.50	45.00	9.70	5.80	59.90	40.10
		39.37 ± 1.0	44.86 ± 0.9	10.17 ± 3.9	5.60 ± 3.1	59.63 ± 0.4	40.37 ± 0.6
D-4	05. 19. 69	31.65	38.08	24.58	5.69	56.67	43.33
		32.02	38.11	24.40	5.47	56.41	43.59
		31.58	38.39	24.79	5.24	56.90	43.10
		31.75 ± 0.7	38.19 ± 0.4	24.59 ± 0.8	5.47 ± 4.1	56.66 ± 0.5	43.34 ± 0.6
E-1	01. 27. 70	38.20	47.50	10.90	3.40	57.10	42.90
		37.90	47.40	11.30	3.40	56.40	43.60
		38.50	47.10	10.70	3.70	57.00	43.00
		38.20 ± 0.8	47.33 ± 0.4	10.97 ± 2.8	3.50 ± 4.9	56.83 ± 0.7	43.17 ± 0.9
E-5	07. 21. 69	34.30	39.13	16.95	9.62	56.80	43.20
		33.82	40.05	16.39	9.74	57.00	43.00
		34.02	39.37	17.70	8.91	56.40	43.60
		34.05 ± 0.7	39.52 ± 1.2	17.01 ± 3.8	9.42 ± 4.8	56.73 ± 0.5	43.27 ± 0.7
G-7	05. 12. 69	31.94	36.30	28.05	3.71	56.00	44.00
		31.93	36.51	27.81	3.75	56.40	43.60
		32.03	36.84	27.26	3.87	56.80	43.20
		31.96 ± 0.2	36.55 ± 0.7	27.71 ± 1.5	3.78 ± 2.2	56.40 ± 0.7	43.60 ± 0.9
H-2	02. 17. 70	33.40	47.00	12.70	6.90	54.60	45.40
		33.80	46.60	12.20	7.40	54.00	46.00
		33.80	46.60	12.30	7.30	53.80	46.20
		33.67 ± 0.7	46.73 ± 0.5	12.40 ± 2.1	7.20 ± 3.7	54.13 ± 0.7	45.87 ± 0.9
H-8	05. 06. 69	27.45	35.50	27.33	9.72	54.90	45.10
		27.27	35.98	27.07	9.68	54.60	45.40
		27.53	35.92	27.26	9.29	54.00	46.00
		27.42 ± 0.5	35.80 ± 0.7	27.22 ± 0.5	9.56 ± 2.5	54.50 ± 0.8	45.50 ± 1.0
J-1	01. 20. 70	29.90	46.70	14.30	9.10	47.30	52.70
		29.80	47.20	14.50	8.50	47.50	52.50
		29.60	47.20	14.40	8.80	47.50	52.50
		29.77 ± 0.5	47.03 ± 0.6	14.40 ± 0.9	8.80 ± 3.4	47.43 ± 0.2	52.57 ± 0.2
j-9	07. 09. 69	22.62	35.80	31.39	10.19	45.95	54.05
		22.61	35.69	31.60	10.10	45.42	54.58
		22.79	35.37	32.09	9.75	45.48	54.52
		22.68 ± 0.4	35.62 ± 0.6	31.69 ± 1.1	10.01 ± 2.3	45.62 ± 0.6	54.38 ± 0.5

Table A. 4-4 Isotopic concentrations of Nd-148, U-238 and Pu-239

Sample No.	A(U-238)x 10 <sup>17</sup> %	A(Pu-239)x 10 <sup>14</sup> %	A(Nd-148)x10 <sup>14</sup> %	Sample No.	A(U-238)x 10 <sup>17</sup> %	A(Pu-239)x 10 <sup>14</sup> %	A(Nd-148)x10 <sup>14</sup> %
A-1	5. 6024	21. 419	1. 1024	D-2	5. 6123	23. 281	0. 9902
	5. 5799	21. 348	1. 1047		5. 5738	23. 180	0. 9870
	5. 5912 ± 0. 20	21. 384 ± 0. 17	1. 1036 ± 0. 10		5. 5930 ± 0. 34	23. 231 ± 0. 22	0. 9886 ± 0. 16
A-3	5. 3510	21. 4084	1. 0493	D-4	5. 5319	23. 954	0. 9149
	5. 2882		1. 0577		5. 5731	23. 906	0. 9238
	5. 4175	1. 0535 ± 0. 40	5. 5525 ± 0. 37		23. 930 ± 0. 10	0. 9193 ± 0. 48	
A-5	5. 1594	21. 182	1. 0193	E-1	5. 5739	23. 401	1. 1237
	5. 1415	21. 063	1. 0186			5. 5718	23. 277
	5. 1504 ± 0. 17	21. 122 ± 0. 28	1. 0189 ± 0. 03		5. 5728 ± 0. 02	23. 339 ± 0. 27	1. 1274 ± 0. 23
A-9	5. 5701	19. 734	1. 4690	E-5	5. 6171	24. 387	0. 9320
	5. 5532		1. 4522		5. 5763	24. 247	0. 9397
	5. 5870	1. 4606 ± 0. 57	5. 5967 ± 0. 36		24. 321	0. 9358 ± 0. 41	
B-1	5. 5701 ± 0. 30	19. 706 ± 0. 14	1. 0209	G-7	5. 4672	23. 577	1. 0790
		5. 6198	22. 271		1. 0323	5. 4999	23. 571
	5. 6254		22. 269		1. 0266 ± 0. 55	5. 4836 ± 0. 30	23. 574 ± 0. 01
B-2	5. 5766	22. 218	1. 0820	H-2	5. 4717	21. 514	1. 2290
	5. 5821	22. 168	1. 0711		5. 4581	21. 574	1. 2118
	5. 5793 ± 0. 05	22. 193 ± 0. 40	1. 0741 ± 0. 64		5. 4649 ± 0. 12	21. 544 ± 0. 14	1. 2204 ± 0. 70
B-8	5. 6335	21. 418	1. 2864	H-8	5. 5095	21. 730	1. 3116
		5. 6297	21. 397		1. 2765	5. 4644	21. 954
	5. 6316 ± 0. 03	21. 408 ± 0. 05	1. 2815 ± 0. 38		5. 4870 ± 0. 40	21. 842 ± 0. 50	1. 3059 ± 0. 44
C-1	4. 9671	20. 144	0. 9933	J-1	5. 5611	20. 999	1. 3291
	4. 9636	20. 118	0. 9895		5. 5542	20. 870	1. 3330
	4. 9653 ± 0. 03	20. 131 ± 0. 06	0. 9914 ± 0. 19		5. 5576 ± 0. 06	20. 934 ± 0. 31	1. 3310 ± 0. 15
C-3	5. 5336	23. 759	0. 9439	J-9	5. 4778	19. 805	1. 4792
	5. 5643	23. 718	0. 9499		5. 4906	19. 860	1. 4904
	5. 5490 ± 0. 28	23. 738 ± 0. 08	0. 9495 ± 0. 30		5. 4842 ± 0. 12	19. 860 ± 0. 14	1. 4848 ± 0. 38